SYNOPTIC MAPPING OF DNA DAMAGE IN THE REPLICATIVE SENESCENCE OF HUMAN FIBROBLASTS

SILA NAZ KÖSE

Thesis for the Master's Program in Bioengineering

Graduate School

Izmir University of Economics

Izmir

2023

SYNOPTIC MAPPING OF DNA DAMAGE IN THE REPLICATIVE SENESCENCE OF HUMAN FIBROBLASTS

SILA NAZ KÖSE

THESIS ADVISOR: ASST. PROF. DR. CİHANGİR YANDIM

A Master's Thesis

Submitted to

the Graduate School of Izmir University of Economics

the Department of Bioengineering

Izmir

2023

ETHICAL DECLARATION

I hereby declare that I am the sole author of this thesis and that I have conducted my work in accordance with academic rules and ethical behaviour at every stage from the planning of the thesis to its defence. I confirm that I have cited all ideas, information and findings that are not specific to my study, as required by the code of ethical behaviour, and that all statements not cited are my own.

Name, Surname: Sıla Naz, Köse

Date: 16/10/2023

Signature:

ABSTRACT

SYNOPTIC MAPPING OF DNA DAMAGE IN THE REPLICATIVE SENESCENCE OF HUMAN FIBROBLASTS

Köse, Sıla Naz

Master's Program in Bioengineering

Advisor: Asst. Prof. Dr. Cihangir Yandım

October, 2023

Replicative cellular senescence is an inherent biological process implicated in aging, distinguished by enduring growth arrest and an associated inflammatory phenotype. Although a strong connection between DNA damage and telomere attrition is recognized in senescence, compelling evidence points to the potential for replicative senescence independent of telomere length. Notably, the accumulation of DNA damage outside telomeres during replicative senescence has been reported, yet the specific genomic loci involved in this process have remained elusive. This thesis aims to map endogenous DNA damage during replicative senescence, identifying regions of the human genome vulnerable to DNA damage. The main research motivation was to expose genes, regulatory elements, and repetitive motifs that are likely to mutate during cellular aging. Leveraging a fibroblast senescence model, molecular characterization of cells, chromatin immunoprecipitation with the DNA-damage marker γ-H2AX and next-generation sequencing were performed. Intriguingly, we observed γ-H2AX occupancies not only in telomeric regions, but also within gene-rich

regions, and repetitive DNA, including LINEs, SINEs, and various satellite sequences. Moreover, gene ontology analysis revealed increased γ-H2AX peaks of affected genes involved in immune system activation, cell death, vascularization, diabetes, and cancer. Our findings posit that mutations may not randomly accumulate in the aging genome; rather, they may demonstrate a discernible bias toward known age-related phenotypes and diseases as cells navigate into senescence. This new knowledge enriches our understanding of aging processes and could guide the development of interventions targeting DNA damage in age-related diseases. This thesis received funding from the TÜBİTAK 3501 program (Project No: 219Z371).

Keywords: Replicative senescence, DNA damage, γ-H2AX, chromatin immunoprecipitation sequencing, repetitive DNA.

ÖZET

İNSAN FİBROBLASTLARINDA REPLİKATİF YAŞLANMA SIRASINDA MEYDANA GELEN DNA HASARININ KAPSAMLI HARİTALANMASI

Köse, Sıla Naz

Biyomühendislik Yüksek Lisans Programı

Tez Danışmanı: Dr. Öğr. Üyesi Cihangir Yandım

Ekim, 2023

Hücrenin doğal yaşlanmasıyla ilişkilendirilen replikatif senesans, büyüme duraklaması ve immün fenotiple ayırt edilir. Telomer kısalamasıyla DNA hasarı arasındaki güçlü bağlantı, senesansın temelinde tanınmış olsa da, çalışmalar, telomer uzunluğundan bağımsız olarak replikatif senesansın potansiyeline işaret etmektedir. Özellikle, replikatif senesans sırasında telomer dışında DNA hasarının biriktiği bildirilmiştir, ancak bu süreçte etkilenen belirli genomik bölgeler henüz belirsiz kalmaktadır. Bu tez, replikatif senesans sırasında endojen DNA hasarını haritalamayı ve DNA hasarına yatkın insan genomunun bölgelerini tanımayı amaçlamaktadır. Ana araştırma motivasyonu, hücresel yaşlanma sırasında muhtemelen mutasyona uğrayan genleri, düzenleyici elementleri ve tekrarlanan motifleri açığa çıkarmaktır. Fibroblast senesans modelinden yararlanarak, genç, erken yaşlı ve geç yaşlı hücrelerin moleküler karakterizasyonu yapılmıştır. Bu süreci takiben, γ-H2AX DNA hasar belirteci ile kromatin immünopresipitasyonu ve yeni nesil dizileme yapılmıştır. Şaşırtıcı bir şekilde, γ-H2AX mekanizmalarının sadece telomerik bölgelerde değil, aynı zamanda

gen zengin bölgelerde, düzenleyici elementlerde ve LINE, SINE ve çeşitli satelit dizileri gibi tekrarlanan DNA'lar içinde de görüldüğü gözlemlenmiştir. Bu, replikatif senesans sırasında meydana gelen endojen DNA hasarının sadece telomerlerle sınırlı olmadığını göstermektedir. Ayrıca, gen ontoloji analizi, etkilenen genlerin bağışıklık sistemi aktivasyonu, hücre ölümü, damarlaşma, diyabet ve kanserle ile ilgili olduğunu ortaya koymuştur. Bulgularımız, mutasyonların yaşlanan genomda rastgele birikmediğini, bunun yerine hücrelerin senesansa ilerlerken bilinen yaşa bağlı fenotiplere ve hastalıklara yönelik belirgin bir eğilim gösterebileceğini düşündürmektedir. Bu yeni bilgi, yaşlanma süreçlerinin anlaşılmasını zenginleştirmekte ve yaşla ilişkili hastalıklarda DNA hasarına yönelik müdahalelerin geliştirilmesine rehberlik edebilir. Bu tez, TÜBİTAK 3501 programından (Proje No: 219Z371) fon desteği almıştır.

Anahtar Kelimeler: Replikatif yaşlanma, DNA hasarı, γ-H2AX, kromatin immünopresipitasyon sekanslama, tekrarlayan DNA.

Dedicated to my beloved family;

My brother Taylan, my mother Sema and my father Birol

ACKNOWLEDGEMENTS

I would like to express my sincere gratitude to my advisor, Assistant Professor Cihangir Yandım, who has supported me since my undergraduate years and encouraged me to go the extra mile. I am immensely thankful for the vision he has brought into my life, and his guidance. I consider him not only as my mentor but also as a part of my family, and I am truly thankful for his presence in my life.

To my dear friend and mentor, H. Saygın Portakal, I am truly appreciative of the consistent motivation you have provided and your patient responses to all my questions. I cannot imagine the lab without your presence. I would also like to express my gratitude to my office mate, A. Buse Andaç, for your loving heart and assistance, which have made this challenging adventure more enjoyable. To both of you, I am forever thankful for lifting me up whenever I fell. To my first student, Yağmur Başkan, thank you for your invaluable support and for being not only a friend but also a beloved sister. Without all of you, it would not have been possible to work with so much joy.

To the Yandım Lab team, who has become my second family, I am deeply grateful for their continuous support, dedication, and companionship throughout this research endeavor. I am grateful for the presence of Gökçe Dağlar, Yağmur Başkan, Mahinur Başcı, Büşranur Çeltik, Helin Su Mete, Ilgım Gül, Hasan Doruk Biçer, Fatma Rabia Çakıcı, and Yaren Derbent. I would like to thanks to my project partner, Elif Duymaz, for being a reliable companion on this journey.

I would like to express my gratitude to Assoc. Prof. Zeynep Fırtına Karagonlar and Asst. Prof. Yavuz Oktay for dedicating their time to read my thesis and provide valuable insights. Furthermore, I extend my thanks to them and their lab teams for their material support and their modest nature, serving as an inspiration to me.

Finally, I would like to extend my heartfelt appreciation to my parents to my family, Sema Köse, Birol Köse, and Taylan Can Köse, for their patience, unwavering support, unconditioned love, and assistance throughout my life. I am incredibly grateful for the endless encouragement they have provided.

TABLE OF CONTENTS

LIST OF TABLES

LIST OF FIGURES

LIST OF ABBREVIATIONS

5'UTR : 5' Untranslated region

ARF : Alternative Reading Frame

ATCC : American Type Culture Collection

ATM : Ataxia-Telangiectasia Mutated

ATR : Ataxia Telangiectasia and Rad3-related

bp : Base pairs

BrdU : 5-Bromo-2'-deoxyuridine

BRE : TFIIB recognition element

cDNA : Complementary DNA

CpG : Cytosine-guanine dinucleotide

CRISPR-Cas9: Clustered Regularly Interspaced Short Palindromic Repeats-CRISPR-associated protein 9

DMSO : Dimethyl Sulfoxide

DNA : Deoxyribonucleic acid

DNMTs : DNA Methyltransferases

DPE : Downstream promoter element

DTT: Dithiothreitol

EDTA: Ethylenediaminetetraacetic acid

FITC : Fluorescein Isothiocyanate

H3K27ac : Acetylation of lysine 27 on histone 3

H3K27me3 : Trimethylation of lysine 27 on histone 3

H3K4me : Methylation of lysine 4 on histone 3

H3K9ac : Acetylation of lysine 9 on histone 3

Inr : Initiator

IP: Immunoprecipitation

IP: Immunoprecipitation

JNK : c-Jun Amino-Terminal Kinase

kb : Kilobases

M: Molar

MAPK : Mitogen-Activated Protein Kinase

MTE : Motif ten element

MYC : Myelocytomatosis

NaCl: Sodium chloride

ncRNA : Non-coding RNA

NF1 : Neurofibromin 1

ORF : Open reading frame

OXPHOS : Oxidative Phosphorylation

PIC : Protease Inhibitor Cocktail

PTEN : Phosphatase and Tensin Homolog

RNA : Ribonucleic acid

ROS : Reactive Oxygen Species

TAE : Tris-Acetate-EDTA

TF : Transcription factor

TSS: Transcription start site

UV : Ultraviolet

PCR : Polymerase Chain Reaction

CHAPTER 1: INTRODUCTION

The genomes of all organisms on our planet give rise to the complex life forms we see around us. Every organism has a genome that carries the biological information needed to create and maintain its specific function and characteristics. Most genomes, including those found in humans and other cell organisms, are composed of DNA, but a few bacteria have RNA genomes. These long-chain molecules consist of monomeric subunits known as nucleotides (Alberts B. *et al*., 2002).

Since Friedrich Mischer discovered human genomic DNA in 1869, scientists have sought to unlock the secrets hidden in this complex structure that records our very existence. Decades later, Watson and Crick were able to reveal the double helical structure of DNA, which was a monumental achievement in the field of molecular biology. Today, many groundbreaking milestones have been reached in cellular and molecular biology, including the sequencing of the 3 billion letters of human DNA, which marked the beginning of the inward journey of exploration for humankind (Lamm, Harman and Veigl, 2020).

1.1. Human Genome and Its Content

1.1.1. DNA

Despite its chemical simplicity, DNA is considered the basic building block of life and genetics. It is a long polynucleotide chain with only four different nucleotide subunits, each with a sugar molecule, a nitrogen base and a phosphate group. It has a double stranded structure where two strands are antiparallel and bases in the strands are paired up complementarily which provides its helical structure. Through the sequence of nucleotides along each strand, DNA encodes information in the human genome (Brown, 2002)

The fundamental role of DNA is to carry genes with the critical information necessary to specify the composition of all living organisms, including details about the production of RNA molecules and proteins by transcription and translation processes. The nuclear DNA of eukaryotes is organized into chromosomes, which serve as the repository for this genetic information. The human genome consists of 23 pairs of chromosomes, which contain approximately 3 billion base pairs of the DNA. Of these, the X and Y chromosomes are sex chromosomes, while the remaining 22 pairs are autosomes, containing protein-coding genes and various non-coding sequences. Protein-coding genes are responsible for synthesizing proteins, which are

essential for cell structure and function. Interestingly, estimates suggest that the human genome contains between 20,000 and 25,000 protein-coding genes, accounting for only 1-2% of the total genome, while the remaining DNA is mostly non-coding, including introns, regulatory regions, and repetitive DNA (Alberts et al., 2002; Chaffey, 2003).

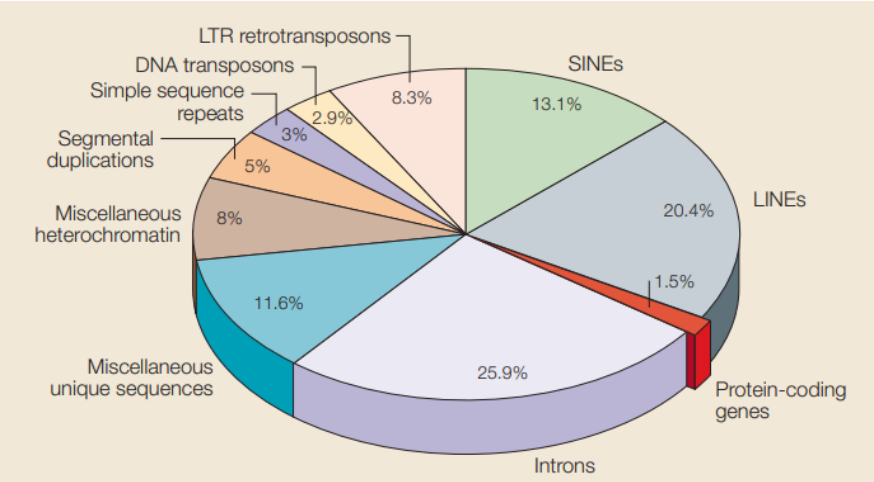

Figure 1. Overview of the various segments comprising the human genome. Merely 1.5% of the genome is comprised of the protein-coding sequences. In contrast, the majority of the genome is composed of non-coding sequences, including introns (approximately 26%) and mostly inactive transposable elements (nearly 45%) (Source: Lander et al., 2001; Gregory, 2005)

1.1.2. Non-coding sequences

The non-coding regions of the genome were once considered as "junk DNA" since they did not directly code for proteins. However, with advancements in genome sequencing and research, it has become clear that non-coding regions play important regulatory roles in gene expression, the 3D organization of the genome, and in embryonic development (Ambros, 2004). Dysregulation of non-coding regions has also been linked to various diseases, including cancer and neurodegenerative disorders.

This non-coding DNA can be further divided into different categories, such as introns, regulatory regions, and repetitive DNA. Introns are non-coding regions that are interspersed between coding regions within genes. They are transcribed into RNA but are later spliced out, leaving only the exons to be translated into protein (Mattick and Makunin, 2006).

1.1.3. Non-coding regulatory regions

Gene promoters, the non-coding regulatory elements located upstream of and partially overlap with the transcription start site (TSS) of the gene they regulate, occupying the first part of the 5'UTR region. They are essential in determining the direction of transcription and regulating gene expression. The length of gene promoters varies between 100 to 1000 base pairs (Le et al., 2019). The RNA polymerase II core promoter is an essential regulatory element in transcription. Although the core promoter is typically defined as a DNA stretch, it is a multidimensional entity with diverse structure and function. Core promoter elements such as the TATA box, initiator (Inr), TCT, BRE, MTE, and DPE motifs play a crucial role in transcriptional initiation. Nevertheless, different types of core promoters can be transcribed by different sets of transcription factors, and their properties, such as their interaction with transcriptional enhancers, are determined by the presence or absence of specific core promoter motifs (Kadonaga, 2012).

Apart from the core promoter, the proximal promoter, located approximately 250 bp upstream of the TSS, can extend up to 1000-2000bp and contains binding sites for both general and sequence-specific transcription factors, acting as an enhancer (Haberle and Stark, 2018). Enhancers on the other hand, DNA sequences that modulate gene expression, can range from 50 to 1500 bp in length and are binding sites for activators and repressors. The interaction between enhancers and activator/repressor proteins results in chromatin loops formation, which shift the enhancer closer to the gene promoter and recruit mediator proteins. Mediator proteins play a crucial role in facilitating the binding of RNA polymerase, which leads to the activation or suppression of gene expression for specific target genes. Enhancer regions, even when located far away from the target gene, can interact with activator and repressor molecules through chromatin loops. These loops are three-dimensional folds of chromatin that occur non-randomly and enable physical interactions between distant genetic sequences. Long-range interactions between regulatory sequences and their corresponding target genes are established through these chromatin loops (Pagni et al., 2022).

Non-coding repetitive sequences also play a crucial role in genome regulation and function. These repetitive structures consist of centromeres, transposable elements, satellite DNA, and telomeres, and are involved in vital cellular processes such as transposon reassembly, genome rearrangements, and the production of small

regulatory RNAs that can generate new exons. In addition, multiple studies have confirmed their crucial role in the assembly of the kinetochore, controlling telomere elongation, capping, and replication. Besides, some of repeats can modulate gene expression through epigenetic regulation and transcriptional response to stress (Hadjiargyrou and Delihas, 2013; Plohl, Meštrović and Mravinac, 2014; Simna and Han, 2022). Although the details of these functions are still an area of research, it is well-established that alterations in the non-coding regions and repetitive structures can lead to a wide range of pathological conditions, including cancer and neurodegenerative diseases (Weinberg and Wood, 2009).

1.2. Chromatin Structure

Within eukaryotic cells, chromosomes are comprised of a single, extended linear DNA molecule that is tightly wrapped and compacted by proteins. Alongside those proteins, many other proteins and RNA molecules interact with chromosomes, facilitating essential cellular functions including DNA repair, DNA replication, and gene expression. These proteins can be broadly categorized as histones or non-histones. Each histone protein is arranged as an octamer, consisting of two copies of four different histone proteins. The fundamental units of DNA and histone are referred to as nucleosomes, which are connected by stretches of "linker" DNA that resemble beads on a string. The precise and highly organized manner in which DNA and histones are packaged together is referred to as chromatin. The different states of chromatin can have a direct impact on transcription, either by modifying the manner in which DNA is packaged to permit or impede access to DNA-binding proteins, or by altering the surface of nucleosomes to enhance or restrict recruitment of protein complexes that effect change (Alberts *et al*., 2002; Park, 2009). Epigenetic modifications can dynamically regulate the chromatin architecture by either compact DNA into heterochromatin or open it up into euchromatin (Siddiqi, Mills and Matushansky, 2010).

In 1928, Heitz observed these two distinct states of chromatin. When cells are terminally differentiated, their nuclei are not homogeneous. Euchromatin, which corresponds to transcriptionally active genes, forms lighter areas that aggregate in the center, while heterochromatin forms darker areas in the periphery. Euchromatin has an open structure and is thought to have a "beads-on-string" organization in interphase, while heterochromatic genes are packed into chromatin fiber (Yandım, 2012). The packed structure of heterochromatin renders the chromatin unable to access

transcription factors, resulting in a silent state. Heterochromatin is a unique property of eukaryotes and is maintained throughout the cell cycle, playing an essential role in genome stability (Evans, Graumann and Bryant, 2013).

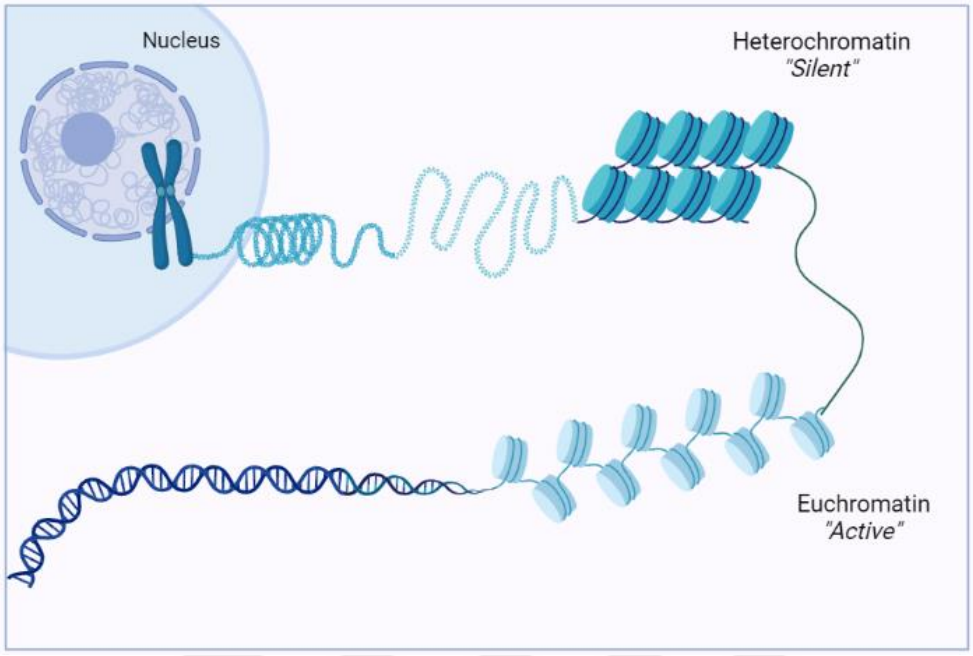

Figure 2. Distinction between Euchromatin and Heterochromatin, adapted from (Source: Murakami, 2013).

Heterochromatin can be further divided into two categories: "constitutive" and "facultative." Facultative heterochromatin refers to euchromatic regions that become heterochromatic and contain genes that should remain silent until activated by certain signals. An example of this form is the inactive X chromosome (Saksouk, Simboeck and Déjardin, 2015; Molnár, 2016). In contrast, constitutive heterochromatin is present in the same regions in all types of cells and generally does not include any genes. Therefore, this form is believed to be more stable than facultative heterochromatin. It is mostly found in pericentromeric regions and at telomeres where most of the repeat sequences are located (Saksouk, Simboeck and Déjardin, 2015).

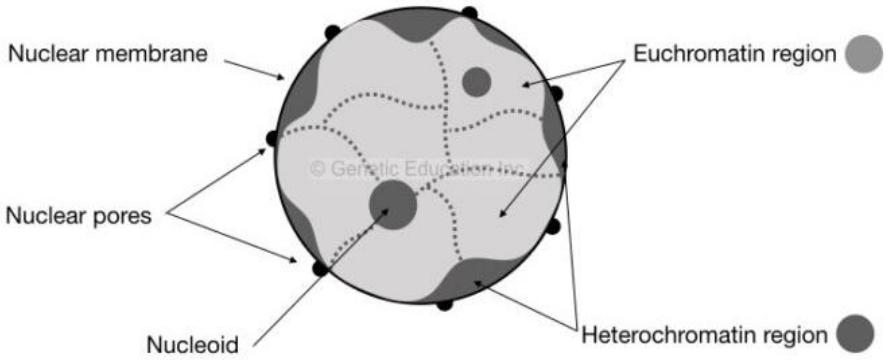

Figure 3. The distinct appearance of euchromatin and heterochromatin regions within the interphase nucleus. Euchromatin is depicted as a more loosely packed and dispersed form of chromatin, represented by the open and extended fiber (Source: Chauhan, 2021).

The regulation of chromatin states is executed by a wide range of chemical modifications on both histones and DNA, known as epigenetic marks. These marks modify the structure of chromatin and create distinctive recognition sites for regulatory factors.

1.3. Epigenetic Mechanisms

Epigenetic mechanisms play a critical role in a variety of cellular processes such as cell identity, differentiation, and cellular adaptation during both embryonic development and adult tissue maintenance. Epigenetic regulation is facilitated by DNA-binding proteins, most notably transcription factors (TFs), which facilitate the recruitment of epigenetic enzymes for the regulation of chemical modifications on DNA and histones. This modification process can lead to the restructuring or remodeling of chromatin architecture (Amtmann, Ma and Wagner, 2015; Sun et al., 2021). There have been three distinct epigenetic mechanisms that have been identified, namely histone modification, DNA methylation, and gene silencing associated with non-coding RNA (ncRNA) (Loscalzo and Handy, 2014).

1.3.1. Histone modifications

Eukaryotic organisms possess DNA that is wrapped around nucleosomes composed of core histones (H3, H4, H2A, H2B). Histone modifications are essential for various cellular events by enabling the binding of non-histone proteins and general transcription factors to the histone tails. These modifications are vital for gene expression, DNA replication and repair, chromatin compaction, cell-cycle control as well as aging by remodeling the chromatin to enable the transcription. Four types of

post-translational modifications to histone proteins are known: acetylation, methylation, phosphorylation, and ubiquitylation. Each of these modifications alters the DNA-histone interactions in nucleosomes (Mah, El-Osta and Karagiannis, 2010).

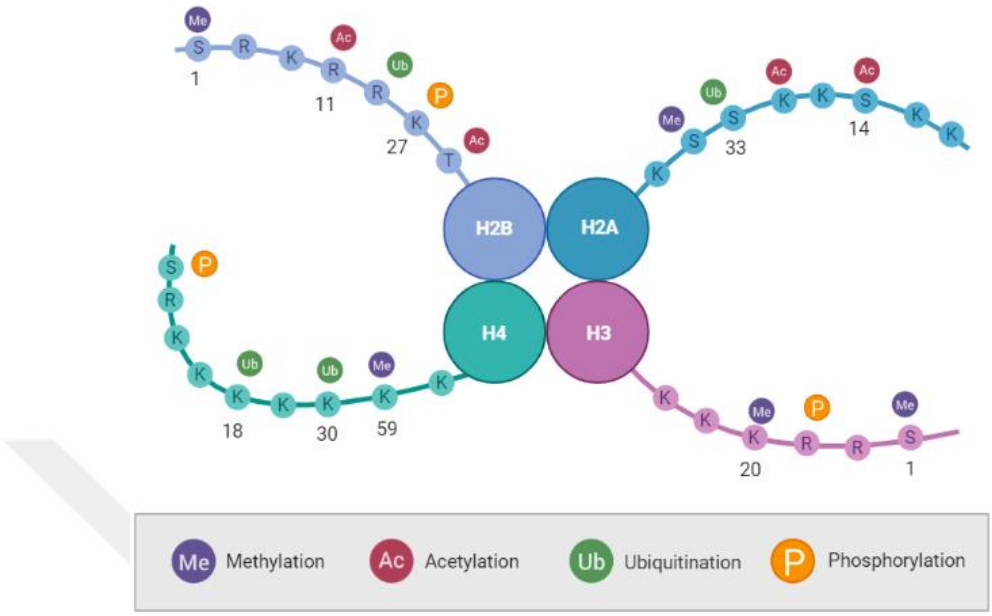

Figure 4. Post-translational modifications of Histone H2A, H2B, H3, and H4 (Source: Created with BioRender.com).

For instance, histone acetylation weakens the DNA-histone interactions, opening the chromatin and facilitating transcription. Histone acetylation frequently occurs at positively charged lysine residues, such as H3K9ac and H3K27ac. These modifications correspond with transcription activation. Histone methylation is more complex as it does not alter the histone protein charge and can involve the addition of 1-3 methyl groups to lysine and 1-2 methyl groups to arginine. It is linked to transcription activation when it occurs at lysine 4 on histone 3 (H3K4me). Trimethylation of lysine 27 on histone 3 (H3K27me3) is associated with transcription repression.

Histone ubiquitination involves adding a large ubiquitin molecule to lysine residues and it is related to gene silencing and transcription.

Histone phosphorylation entails adding a negative phosphate group to the histone tail, and phosphorylation plays a role in responding to DNA damage and subsequent repair. However, less is known about its function besides the phosphorylation of H2A(X) (Al Aboud, Tupper and Jialal, 2023). The presence of phosphorylated serine-139 residue on the H2AX histone variant, known as γ-H2AX, at a locus where a double-strand break (DSB) occurs, facilitates the recruitment of

DNA damage repair enzymes to the site of damage. This recruitment serves to promote efficient repair of the DSB and facilitate the transmission of signals involved in the DNA damage response (DDR) (Mah, El-Osta and Karagiannis, 2010).

1.3.2. DNA Methylation

DNA methylation is an epigenetic modification that involves the addition of a methyl group to the C-5 position of cytosine rings in DNA, catalyzed by DNA methyltransferases (DNMTs). This modification regulates gene expression by influencing the binding of transcription factors and other regulatory proteins to DNA, and it frequently occurs in the promoter region of genes. Methylation of CpG islands, which are typically located near gene promoters, can lead to gene repression by inhibiting the binding of transcription factors, whereas demethylation can promote gene expression (Jin, Li and Robertson, 2011). Furthermore, DNA methylation is involved in developmental processes, such as X-chromosome inactivation and genomic imprinting. During development, DNA methylation patterns change dynamically due to de novo DNA methylation and demethylation, resulting in a unique DNA methylation pattern in each differentiated cell that regulates tissue-specific gene transcription. Additionally, DNA methylation helps to maintain genome stability by silencing transposable elements and other repetitive sequences that could cause mutations and chromosomal abnormalities. However, aberrant global DNA methylation patterns and variations in the methylation levels of repetitive sequences can exert deleterious effects on cellular function and have been linked to various diseases, including cancer, neurological disorders, cardiovascular disease (Moore, Le and Fan, 2013) as well as global hypomethylation is observed during both stress-induced and replicative senescence in human embryonic lung fibroblasts (Issa, 2003; Zhang et al., 2008).

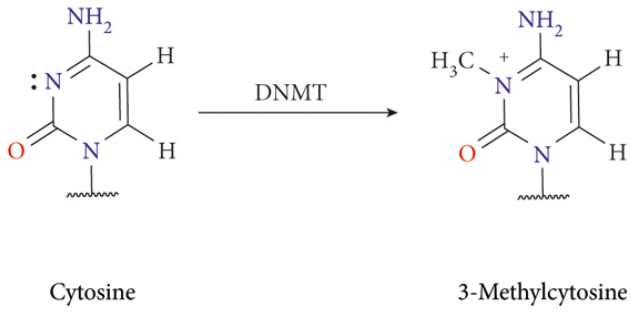

Figure 5. The reaction scheme depicting the enzymatic conversion of cytosine to 3 mC (3-methylcytosine) under the catalysis of DNMT (DNA methyltransferase). DNMT

plays a crucial role in the addition of a methyl group to the fifth carbon position of the cytosine ring, resulting in the formation of 3 mC (Almatarneh et al., 2022).

1.4. Repetitive DNA

Only a small fraction of the entire genomic sequence is responsible for encoding proteins, whereas the majority, exceeding 50%, comprises repetitive sequences commonly referred to as "junk" DNA (Lander et al., 2001). Although the precise role of these repetitive elements in sub-nuclear regulation remains incompletely understood, their expression has consistently been associated with crucial biological processes, including the response to heat stress (Porokhovnik et al., 2021), cellular senescence (Karakülah and Yandim, 2020), and their significant involvement in embryonic development (Ulitsky et al., 2011; Yandım and Karakülah, 2019b). Furthermore, aberrations in these repetitive sequences have been linked to genomic instability (Zhu et al., 2011; Anwar, Wulaningsih and Lehmann, 2017) and an increased vulnerability to DNA damage (Zhu et al., 2011; De Azambuja et al., 2014; Kishikawa et al., 2016; Anwar, Wulaningsih and Lehmann, 2017) through the disruption of chromatin architecture (Lee et al., 2012). The genome contains two types of repeat sequences: tandem repeats and interspersed repeats. Tandem repeats play a critical role in the formation of kinetochores, which are essential for proper chromosome segregation during cell division (Vos, Famulski and Chan, 2006; Zhu et al., 2011). On the other hand, interspersed repeats primarily serve as a mutagenic force, posing a risk for genomic alterations and genetic instability (Lee et al., 2012; Helman et al., 2014).

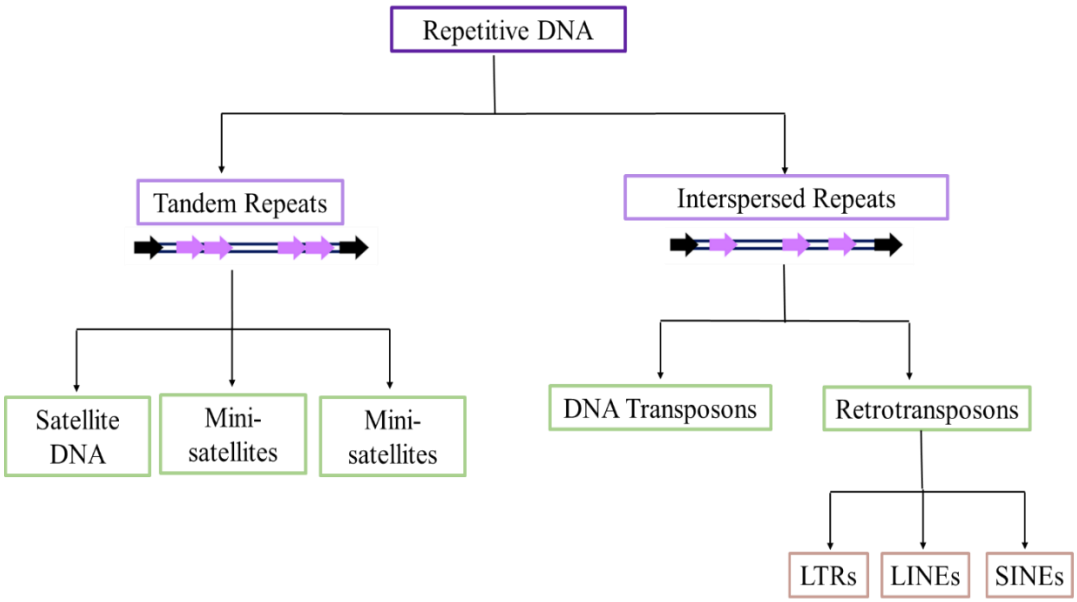

Figure 6. Repetitive DNA sequences in eukaryotic genomes. This schematization collects the information of several works in the information above.

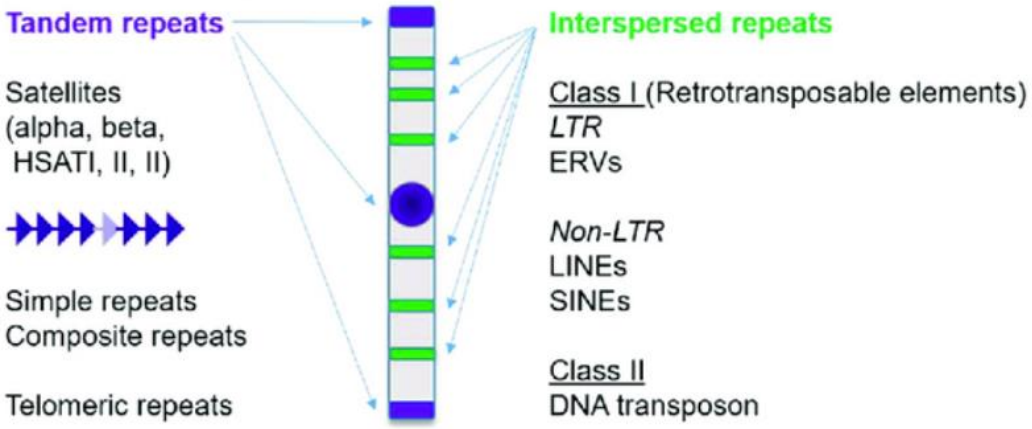

Figure 7. Chromosomal Distribution of Repetitive Elements. This figure illustrates the distribution pattern of repetitive elements along the chromosome (Source: Dumétier et al., 2022)

1.4.1. Tandem Repeats

Tandem repeat arrays refer to sequences in which repeating units are arranged in a consecutive manner, with each unit positioned in a head-to-tail orientation (Pavlicek, Kapitonov and Jurka, 2006). The length of these repeat units can vary, ranging from 2 to 171 bases (Shammas, 2011). Tandem repeats are predominantly found in regions of the genome that exhibit heterochromatin and centromeres, constituting approximately 3% of the human genome as determined by sequencing studies (Pavlicek, Kapitonov and Jurka, 2006). They can be classified as satellite DNA,

mini satellites and microsatellites.

1.4.1.1. Satellite DNA

Satellite DNAs predominantly occupy heterochromatic regions within the pericentromeres, subtelomeres, and sex chromosomes. Their sizes exhibit significant variability, ranging from 100 kb to over 1 mb. These repetitive DNA elements play critical roles in essential cellular processes such as chromosome segregation, maintenance of chromatin structure, and preservation of genomic stability (Wei et al., 2021). Typically, satellite DNAs exist in a repressed state, and their aberrant activation has been associated with various pathologies, including pancreatic cancer (Ting et al., 2011; Yandım and Karakülah, 2022), breast cancer (Densham and Morris, 2017; Yandım and Karakülah, 2019a) and hepatocellular carcinoma (Karakülah and Yandim, 2021) as well as senescence (Karakülah and Yandim, 2020; Wei et al., 2021)

1.4.1.2. Minisatellites

Minisatellites exhibit considerable variation in length and are composed of repeat units ranging from 6 to 100 base pairs. These satellite sequences are primarily located in subtelomeric regions and are recognized as hotspots for genomic rearrangements through homologous recombination. These repetitive sequences also contain hexameric TTA GGG repeats found in human telomeric DNA, and therefore play a crucial role in preserving the integrity of coding sequences located at the ends of chromosomes during the cell division (Wahls, Wallace and Moore, 1990; Ramel, 1997).

1.4.1.3. Microsatellites

Microsatellites are characterized by their high variability, consisting of repeat units with lengths typically ranging from 1 to 5 base pairs. Mononucleotide, dinucleotide, trinucleotide, and tetranucleotide repeats are the predominant types of microsatellites, although repetitive sequences composed of five (pentanucleotide) or six (hexanucleotide) nucleotides are also commonly classified as microsatellites (Ellegren, 2004). The specific combination of these repeated units can be distinctive to each individual, yet they can also be inherited from parents to their offspring (Morris, 2023). Expansion of these repetitive sequences has been linked to the manifestation of various disorders, including Fragile X syndrome and Huntington's disease (Ramel, 1997).

1.4.2. Interspersed Repeats

Interspersed repeats account for the predominant portion of repetitive sequences, making up approximately 45% of the human DNA. These repeats are dispersed randomly across the genome and possess the capability to insert their copies at various genomic locations. Originating mainly from transposable elements, interspersed repeats possess the capacity to initiate chromosomal instabilities by means of homologous recombination between dispersed copies, thereby contributing to the occurrence of diverse pathologies including cancer (Pavlicek, Kapitonov and Jurka, 2006; Shammas, 2011).

1.4.2.1. DNA Transposon Elements

Accounting for roughly 3% of the human genome, these evolutionarily conserved and inactive mobile genetic elements utilize a mechanism referred to as "cut and paste" (Pace and Feschotte, 2007). They encode the transposase enzymes, facilitate the excision of transposons from their original genomic sites and subsequent integration into alternative genomic locations (Feschotte and Pritham, 2007). The dynamic nature of these elements not only impacts gene expression modulation but also serves as a catalyst for recombination events and gene inactivation processes (Muñoz-López and García-Pérez, 2010).

1.4.2.2. Retrotransposons

Retrotransposons, comprising a substantial portion of repetitive sequences within the human genome, constituting approximately 45% of the genome. In the process of retrotransposition, retrotransposons are transcribed into RNA molecules by host RNA polymerases. Following, reverse transcription takes place, leading to the synthesis of complementary DNA (cDNA) copies. These cDNA copies, which contain the genetic information of the retrotransposon, are subsequently integrated into new genomic locations while the original transposon remains in its initial location . However, this processes is an error prone mechanism, it can lead to genomic instability by point mutations or truncations (Shammas, 2011). Therefore, they are recognized as one of the major contributor to genetic variation and their insertions have the capacity to influence protein function, modify gene expression, and induce genomic instability (Helman et al., 2014).

1.4.2.2.1. Long terminal repeat (LTR)

Long terminal repeat (LTR) retrotransposons, which are remnants of ancient endogenous retroviruses, contain coding sequences for env, gag, and pol genes. These elements, although currently inactive, constitute approximately 8% of the human genome (Shammas, 2011). Similar to other retrotransposons, LTR retrotransposons mobilize through the reverse transcription of their mRNA molecules. involving the conversion of their mRNA transcripts into complementary DNA (cDNA) molecules. Subsequently, these cDNA copies are integrated into novel genomic sites. The presence of LTR retrotransposons within the genome contributes to its intricate structure and enhances genomic diversity (Zhang et al., 2014).

1.4.2.2.2. Long interspersed nuclear elements (LINE)

LINEs are a class of non-long terminal repeat (non-LTR) retrotransposons that are autonomously transposable elements. In the human genome, they constitute almost a quarter of the total genomic content. Among the LINEs, the most prevalent and extensively studied member is LINE-1, which is present in around half a million copies scattered throughout the genome (Shammas, 2011). LINE-1 repeats consist of distinct structural components, including a 5' untranslated region (UTR), two open reading frames (ORFs), and a 3' UTR. The ORFs within LINE-1 repeats encode essential proteins called ORF1p and ORF2p, each with distinct functional properties. ORF1p exhibits RNA binding and chaperone activities, while ORF2p possesses endonuclease and reverse transcriptase activities (Dai et al., 2014). Their capacity for insertional mutagenesis promotes genetic diversity and potentially shapes the evolutionary course of the human genome. Disrupting gene function, L1 insertions near or within protein-coding genes can affect gene expression and lead to gene mutations. Additionally, L1 retrotransposition is linked to genomic instability, genetic disorders, and the pathogenesis of specific cancer types (Beck et al., 2011) as well as their activation can contribute to age-related inflammation (De Cecco et al., 2019).

1.4.2.2.3. Short interspersed nuclear elements (SINE)

As non-autonomous retrotransposons, these non-coding sequences are typically characterized by their lengths, which are usually below 500 base pairs. Notably, Alu elements, which make up around 11% of the human genome, are a prominent representative of this group (Shammas, 2011). With a length of approximately 300 base pairs, Alu elements originate from the 7SL RNA gene, an essential component involved in protein synthesis. While the majority of Alu repeats

are considered inactive and incapable of retrotransposition, a subset of Alu elements retains their mobilization potential. The mobility of active Alu elements can have significant implications, including genomic rearrangements, insertional mutagenesis, and the generation of genetic diversity (Okada, 1991; Deininger, 2011).

1.5. DNA Damage

As the fundamental genetic material, DNA is a highly dynamic molecule that undergoes numerous chemical modifications daily in response to both internal and external factors. However, the essential processes of DNA replication and repair, while critical for maintaining genomic fidelity, are inherently prone to errors, resulting in the accumulation of deleterious mutations (Chatterjee and Walker, 2017). These mutations can disrupt the precise transcription of genetic instructions, leading to impaired translation of proteins essential for cellular function. Moreover, if left unrepaired during cell division, these mutations can be perpetuated through subsequent generations. When a cell loses its capacity to effectively repair DNA damage, it may undergo programmed cell death (apoptosis), acquire malignant properties, or enter a state of cellular senescence. Thus, these DNA lesions exert a significant influence on the initiation and progression of diverse pathological conditions, encompassing neoplastic transformation and age-related disorders (Bernstein et al., 2013).

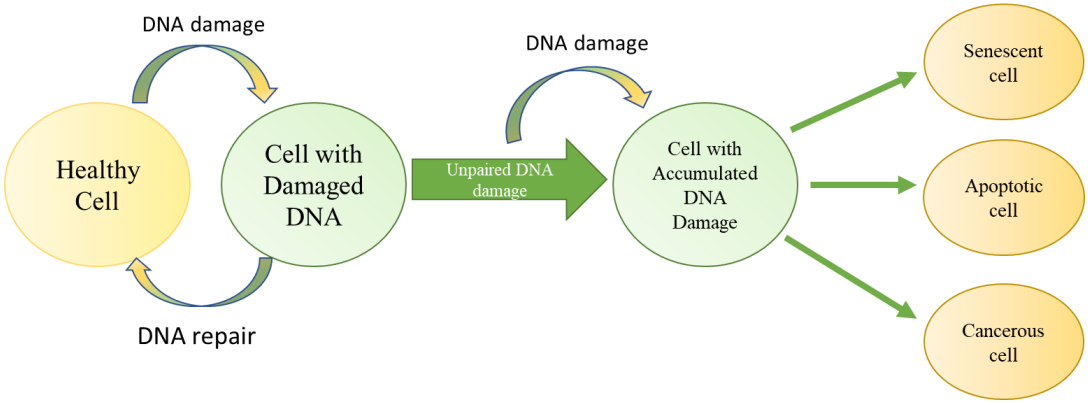

Figure 8. The cellular pathway of DNA damage and repair plays a critical role in determining cell fate, which can result in senescence, apoptosis, or cancer development, adapted from (Source: Merck, no date).

1.5.1. DNA Damage Response

To protect the cells from threats coming from DNA damage, and preserve genomic integrity and stability, cells evolved a complex response mechanism which is called DNA damage response (DDR). The DDR orchestrates a comprehensive set of cellular responses, including precise regulation of cell cycle progression, metabolic

adjustments, determination of cell fate, chromatin remodeling, immunogenicity, and apoptosis. This intricate network of processes ensures cell survival and facilitates adaptation to different forms of DNA damage, including replicative stress (Campisi and d'Adda di Fagagna, 2007; Bernstein et al., 2013; Pilié et al., 2019).

The activation of specific repair mechanisms depends on the nature of the DNA damage encountered, including single-strand breaks, double-strand breaks, base modifications, and DNA crosslinks. These diverse forms of DNA damage can trigger distinct repair pathways within the DDR (Jackson and Bartek, 2009). Furthermore, the selection of repair mechanisms is influenced by the phase of the cell cycle in which the damage occurs.

1.5.2. The Role of Gamma-H2AX in DNA Damage

Gamma-H2AX (γ-H2AX) is a pivotal component in the DNA damage response (DDR) pathway, specifically tasked with detecting and facilitating the repair of DNA double-strand breaks (DSBs). When DSBs occur in the DNA molecule, often due to external factors or exposure to certain chemicals, the cell's intricate surveillance system goes into action. The initial responder is the ATM kinase, which quickly localizes to the DSB site and becomes activated (Kuo and Yang, 2008).

Once activated, ATM undertakes a critical action: it phosphorylates a specific serine residue on a histone protein called H2AX, converting it into γ-H2AX. This phosphorylation of H2AX is not limited to just the immediate vicinity of the DSB; it spreads throughout the neighboring chromatin regions. Multiple γ-H2AX molecules accumulate around the break site, forming discrete foci that can be visualized under a microscope (Burma et al., 2001; Kuo and Yang, 2008).

These γ-H2AX foci serve as potent signals, precisely marking the location of the DSB within the genome. They act as scaffolds for recruiting various repair proteins to the damaged site. Importantly, γ-H2AX is instrumental in the assembly of repair complexes, including proteins responsible for two primary DNA repair pathways: non-homologous end-joining (NHEJ) and homologous recombination (HR). These recruited repair machinery components work either to directly rejoin the broken DNA ends (NHEJ) or exchange genetic material with an undamaged homologous DNA strand (HR), depending on the specific repair pathway involved (Chowdhury et al., 2005; Lowndes and Toh, 2005).

Moreover, γ-H2AX doesn't stop at recruiting repair factors; it also contributes to modifying the chromatin structure around the break site. These modifications

induced by γ-H2AX make the surrounding DNA more accessible to repair enzymes, thus facilitating the repair process. Additionally, γ-H2AX plays a role in activating cell cycle checkpoints that temporarily arrest the cell cycle, allowing time for DNA repair. If the damage is beyond repair, it can trigger apoptosis (Lowndes and Toh, 2005; Liao et al., 2021).

Ultimately, the presence of γ-H2AX foci signifies a commitment to efficient and accurate DNA damage repair, maintaining genomic stability, and preventing the inheritance of DNA errors or mutations.

1.5.3. Cell Cycle and DNA Damage

The cell cycle in eukaryotic cells is a highly intricate process that governs cell growth, replication, and division. It consists of well-defined phases, each with distinct characteristics and functions. Throughout the cell cycle, DNA damage can occur at different stages, and the cellular response to this damage depends on the specific phase in which it arises.

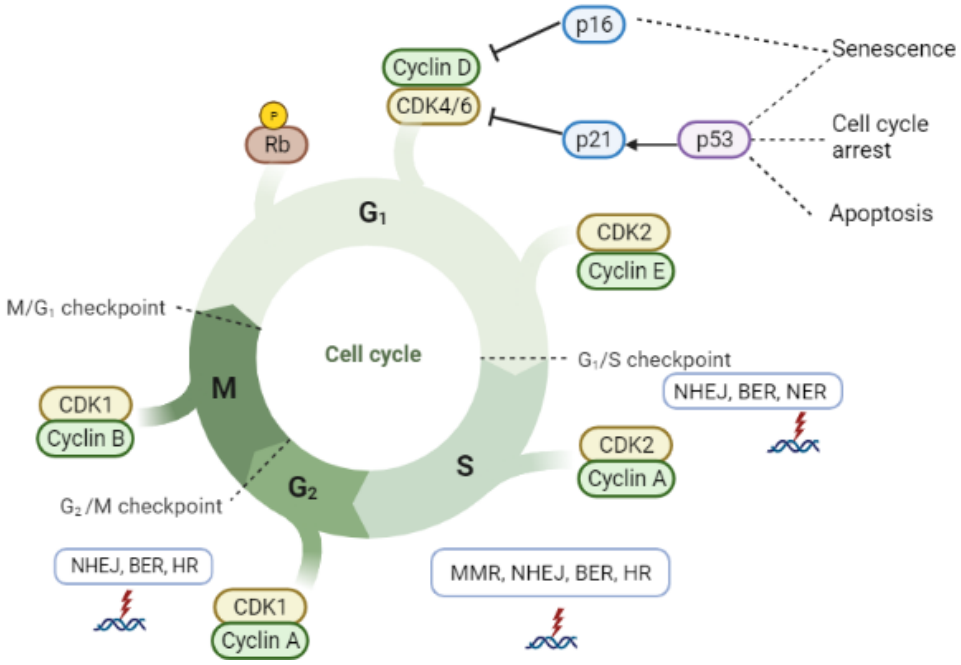

Figure 9. A comprehensive overview of the relationship between the cell cycle phases and the DNA repair mechanisms active during each stage. The cell cycle consists of distinct phases, including G1 (Gap 1), S (Synthesis), G2 (Gap 2), and M (Mitosis), adapted from (Source: Gee et al., 2018; Tomasova et al., 2020).

In the G1 phase, which begins the cell cycle, cells are ready to replicate DNA. When DNA is damaged during this phase, it triggers DNA damage response pathways,

causing cell cycle arrest and initiation of repair. Cyclin-dependent kinases (CDKs) play an important role in regulating the transition from G1 to S phase. CDK4 and CDK6, in complex with cyclin D, promote retinoblastoma protein (Rb) phosphorylation, eliminate E2F transcription factors and induce expression of genes required for S phase entry.

The S phase follows, where DNA replication takes place. During S phase, DNA damage activates complex signaling pathways to ensure accurate replication and activate repair mechanisms. Cells have evolved surveillance mechanisms, such as the activation of checkpoints, to ensure the accurate and complete replication of DNA before proceeding to subsequent phases. Cyclin A-CDK2 complex is involved in regulating the S phase progression and is implicated in the DNA damage response during this phase (Western Oregon University, no date)

After DNA replication, cells enter the G2 phase to prepare for cell division. In G2 phase, DNA damage activates DNA damage response pathways, causing cell cycle arrest. Repair processes are initiated, and the integrity of the DNA is assessed before progressing to the next phase (Limas and Cook, 2019). Cyclin A and cyclin B, in complex with CDK1, regulate the transition from G2 to M phase. Activation of CDK1 leads to the phosphorylation of various target proteins involved in mitotic progression. At the G2/M checkpoint, cells assess DNA integrity and repair any remaining DNA damage before entering mitosis.

Finally, during the M phase, also known as mitosis, cell division occurs, and the duplicated chromosomes are distributed to the daughter cells. Since, in this phase chromosomes are condensed, homology search is difficult and therefore DNA damage during this phase can disrupt chromosome segregation and lead to genomic instability (Branzei and Foiani, 2008).

Overall, the DNA damage response is tightly regulated during cell cycle to maintain genome integrity. The DDR mechanisms ensure correct recognition and removal of DNA lesions, provide the proper DNA synthesis and transcription, and ultimately promote genetic stability at each phase of the cell cycle. These mechanisms include the activation of various DNA repair pathways, such as base excision repair (BER), nucleotide excision repair (NER), homologous recombination (HR), and non-homologous end joining (NHEJ), among others (Chen et al., 2022).

1.5.4. DNA Damage Repair Mechanisms

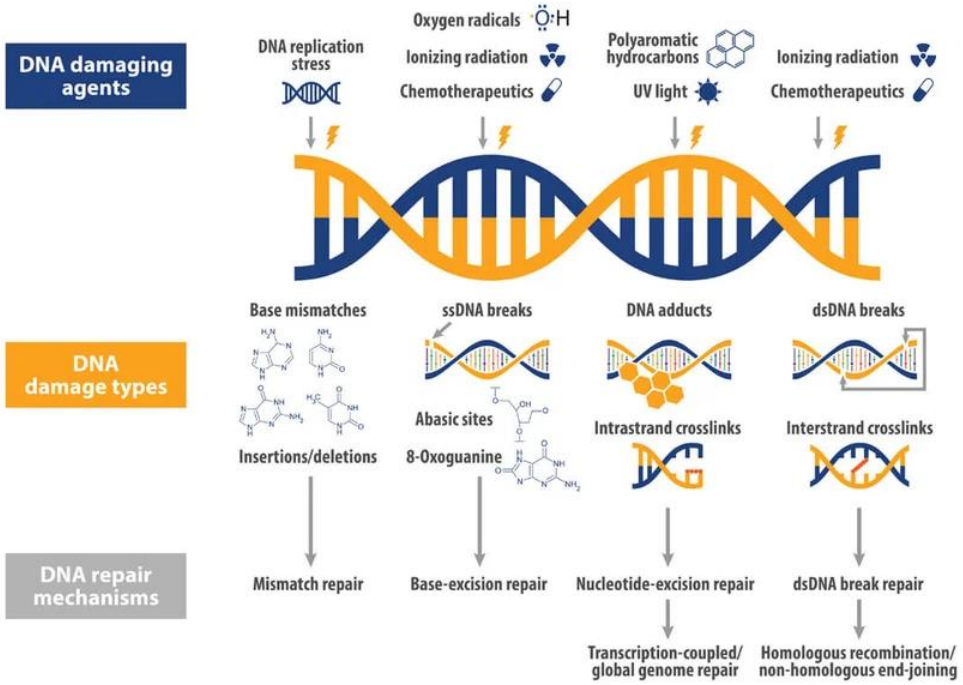

Figure 10.The major types of DNA repair mechanisms (Source: Mitra, 2019; Bourré, 2020)

1.5.4.1. Base Excision Repair

Base excision repair (BER) is a well-established DNA repair pathway that works to repair damaged or damaged bases in a DNA molecule. It works by using special enzymes (DNA glycosylases) that recognize and remove damaged bases, creating an apurinic/apyrimidinic (AP) site. Then, AP endonuclease enzymes subsequently processes the AP site. In the final step, appropriate bases are accurately inserted, complementing the DNA sequence, and subsequent recombination of the DNA strands occurs. BER plays a critical role in protecting genome integrity by efficiently repair DNA lesions caused by oxidation, deamination, methylation, and single-strand breaks (Rahimian et al., 2020).

1.5.4.2. Nucleotide Excision Repair

Nucleotide Excision Repair (NER) responsible for the removal of DNA lesions, resulting from bulky adducts and UV-induced pyrimidine dimers. It functions by recognizing and excising a section of DNA encompassing the damaged site, resulting in the formation of a gap. This gap is then filled through DNA synthesis, utilizing the intact complementary strand as a template. Finally, the reconstruction process is completed by joining the repaired DNA strands. Failure in this mechanism causes a serious threat to genome integrity and can result in carcinogenicity,

developmental abnormalities and premature aging (Rahimian et al., 2020).

1.5.4.3. DNA Mismatch Repair

DNA Mismatch Repair (MMR) is a highly conserved cellular mechanism that repairs errors that occur during DNA replication, such as mismatches in base pairing and short insertions or deletions. MMR functions by distinguishing the newly synthesized DNA strand from the template strand and promptly recognizing any mismatches. Once identified, MMR removes the erroneous nucleotide and replaces it with the correct one, thereby restoring DNA structure. This complex process requires a carefully coordinated set of steps, including discrimination of the DNA strands, mismatch region removal, and replication of corrected DNA fragments. By correcting replication errors, MMR plays a pivotal role in preserving genomic stability and preventing the accumulation of mutations that can lead to genetic disorders or contribute to the initiation and progression of cancer (Li, 2008; Rahimian et al., 2020).

1.5.4.4. Homologous Recombination

Homologous recombination (HR) acts as a major DNA repair pathway in the S and G2 phases of the cell cycle, with peak DNA replication and the presence of sister chromatids. During the repair process of double-strand breaks (DSBs) through HR, sister chromatids serve as templates for DNA repair. Therefore, HR is widely recognized as an error-free mechanism (Rahimian et al., 2020). Initially, the DSB undergoes processing, leading to the generation of single-stranded DNA (ssDNA) ends. These ssDNA ends search for homologous sequences within the sister chromatid. Upon locating a suitable homologous sequence, the ssDNA initiates an invasion into the homologous DNA, forming a distinctive displacement loop (D-loop) structure. Subsequently, DNA synthesis takes place, extending the invading strand and displacing the complementary DNA strand. This intricate process culminates in the formation of a Holliday junction, wherein the two DNA molecules intertwine. Ultimately, the Holliday junction is resolved, resulting in the formation of accurately repaired DNA strands (Elbakry and Löbrich, 2021).

1.5.4.5. Non-Homologous End Joining

Non-Homologous End Joining (NHEJ) is a prominent DNA repair pathway that plays a crucial role in efficiently repairing double-strand breaks (DSBs). NHEJ primarily operates during the G1 phase of the cell cycle, but it is also active throughout most of the cell cycle (Hinz et al., 2005). This repair mechanism involves a series of well-coordinated steps. Initially, the broken DNA ends are recognized and processed

by the Ku70/Ku80 heterodimer, which facilitates the recruitment of additional proteins essential for the repair process. Subsequently, the DNA ends undergo trimming to remove damaged or non-complementary nucleotides. Following this, the DNA ligase IV complex, along with associated factors like XRCC4 and XLF, mediates the joining of the processed DNA ends, leading to the reconnection of the broken strands. Notably, unlike homologous recombination, NHEJ does not rely on a homologous template and can effectively repair DSBs throughout the cell cycle, making it particularly important in non-dividing cells. While NHEJ exhibits efficiency in repairing DSBs, it has a tendency to introduce small insertions or deletions at the repair junction, potentially resulting in mutations or alterations in the DNA sequence. This inherent characteristic renders NHEJ an error-prone repair mechanism. Nevertheless, the advantage of NHEJ lies in its rapid and flexible nature in repairing DSBs, which is crucial for cellular survival and the maintenance of genome stability (Chang et al., 2017; Rahimian et al., 2020)

1.6. Biology of Aging and Its Impact

Aging is a universal phenomenon that impacts almost all living organisms and characterized by the gradual deterioration of physiological functions essential for survival. It encompasses a wide range of biological, physiological, environmental, psychological, and social factors. While some age-related changes are benign, most contribute to the decline of bodily functions and increase susceptibility to chronic diseases. Factors such as oxidative damage, mitochondrial dysfunction, telomere shortening, and defects in DNA repair enzymes can contribute to the aging process (Gilbert, 2000; National Insitute on Aging (NIA), 2023).

According to evolutionary theory, aging is believed to the result of diminished natural selection as individuals grow older. Factors such as accidents, predators, infection, and limit the life span of most species, leading to a scarcity of older individuals in natural populations. Consequently, there are fewer living elderly populations in which natural selection can act to eliminate favorable alleles that confer advantages in childhood but inadvertently contribute to decreases in life expectancy. This concept is called antagonistic pleiotropy, and it is critical to understanding a variety of aging phenomena, including the relationship between aging and some pathologies (Campisi, 2013).

Furthermore, DNA damage is a crucial aspect for aging. The accumulation of DNA damage over time is believed to play a role in cellular senescence and the decline

of tissue function associated with aging. Upon DNA damage, DDR pathways are activated to repair the damage. However, as the age increases, the efficiency of DNA repair mechanisms diminishes, leading to the persistence of DNA damage and increased genomic instability (Campisi, 2013; Guo et al., 2022).

The dysregulation of cyclins and CDKs is another factor implicated in age-related changes. Disruptions in the balance between cell proliferation and senescence caused by altered cyclin-CDK activity contribute to age-related phenotypes. Additionally, cyclin-dependent kinase inhibitors (CDKIs), such as p16INK4a and p21Cip1, are known to increase with age and play a role in establishing and maintaining cellular senescence (Capparelli et al., 2012; Hernandez-Segura, Nehme and Demaria, 2018; Guo et al., 2022).

The impact of aging extends beyond the cellular level and affects the functioning of tissues and organs. Aging is associated with a decline in tissue regenerative capacity, compromised immune responses, and heightened susceptibility to age-related diseases, such as cancer, neurodegenerative disorders, and cardiovascular diseases. The mechanisms underlying these age-related pathologies are multifaceted and involve processes such as chronic inflammation, mitochondrial dysfunction, and impaired proteostasis (Guo et al., 2022).

Increasing evidence suggests that cellular senescence plays a role in the development of various age-related pathologies, encompassing both degenerative and hyperplastic conditions. Although a complete understanding of aging remains elusive, it is worth noting that a significant number of age-related diseases have been associated with the senescence response, whether directly or indirectly. While cellular senescence may not encompass all aspects of aging, its involvement in age-related diseases is noteworthy (Campisi, 2013).

1.7. Molecular Senescence Mechanisms

Senescence is firstly recognized in 1961 by Hayflick and Moorhead's groundbreaking study. They revealed that human fibroblast cells had a limited capacity for division in culture. After a certain number of divisions, these cells would enter a state of growth arrest, known as senescence (Hayflick and Moorhead, 1961). Once cells enter senescence, they are unable to re-enter the cell cycle in response to any known stimuli.

Senescence represents a metabolically active but non-proliferative phase characterized by distinct changes in cell morphology. One of the primary causes of

senescence is believed to be the shortening of telomeres, which are repetitive sequences located at the ends of chromosomes that contribute to the maintenance of genomic stability (Hachmo et al., 2020). As telomeres shorten, signals for DNA damage, mediated by ATM and ATR, are triggered, eventually leading to cell cycle arrest (d'Adda di Fagagna et al., 2003; Jullien et al., 2013). Also, the p53/p21 and p16INK4a/pRB pathways, both of which are tumor suppressors, play critical roles in regulating senescence. In addition to growth arrest, senescent cells also exhibit changes in chromatin structure and alterations in gene expression patterns. These changes manifest as the secretion of chemokines, cytokines, growth factors, and proteases. Collectively, these alterations are referred to as the senescence-associated secretory phenotype (SASP), which will be further discussed in the subsequent sections (Campisi, 2013; Di Micco et al., 2021).

Also, during embryogenesis, a precisely orchestrated balance between cell proliferation and differentiation is essential for the formation of complex tissues and organs. Cellular senescence has been identified as a regulatory mechanism that contributes to this balance. Some cells undergo senescence to prevent excessive proliferation, ensuring that the correct number of cells is generated and preventing overgrowth. This controlled senescence can also aid in tissue remodeling and sculpting during organogenesis. Moreover, senescent cells can secrete signaling molecules that influence neighboring cells, contributing to tissue patterning and differentiation. While the role of senescence in embryogenesis is still a topic of active investigation, it underscores the multifaceted nature of this process, extending beyond aging and pathology to encompass fundamental aspects of development and tissue homeostasis (Muñoz-Espín et al., 2013; Storer et al., 2013).

1.7.1. Key Characteristics Shaping the Landscape of Senescence

Understanding these core characteristics offers a cohesive foundation for gaining a comprehensive insight into the aging process, particularly in the context of senescence across diverse organisms, with a specific emphasis on the aging processes in mammals. These defining attributes encompass *Stable Cell Cycle Arrest, Metabolic Alterations, Morphological Modifications, Epigenetic Changes, DNA Damage and Persistent DNA Damage Response, Resistance to Apoptosis, Secretory Phenotype, Senescence-associated heterochromatin foci, and Reactive Oxygen Species*.

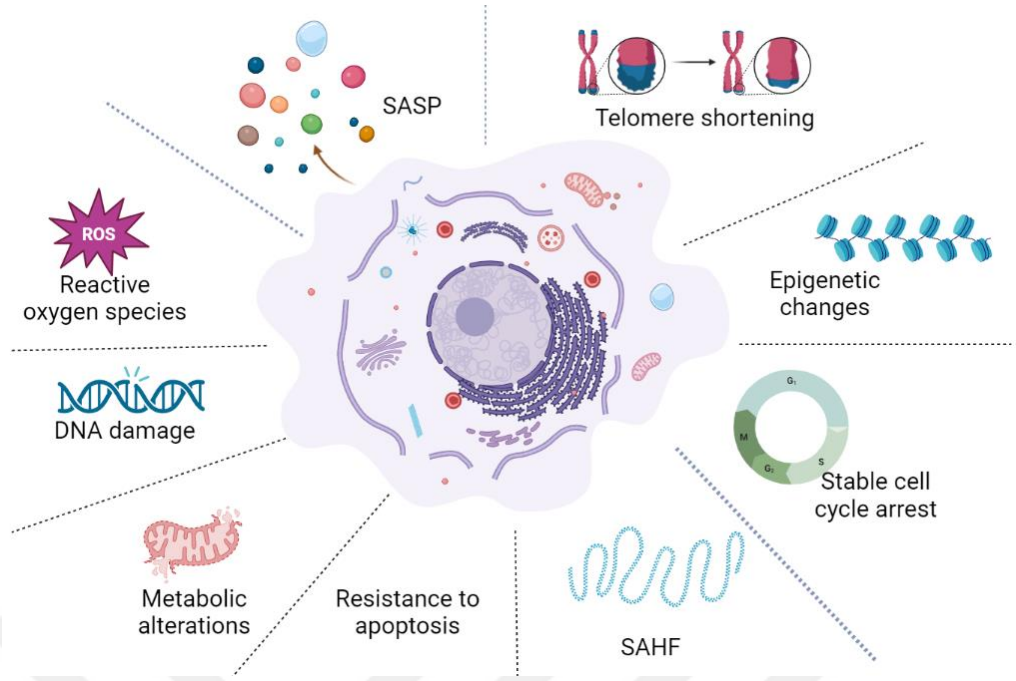

Figure 11. Overview of Key Characteristics Shaping the Landscape of Senescence. This scheme illustrates the key hallmarks associated with senescence, as described in this thesis, adapted from (Source: Di Micco et al., 2021).

1.7.1.1. Stable Cell Cycle Arrest

Cell cycle arrest is a crucial aspect of cellular senescence, referring to the state where cells cease to divide and enter a permanent growth arrest phase. This process is regulated by various molecular mechanisms involving specific signaling pathways and key regulatory molecules.

One of the well-established pathways involved in cell cycle arrest during senescence is the p53/p21 pathway. The tumor suppressor protein p53 plays a central role in sensing cellular stress and initiating appropriate cellular responses, including senescence. Upon activation, p53 induces the expression of p21, a cyclin-dependent kinase inhibitor (CDKI). p21 inhibits the activity of cyclin-dependent kinases (CDKs), which are essential for cell cycle progression, leading to cell cycle arrest (Kanaki, Makrantonaki and Zouboulis, 2016; Hernandez-Segura, Nehme and Demaria, 2018).

The p16INK4a/pRB pathway has been implicated as another pathway involved in senescence-associated cell cycle arrest. The activity of CDK4 and CDK6, which play a role in promoting cell cycle progression, is inhibited by the tumor suppressor protein p16INK4a. By inhibiting CDK4/6, the phosphorylation of the retinoblastoma protein (pRB) is prevented by p16INK4a. Consequently, E2F transcription factors are sequestered, leading to cell cycle arrest (Kastenhuber and Lowe, 2017; Hernandez-

Segura, Nehme and Demaria, 2018; Sanidas et al., 2019).

1.7.1.2. Metabolic Alterations

One of the hallmarks of cellular senescence is the presence of metabolic changes, which include modifications in metabolic pathways and cellular processes. These changes are characterized by shifts in energy metabolism, nutrient sensing, and metabolic signaling pathways.

During senescence, a transition from oxidative phosphorylation (OXPHOS) to glycolysis occurs, which is commonly referred to as the Warburg effect or aerobic glycolysis. This metabolic reprogramming allows cells to meet their energy requirements and fulfill the biosynthetic demands associated with the senescent state. The shift to glycolysis is accompanied by an increase in lactate production, even in the presence of oxygen (López-Otín et al., 2013; Mylonas and O'Loghlen, 2022).

Apart from changes in energy metabolism, senescent cells exhibit changes in nutrient sensing and signaling pathways. The mechanistic target of rapamycin (mTOR) pathway, which plays a critical role in nutrient sensing and cellular growth, becomes dysregulated in senescence. mTOR activity is often upregulated in senescent cells, resulting in enhanced protein synthesis, cell growth, and inhibition of autophagy (Nacarelli and Sell, 2017).

Furthermore, senescent cells display disruptions in other metabolic pathways, such as lipid metabolism and mitochondrial function. Dysregulated lipid metabolism can contribute to the accumulation of lipids and lipotoxicity, which are associated with age-related diseases (Hamsanathan and Gurkar, 2022). Senescent cells also exhibit mitochondrial dysfunction, characterized by impaired oxidative phosphorylation and increased production of reactive oxygen species (ROS) (López-Otín et al., 2013; Rabinovitch et al., 2017).

1.7.1.3. Resistance to Apoptosis

Apoptosis resistance is a characteristic feature of senescence and refers to the reduced ability of senescent cells to undergo programmed cell death or apoptosis. This resistance enables senescent cells to survive for an extended period and accumulate in tissues. Apoptosis is a vital process for maintaining tissue balance by eliminating damaged or dysfunctional cells. Nonetheless, senescent cells develop a resistance to apoptosis, enabling their persistence and involvement in age-related diseases (Hu et al., 2022).

One mechanism involves the disruption of apoptotic pathways. For instance, the tumor suppressor protein p53, known for its role in promoting apoptosis under cellular stress, is often upregulated in senescent cells. However, in senescence, p53 promotes cell cycle arrest instead of apoptosis, contributing to the resistance to cell death (Hu et al., 2022).

Another factor contributing to apoptosis resistance in senescent cells is the alteration of anti-apoptotic and pro-survival signaling pathways. Senescent cells exhibit increased levels of anti-apoptotic proteins, such as members of the Bcl-2 family, which inhibit the activation of downstream apoptotic factors such as c-Jun amino-terminal kinase (JNK) (Hernandez-Segura, Nehme and Demaria, 2018; Fan et al., 2020; Bulbiankova et al., 2023).

1.7.1.4. Reactive Oxygen Species

Reactive oxygen species (ROS) are highly reactive molecules generated as natural byproducts of cellular metabolism. They include superoxide anion, hydrogen peroxide, and hydroxyl radical, and can cause oxidative damage to cellular components like lipids, proteins, and DNA. The accumulation of ROS is associated with aging and is considered a hallmark of senescence (Borodkina et al., 2014).

During senescence, various factors such as mitochondrial dysfunction, increased metabolic activity, and activation of inflammatory pathways lead to increased ROS production. The elevated levels of ROS in senescent cells induce oxidative stress, resulting in cellular damage and dysfunction. ROS can directly cause DNA DSBs, leading to the accumulation of DNA damage and genomic instability (Di Micco et al., 2021). ROS also activate the DDR pathway, which triggers the activation of tumor suppressor proteins like p53, playing a role in senescence induction.

Moreover, ROS can also modulate signaling pathways involved in senescence. For example, ROS can trigger stress-responsive kinases such as p38MAPK and JNK, which promote senescence-associated phenotypes (Tiedje et al., 2012; Hernandez-Segura, Nehme and Demaria, 2018).

Furthermore, the activity of crucial enzymes involved in regulating senescence can be influenced by ROS. For example, it has been demonstrated that the activity of telomerase, an enzyme responsible for preserving the length of telomeres, can be inhibited by ROS, resulting in telomere shortening, which is a distinctive characteristic of cellular senescence (von Zglinicki, 2002).

1.7.1.5. DNA Damage and Persistent DNA Damage Response in Senescence

When DNA damage occurs in cells, a mechanism known as the DNA damage response (DDR) is initiated. As part of this response, certain proteins, such as γ-H2AX (phosphorylated at Ser139) and p53 binding protein (53BP1), accumulate at the locations where double-strand breaks (DSBs) have occurred. The kinases ATM and ATR are recruited to these damaged sites, where they convert the H2AX protein to its phosphorylated form, known as Activation of ATM, leads to the phosphorylation of certain checkpoint kinases and subsequent activation of downstream phosphorylation cascades to mark the damaged sites. As a result, the p53/p21 pathway is activated, p53 stimulates the expression of p21, which is a cyclin-dependent kinase inhibitor that plays a vital role in causing cell cycle arrest associated with senescence. Another important player in various types of senescence is p16, which inhibits the activity of CDK4 and CDK6. While p21 is activated early during the initiation of senescence, p16 is activated at a later stage, likely contributing to the maintenance of the senescence phenotype (Di Micco et al., 2021).

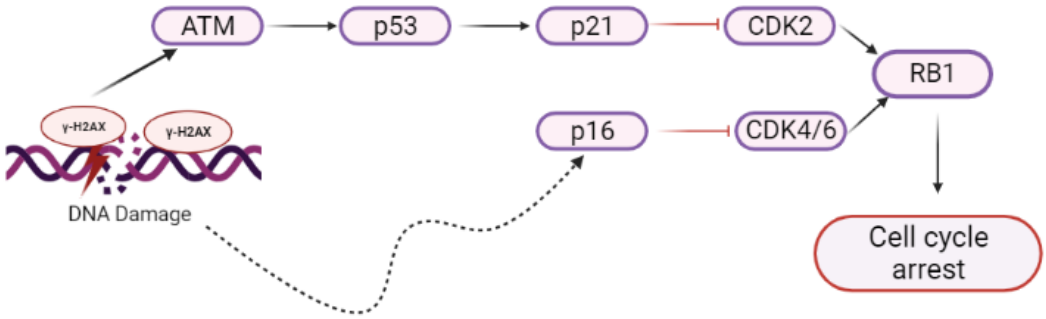

Figure 12. DDR Induced Cell Cycle Arrest. This schematic diagram illustrates the process of cell cycle arrest induced by the DNA damage response (DDR). When DNA damage occurs, the ataxia telangiectasia-mutated (ATM) kinase is activated and phosphorylates the histone protein H2AX at Ser139, resulting in the formation of γ-H2AX. The presence of γ-H2AX activates the p53 pathway, adapted from (Smith et al., 2021).

1.7.1.6. Telomere Shortening

Telomeres play a crucial role in cellular senescence as protective structures located at the ends of chromosomes. They consist of repetitive DNA sequences and associated proteins that serve to preserve genomic stability. Telomeres act as caps that prevent the erosion of essential genetic information during DNA replication and

protect the integrity of chromosomes. However, they undergo a gradual reduction in length as cells replicate. The replication machinery is unable to fully replicate the terminal regions of linear chromosomes, leading to the gradual erosion of telomeres. Normally, the enzyme telomerase replenishes and preserves telomeric DNA length. However, in most human somatic cells, telomerase activity is limited, resulting in progressive telomere shortening. This process eventually reaches a critical threshold, leading to replicative senescence, a cellular response that limits further cell division (López-Otín et al., 2013).

When telomeres become critically short, they activate a DNA damage response, perceiving the unprotected chromosome ends as DNA double-strand breaks. This activates signaling pathways involving ATM and ATR kinases, which further phosphorylates H2AX and activate tumor suppressor proteins, including p53, resulting in cell cycle arrest and senescence. Additionally, telomeres inhibit non-homologous end joining (NHEJ) mechanism by preventing end-to-end fusions. Consequently, this prevents the repair of double-strand breaks (DSBs) and ultimately leads to irreversible cell cycle arrest (Hewitt et al., 2012).

Studies indicate that telomere shortening serves as a mechanism to restrict cell proliferation, preventing uncontrolled growth and potential development of tumors. Additionally, dysfunctional telomeres and accelerated telomere shortening have been associated with various age-related diseases and conditions. In a study involving mice lacking telomerase, it was demonstrated that the progressive shortening of telomeres resulted in cellular senescence and accelerated aging-associated characteristics (Rudolph et al., 1999; Armanios et al., 2009). Also, research has demonstrated that the ectopic expression of telomerase can provide immortality in human fibroblasts without causing development of tumors (Bodnar et al., 1998).

1.7.1.7. Epigenetic Changes

Epigenomic changes are a distinctive characteristic of senescence and refer to modifications in the epigenetic profile of senescent cells. Epigenetic modifications are heritable alterations in gene expression that do not involve changes in the DNA sequence. These changes are pivotal in regulating gene expression patterns and cellular functions. Senescence entails significant alterations in the epigenome, including modifications in DNA methylation patterns, histone marks, and chromatin structure (López-Otín et al., 2013).

While the exact relationship between methylation and senescence remains unclear, it is established that there is a global decrease in DNA methylation levels. However, specific regions, such as CpG islands related to tumor suppressor genes, can undergo hypermethylation, leading to the silencing of these genes. This modification in DNA methylation patterns plays a role in the altered gene expression observed during senescence (de Magalhães, 2013; Pérez et al., 2018; Bulbiankova et al., 2023).

Additionally, non-coding RNAs, including microRNAs and long non-coding RNAs, play a role in senescence-associated epigenomic changes. They influence gene expression by degrading specific mRNAs or modulating chromatin structure and transcriptional regulation. These non-coding RNAs contribute to the propagation of senescence-associated signals and the establishment of the senescent phenotype (Ugalde, Español and López-Otín, 2011; López-Otín et al., 2013). It has been demonstrated that the modulation of expression levels or activity of specific miRNAs can have an impact on longevity in these organisms (Shen et al., 2012).

Histone modifications also undergo significant changes in senescent cells. Repressive histone marks, like H3K9me3 and H4K20me3, are often increased, leading to the formation of senescence-associated heterochromatin foci (SAHF) and the silencing of specific genes. Conversely, active transcription marks, like H3K4me3, may decrease in senescent cells (López-Otín et al., 2013).

1.7.1.8. Senescence-associated heterochromatin foci

Senescence-associated heterochromatin foci (SAHF) are considered a characteristic feature of senescence, representing specific structural and functional changes in chromatin organization in senescent cells. SAHF are localized areas of condensed chromatin marked by repressive histone modifications and chromatin-binding proteins. Formation of these regions is a defense mechanism against genomic instability and unwanted gene expression during cellar senescence. By sequestering specific genomic regions into a transcriptionally repressive state, SAHF contributes to the maintenance of the senescent phenotype (Bulbiankova et al., 2023).

SAHF formation requires chromatin reorganization and recruitment of specific chromatin modifying proteins. Key modifications associated with SAHF include the addition of repressive marks, such as histone H3 lysine 9 trimethylation (H3K9me3), mediated by the enzyme Suv39h1. This modification leads to chromatin compaction and transcriptional repression within the SAHF. Additionally, SAHF contain proteins like heterochromatin protein 1 (HP1) and high mobility group proteins (HMGA) that

contribute to chromatin compaction and gene silencing (Koso et al., 2012; Aird and Zhang, 2013; Kumari and Jat, 2021; Bulbiankova et al., 2023). The retinoblastoma protein (Rb) pathway also plays a role in SAHF formation by controlling cell cycle progression and senescence-associated gene expression (Narita et al., 2003).

1.7.1.9. Secretory Phenotype

The senescence-associated secretory phenotype (SASP) is a characteristic feature of senescent cells, where they release a variety of substances such as pro-inflammatory cytokines, chemokines, growth factors, and proteases into their environment. SASP facilitates communication between senescent cells and their environment, influencing adjacent cells, immune responses, and tissue balance. It helps in tissue repair and increases immune surveillance by attracting immune cells to the damaged tissue. However, prolonged exposure to SASP factors can lead to chronic inflammation, tissue dysfunction, angiogenesis, and the development of age-related diseases (Coppé et al., 2010; Lopes-Paciencia et al., 2019).

The senescence-associated secretory phenotype (SASP) involves the release of various substances by senescent cells. These substances include pro-inflammatory cytokines like IL-6, IL-8, IL-1α, and TNF-α, which can trigger chronic inflammation and attract immune cells (Davalos et al., 2010; Campisi, 2013). Chemokines such as CCL2, CCL5, and CXCL1 are also secreted, contributing to immune responses. Growth factors like TGF-β, IGFBPs, and PDGFs are released, affecting nearby cells and influencing tissue remodeling. Senescent cells also increase the production of matrix metalloproteinases (MMPs), which can remodel the extracellular matrix and potentially disrupt tissue structure. Moreover, senescent cells generate higher levels of reactive oxygen species (ROS), which act as signaling molecules, activating transcription factors such as NF-κB and promoting the production of pro-inflammatory factors (Coppé et al., 2010; Davalos et al., 2010; Lopes-Paciencia et al., 2019; Paramos-de-Carvalho, Jacinto and Saúde, 2021). Lastly, senescent cells release non-coding RNAs, including microRNAs and long non-coding RNAs, which can influence gene expression in adjacent cells and contribute to the spread of senescence-associated signals (Lettieri-Barbato et al., 2022).

1.7.2. Morphological Modifications of Senescent Cells

Senescent cells undergo specific physiological changes that reflect their altered state. At the cellular level, senescent cells typically exhibit a diffuse, flattened, and disorganized shape, and exhibit a different phenotype from the actively dividing cells.

Additionally, their nuclei are also altered as, they have multiple nuclei, lobulation, and altered heterochromatin content due to the changes in chromatin organization and gene expression patterns. These cells also tend to be larger in size due to changes in the cytoskeleton, specifically the loss of LaminB, and increased protein synthesis (Hernandez-Segura, Nehme and Demaria, 2018; Neurohr et al., 2019).

1.7.3. Biomarkers of Senescence

Senescence biomarkers are specific markers at the molecular or cellular level that can be used to detect and assess the presence of senescent cells. These biomarkers provide valuable insights into the process of senescence and its association with various biological and pathological conditions.

1.7.3.1. Senescence-associated β-galactosidase (SA-β-gal)

Senescence-associated β-galactosidase (SA-β-gal) activity is a widely used biomarker for detecting and measuring senescent cells. As cells age, the acidity within lysosomes, and altered gene expression led to increased activity of β-galactosidase. This enzyme specifically acts on a substrate called 5-bromo-4-chloro-3-indolyl β-D-galactoside (X-gal), which is cleaved by β-galactosidase present in senescent cells. The cleavage of X-gal generates a blue-colored precipitate, serving as an indicator for the presence of senescent cells. This staining can be observed under a microscope or quantified using biochemical assays and flow cytometry techniques (Dimri et al., 1995).

1.7.3.2. Senescence-associated secretory phenotype (SASP) factors

The SASP consists of a range of molecules secreted by senescent cells as mentioned in *Section 1.7.1.9*. Senescent cells exhibit an elevated release of these factors, making them useful biomarkers for identifying and characterizing senescence. The levels of SASP factors can be quantified using techniques such as quantitative reverse transcription polymerase chain reaction (qRT-PCR), Enzyme-Linked Immunosorbent Assay (ELISA), or Western Blotting (Coppé et al., 2008).

1.7.3.3. DNA damage markers

Senescent cells exhibit elevated levels of DNA damage. Specific markers, such as phosphorylated histone H2AX (γ-H2AX) or 8-oxo-2'-deoxyguanosine (8-oxo-dG), can be used to detect DNA damage in senescent cells through immunostaining or biochemical assays (Rogakou et al., 1998; Chen et al., 2015).

1.7.3.4. Telomere length

Telomeres, which protect the ends of chromosomes, gradually shorten with each cell division. Measuring telomere length can serve as a biomarker for cellular aging and senescence. Techniques like qRT-PCR or fluorescence in situ hybridization (FISH) are used to assess telomere length (von Zglinicki, 2002; Fumagalli et al., 2012).

1.7.4. Early and Late Senescence

When human cells enter an early stage of senescence, they activate specific pathways that act as protective mechanism against uncontrolled cell growth. These pathways, such as the p53 and p16INK4a pathways, halt the cell cycle and promote the expression of genes associated with senescence (Alessio et al., 2023). In this early stage, the nucleus of the cell maintains its structure, and the arrangement of chromatin, remains relatively intact (Sun, Yu and Dang, 2018).

As senescence progresses to a later stage, there are notable changes at the molecular level. The cell undergoes significant modifications to its chromatin structure, resulting in the formation of condensed regions known as SAHF. These foci display specific chemical marks on histones and DNA itself, contributing to the irreversible growth arrest and decreased gene activity observed in late senescence (Criscione, Teo and Neretti, 2016).

In addition, late senescent cells exhibit a distinct secretory behavior referred to as the SASP. The SASP factors can affect neighboring cells and the surrounding microenvironment, influencing tissue maintenance, immune responses, and potentially contributing to age-related conditions (Coppé et al., 2010; Alessio et al., 2023).

Along with changes in gene expression profiles (Marthandan et al., 2015, 2016), the non-coding portion of the genome also undergoes modifications during senescence. Specifically, there are alterations in non-coding RNA transcripts, particularly in satellite regions as observed in RNA-seq data. These findings shed light on the complex regulatory landscape of senescence and hint at the involvement of non-coding elements in this process (Karakülah and Yandim, 2020).

1.8. γ-H2AX: A Crucial Player Linking DNA Damage and Senescence

Cellular senescence is intrinsically associated with the accrual of DNA damage, and γ-H2AX serves as a vital molecular player in signifying this DNA damage. Cells on the path to senescence often exhibit persistent γ-H2AX foci, which act as a telltale sign of their journey towards the senescent state. These foci represent regions in the genome where DNA DSBs, have occurred. The presence of γ-H2AX

foci in senescent cells underscores the substantial genomic stress they have undergone, reflecting the intricate interplay between DNA damage and senescence (d'Adda di Fagagna, 2008).

Beyond its role as a mere marker, γ-H2AX potentially wields influence over several key senescence-associated processes. One notable facet is its involvement in triggering and sustaining the SASP. While the precise mechanisms governing SASP activation are still a subject of research, γ-H2AX could play a role in initiating or perpetuating this phenomenon (Coppé et al., 2008).

Moreover, senescent cells are characterized by their resistance to apoptosis, a programmed cell death process. γ-H2AX's engagement in DNA damage response pathways might contribute to this resistance. Senescent cells may activate cellular pathways that inhibit apoptosis, potentially involving γ-H2AX in modulating cellular responses to DNA damage and stress, thus aiding in their survival (Childs et al., 2015; Liao et al., 2021).

1.9. Senescence Types

1.9.1. Oncogene-induced Senescence

When certain oncogenes are activated, normal cells undergo a cellular response called oncogene-induced senescence (OIS). This phenomenon was first observed in human fibroblasts when an oncogenic form of RAS was expressed (Serrano et al., 1997). Subsequent studies have identified approximately 50 oncogenes (Gorgoulis and Halazonetis, 2010), including BRAF and MYC, capable of inducing senescence (Novak, 2005; Collado and Serrano, 2010). Loss of tumor suppressor genes such as PTEN, NF1, or VHL can also trigger senescence. OIS acts as a protective mechanism during early stages of tumor development and has been observed in vivo (Muñoz-Espín and Serrano, 2014).

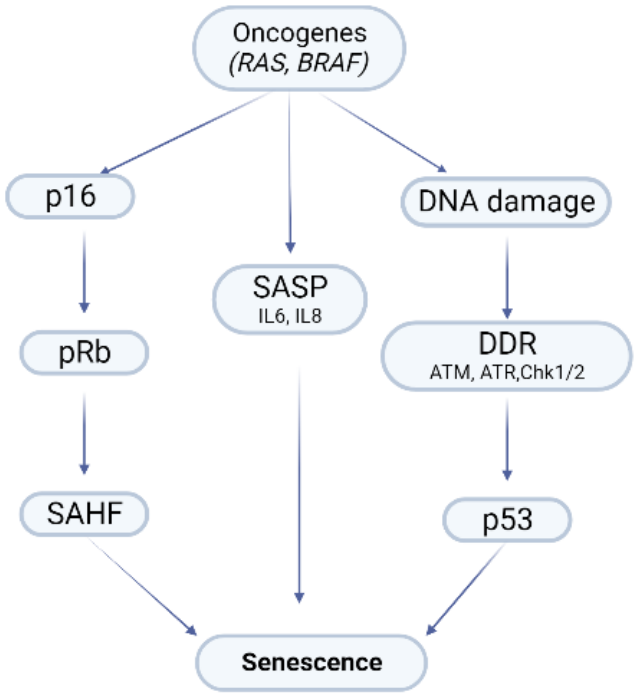

Figure 13. Illustration of the mechanisms involved in oncogene-induced senescence (OIS). Oncogenic stress triggers multiple pathways in response to hyper-replication caused by oncogenes. This leads to the accumulation of DNA damage, which activates the DNA damage response (DDR). The activation of p53, a potent mediator of senescence, is a crucial outcome of the DDR. Key activators of p53 in this response include ATM, ATR, Chk1, and Chk2. Additionally, oncogenes can activate the p16-Rb tumor suppressor pathway, leading to the formation of senescence-associated heterochromatin foci (SAHF). Moreover, oncogenic stress results in the accumulation of reactive oxygen species (ROS), which, when present in excess, can cause DNA damage and trigger the DDR, adapted from (Source: Reddy and Li, 2011).

A key feature of OIS is the derepression of the CDKN2A locus (Muñoz-Espín and Serrano, 2014). Additionally, OIS can activate a robust DDR due to aberrant DNA replication and increased levels of ROS. The specific mechanisms involved, such as p16, ARF, or DDR-induced p53, can vary across different cell types (Rayess, Wang and Srivatsan, 2012; Mijit et al., 2020). In mice, the ARF-p53 pathway plays a crucial role in OIS (Efeyan and Serrano, 2007), whereas in humans, the DDR-p53 pathway appears to be more significant than the ARF-p53 pathway (Halazonetis, Gorgoulis and Bartek, 2008).

Moreover, OIS is associated with changes in chromatin structure and gene expression patterns. It involves alterations in the expression of genes related to cell

cycle regulation, DNA repair, inflammation, and the SASP (Acosta et al., 2013).

1.9.2. Stress Induced Senescence

In stress-induced senescence, a key molecular player is the RAS-RAF-MEK-ERK cascade, which triggers increased intracellular production of ROS. This elevation of ROS levels initiates a chain reaction, activating the p38 MAPK pathway. As a result, the transcriptional activity of p53 increases, upregulating p21, an essential cell cycle regulator. The activation of p53 and subsequent p21expression contribute to cell cycle arrest and the establishment of a senescent phenotype. These complex signaling pathways play integral roles in coordinating the cellular response to stress and ultimately results in the execution of the senescence program (Sun et al., 2007; Muñoz-Espín and Serrano, 2014).

1.9.3. DNA Damage Induced Senescence

DNA damage-induced senescence is a cellular response that occurs when cells experience significant DNA damage, leading to permanent growth arrest or senescence. Multiple types of DNA damage, such as DSBs, oxidative damage, and UV-induced lesions, can trigger senescence. These DNA lesions activate a complex signaling network involving various molecular players, including DNA damage sensors, signaling kinases, and effector molecules such as ATM, ATR kinases, CDKs, p53, p21, p16INK4a/Rb pathways. These include the formation of DNA damage foci marked by γ-H2AX and other DNA damage response factors, chromatin remodeling, activation of DNA repair mechanisms, and the secretion of various factors collectively known as SASP (Chen, Hales and Ozanne, 2007; Muñoz-Espín and Serrano, 2014)

1.9.4. Replicative Senescence

Replicative senescence is a state where cells undergo a permanent halt in their ability to divide and undergo changes in their function. This process is closely linked to the gradual shortening of telomeres. It is controlled by specific genes and is determined by number of cell divisions rather than the passage of time (Campisi, J., Dimri, G., and Hara, 1996).

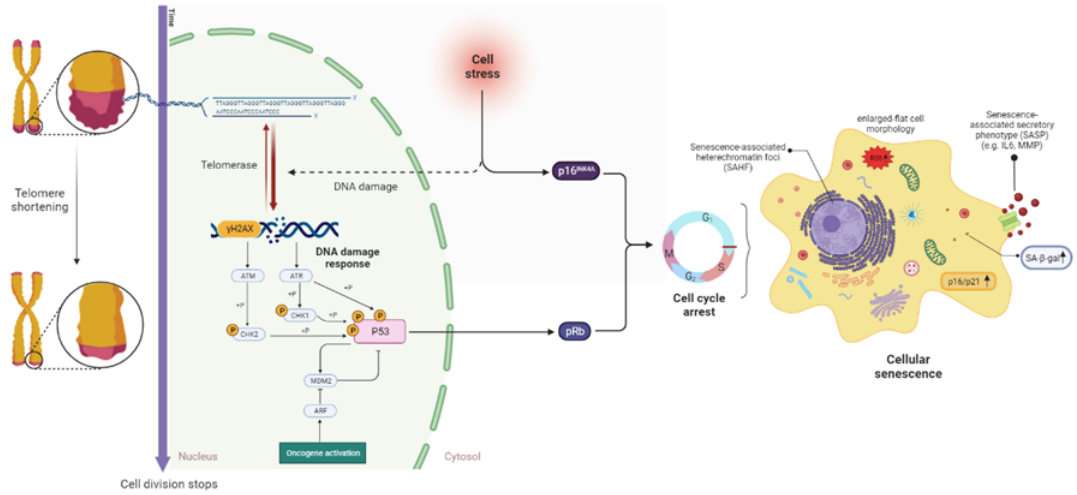

Figure 14. The diagram demonstrates the process of replicative senescence, where the telomere structures at the chromosome ends gradually shorten with each cell division. As telomeres reach a critical length, DDR mechanism gets activated and the cell enters a senescent state, displaying characteristic features (Created with BioRender.com).

During replicative senescence, cells exhibit three distinct characteristics. Firstly, they enter a stable growth arrest phase, typically in the G1 phase. Consequently, they lose the ability to respond to normal growth signals and progress to the S phase. Although senescent cells remain metabolically active and certain genes can still be stimulated by growth signals, the expression of specific cell growth regulators is altered. Second, senescent cells undergo functional changes and resemble terminally differentiated cells due to growth arrest and dysfunction. Lastly, cells become resistant to apoptosis, making them more stable (Campisi, 1996).

1.9.4.1. Replicative Senescence and Telomeres

Telomeres consist of repetitive DNA sequences, primarily TTAGGG in humans, along with associated proteins known as shelterin complex. Shelterin plays a crucial role in protecting telomeres from being recognized as DNA damage sites and prevents activation of DNA repair pathways. It also helps to maintain the structural integrity of telomeres and regulates their length (Victorelli and Passos, 2017).

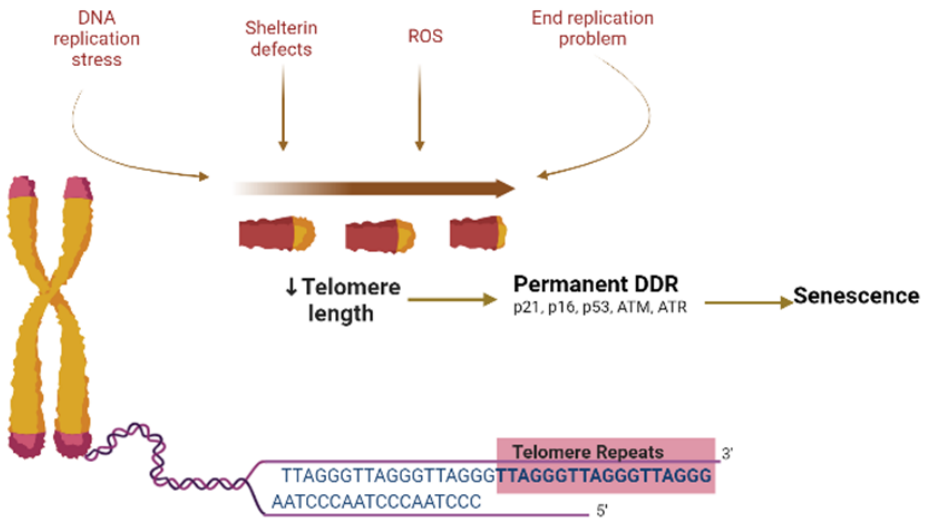

Figure 15. The figure illustrates the relationship between telomere length, DNA damage response (DDR), and the process of senescence. Telomeres, naturally undergo a gradual shortening process due to end replication problem, increased levels of ROS, malfunctioning of shelterin proteins, or exposure to various stressors. This progressive shortening of telomeres ultimately elicits a DNA damage response, triggering the activation of diverse signaling pathways, adapted from (Source: Rutgers Medical School, 2023).

During replicative senescence, the progressive shortening of telomeres causes the shelterin complex to become less stable. As a result, the interaction between shelterin and telomeric DNA weakens, leaving telomeres vulnerable to DNA damage response pathways such as p53, p21, ATM and ATR (Fagagna et al., 2003; Herbig et al., 2006; Jullien et al., 2013).Once activated, these pathways induce the phosphorylation of H2AX, cell cycle arrest, triggering the onset of replicative senescence and effectively halting further cell division (Victorelli and Passos, 2017).

1.9.4.2. Replicative Senescence and Potential Non-Telomeric Triggers

Telomeres have been extensively studied for their role in cellular senescence, particularly in replicative senescence. While telomeres are known to play a significant role, recent studies have revealed that DNA damage occurring during replicative senescence is not limited to telomeres alone. Researchers have used fibroblasts as a model to investigate natural replicative senescence to detect DNA damage occurring in regions of the genome beyond telomeres, techniques such as immunofluorescence and telomere fluorescence in situ hybrid staining have been used. The findings from these studies suggest that DNA damage can occur in regions of the genome other than telomeres during replicative senescence (Nakamura et al., 2009).

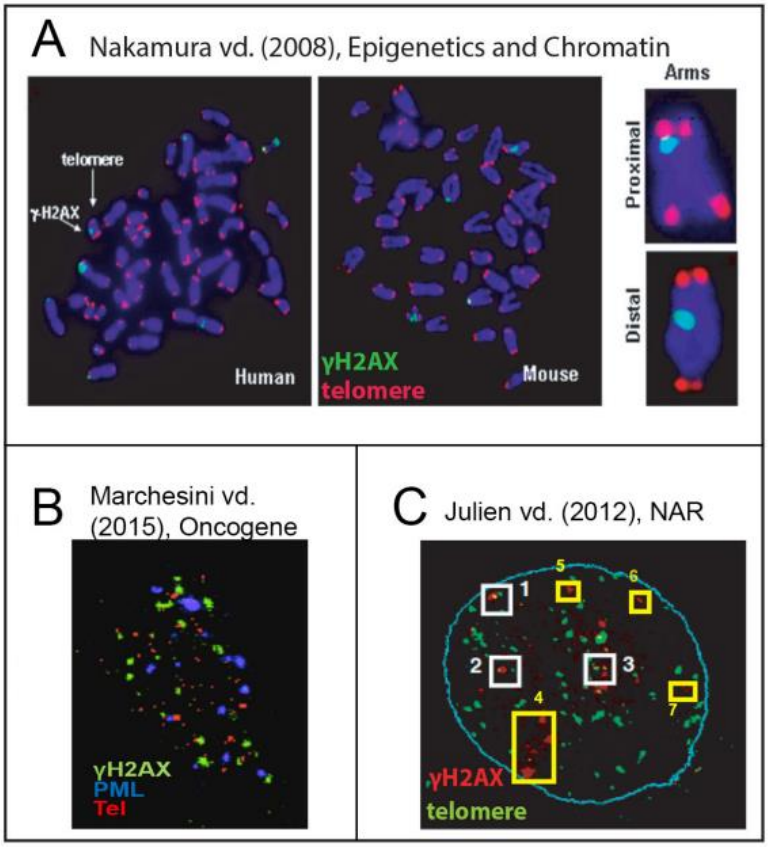

Figure 16. Endogenous DNA damage in non-telomeric regions during replicative senescence. Immunofluorescence staining images presented in the figure were obtained from the mentioned publications. All images belong to different fibroblast cell lines. (A) Nakamura *et al*. (2008) demonstrated γ-H2AX DNA damage localized in chromosomal arms of senescent-like fibroblasts, which do not overlap with telomeres (Nakamura et al., 2008). (B) Marchesini *et al*. (2015) and (C) Jullien et al. (2012) conducted DNA damage and telomere staining studies that support this finding. In panel C, telomeric DNA damage is indicated by white boxes labeled as 1, 2, and 3, while DNA damage not overlapping with telomeres is shown by yellow boxes labeled as 4, 5, 6, and 7.

Furthermore, researchers have been investigating the role of repeat elements in the process of replicative senescence. It is understood that alternative DNA structures can impede the accurate replication of repetitive DNA sequences, and they are often associated with mechanisms involved in mismatch repair (Iyer et al., 2015; Massey and Jones, 2018). Several studies have demonstrated that replication under stress can result in imbalances in microsatellites (Matsuno et al., 2019). Notably, certain repeat elements, such as HSAT II and HSATIII, have been implicated in cancer development and aging, respectively (Ting et al., 2011; De Cecco et al., 2013; Ershova et al., 2019).

Also, the activity of the transposon L1, as well as other retrotransposable elements, has been reported to contribute to inflammaging, a state of chronic inflammation during aging in mice (De Cecco et al., 2019). In addition, other repetitive regions play a crucial role in shaping chromosome structure and regulating chromatin dynamics. These regions have the capacity to form different DNA structures like G-quadruplexes, hairpin loops, and triplex DNA. However, the formation of these structures can present challenges during DNA replication, potentially causing expansions or contractions of these repetitive sequences as cells divide over time (Mirkin, 2007; Gadgil et al., 2017). Changes in the length of these repeats have been linked to various diseases, especially neurological disorders and different types of cancer. Investigating the impact of DNA damage in these specific genomic regions can offer valuable insights into the mechanisms that drive cellular senescence and may contribute to the development of age-related diseases and cancer (Bonneville et al., 2017; Nojadeh, Behrouz Sharif and Sakhinia, 2018).

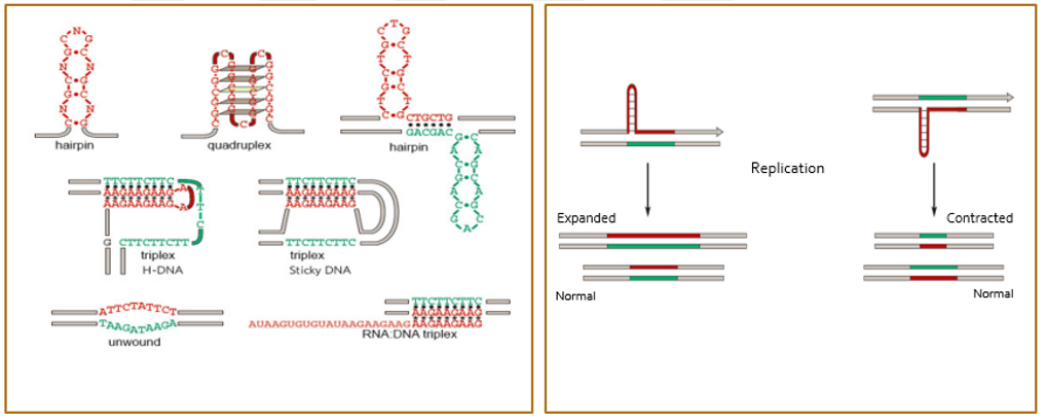

Figure 17. Overview of the various segments comprising the human genome. Alternative DNA structures (Source: Lander et al., 2001; Gregory, 2005; Mirkin, 2007).

Repetitive DNA, including microsatellites and HSATIII, can cause not only mispairing damage but also double-strand breaks due to alternative DNA structures and problems at the replication fork (Argueso et al., 2008; Shastri et al., 2018). In yeast cells, elongated microsatellites have been shown to arrest the cell cycle, but similar studies in mammals are lacking (Sundararajan and Freudenreich, 2011). Additionally, certain classical satellites and microsatellites have been found to exhibit changes in RNA expression levels as cells age (Karakülah and Yandim, 2020).

Despite these findings, there is still a lack of comprehensive genome-wide studies covering the entire genome and examining a wide range of repeat motifs.

Currently, no DNA sequences other than telomeres have been identified as directly associated with aging, despite the occurrence of non-telomeric DNA damage during the aging process. Furthermore, it remains unclear whether microsatellite imbalances are a consequence or a contributing factor to aging.

1.10. Next Generation Sequencing Technologies

Following the completion of the Human Genome Project, the field of genomics experienced remarkable advancements, primarily driven by the emergence of next-generation sequencing (NGS) technologies. NGS platforms, such as Illumina sequencing, Ion Torrent's semiconductor sequencing, Oxford Nanopore and Pacific Biosciences' single-molecule real-time sequencing, revolutionized the field by enabling faster, more cost-effective, and high-throughput sequencing of entire genomes. These state-of-the-art technologies has enable to sequence millions to billions of short DNA or RNA sequences in a single run, facilitating the detection of genetic variations, including single nucleotide polymorphisms (SNPs), insertions, deletions, and structural variations, with increased precision and resolution (Lander et al., 2001; Mardis, 2008; Metzker, 2010).

In Illumina sequencing, the 3’-OH group of ribose is blocked to prevent the elongation process. The process begins with the genomic DNA being cleaved into small pieces and linked by unique sequences for amplification and sequencing. These pieces also have a unique barcode that allows multiple samples to be sequenced. The prepared DNA fragments are then placed on a surface called a flow cell, where they bind to specific molecules.

Next, the DNA fragments are amplified and are spread out across the flow cell surface. This process creates clusters of identical DNA fragments through a technique called bridge amplification. Each cluster contains thousands of copies of the same segments of DNA.

The actual sequencing takes place through a series of cycles. In each cycle, a single nucleotide is added to the DNA fragments, and its presence is detected through a fluorescent signal. After detection, the fluorescent label is removed to prepare for the next cycle. By analyzing the order of nucleotide additions and the emitted signals, the DNA sequence is determined.

Illumina sequencing is known for its accuracy, with very low error rates per base. It also has the advantage of generating many reads in a single run, ranging from millions to billions, depending on the specific Illumina platform. This high throughput

makes it suitable for various applications, including whole genome sequencing, transcriptome analysis, DNA methylation studies, ChIP-seq, metagenomics, and more (Mardis, 2008; Morozova, Hirst and Marra, 2009; Goodwin, McPherson and McCombie, 2016).

1.10.1. Whole Genome Sequencing

Whole genome sequencing (WGS) is a powerful technique used to decipher the complete DNA sequence of an organism's genome. It involves the determination of the order of nucleotides in the entire genome, including both coding and non-coding regions. WGS provides a comprehensive overview of an individual's or a species' genetic composition, enabling the identification of variations and mutations across the entire genome (Lander et al., 2001).

The process of whole genome sequencing typically involves the following steps: DNA extraction, library preparation, sequencing, and data analysis. Initially, DNA is extracted from the organism under study, be it a human, plant, or microorganism. Subsequently, the DNA is fragmented into smaller pieces to facilitate the sequencing process. These fragments are then sequenced using high-throughput sequencing technologies, such as next-generation sequencing NGS platforms.

Once the sequencing is complete, the generated reads are computationally analyzed. They are either aligned to a reference genome or assembled de novo into a new genome. Alignment involves matching the short reads to a reference sequence, allowing for the identification of genetic variations, including single nucleotide polymorphisms (SNPs), insertions, deletions, and structural variants. Advanced bioinformatics tools are utilized to handle and interpret the vast amount of sequencing data, extracting valuable genomic information (Kim et al., 2009; Goodwin, McPherson and McCombie, 2016).

1.10.2. Chromatin-immunoprecipitation Sequencing

To fully understand how genes are regulated, it is important to map the interactions between proteins and DNA as well as identify epigenetic marks throughout the entire genome. This allows us to accurately determine where transcription factors, core transcriptional machinery, histone modifications, and other DNA-binding proteins bind, revealing the complex networks that control various biological processes (Barski et al., 2007; Henikoff, 2008; Jiang and Pugh, 2009). Chromatin immunoprecipitation (ChIP) is the primary technique used to study these mechanisms and enables us to examine protein-DNA interactions across the entire

genome. By combining ChIP with high-throughput sequencing, detailed map of these interactions and marks can be generated.

The process of ChIP-seq involves several steps. First, cells or tissues are treated with a cross-linking agent to preserve the interactions between proteins and DNA. The chromatin, which contains DNA and associated proteins, is then fragmented into smaller pieces using methods like sonication or enzymatic digestion. This generates DNA fragments that specifically capture regions where proteins are bound. Antibodies specific to the protein of interest are utilized to selectively immunoprecipitate the protein-DNA complexes. Afterwards, the protein-DNA complexes are separated, and the cross-links between proteins and DNA are reversed, freeing the DNA fragments.

The isolated DNA fragments are then sequenced using high-throughput methods, producing millions of short sequences reads. These sequence reads are then aligned to a reference genome using bioinformatics tools. By analyzing the distribution and frequency of the aligned reads throughout the genome, the genomic regions where the protein of interest binds can be identified.

ChIP-seq provides valuable insights into how genes are regulated, the modifications that occur on histones, and the functional annotation of the genome (Park, 2009; Nakato and Sakata, 2021).

1.11. Hypothesis of the Study

During the natural process of cell division, somatic cells undergo genetic and metabolic changes that contribute to replicative senescence. One of the key changes is the progressive shortening of repetitive DNA sequences called telomeres located at the ends of chromosomes. This phenomenon activates DNA damage repair mechanisms, specifically those involved in addressing double-strand DNA breaks. Notably, the occurrence of DNA damage extends beyond telomeric regions, as indicated by prior studies (Nakamura et al., 2008; Jullien et al., 2013; Marchesini et al., 2016), although the specific genomic regions affected, and the spontaneous nature of such damage remain unexplored. Based on these observations, this thesis puts forward the following hypothesis: Endogenous DNA damage occurring during replicative senescence is not restricted to telomeres alone, other specific regions that likely to mutate during cellular aging may be vulnerable to DNA damage including gene-rich regions, and repetitive DNA.

1.12. Aims of the Study

The primary objective of this thesis is to map endogenous DNA damage during replicative senescence, identifying regions of the human genome vulnerable to DNA damage. This will be achieved through the utilization of immunofluorescence techniques, allowing for the simultaneous detection of γ-H2AX, a marker of DNA damage, and telomeres. Furthermore, this study aims to identify specific repetitive DNA motifs that contribute to DNA damage in senescent cells by using ChIP-sequencing technology.

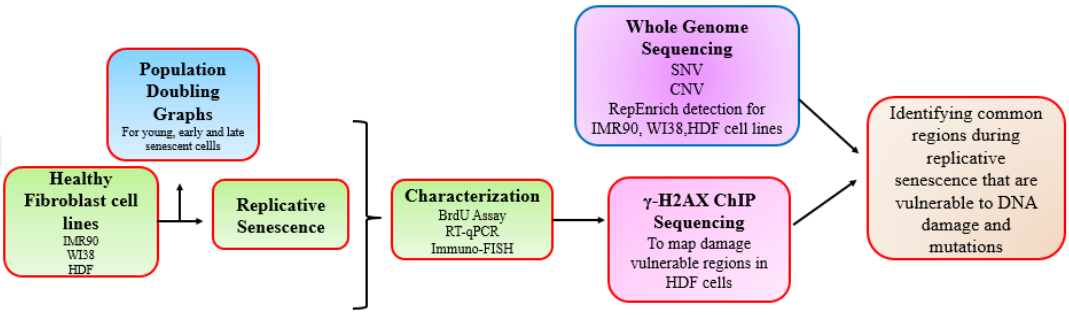

Figure 18. Schematic representation of the methods used in this thesis.

CHAPTER 2: METHODS

2.1. Cell Culture

IMR-90 (embryonic lung fibroblast, CCL186), WI-38 (embryonic lung fibroblast, CCL75) cells were purchased from ATCC and HDF (neonatal dermal fibroblast, C0045C) cell line was purchased from Gibco. Cells were cultured in low glucose Dulbecco's modified Eagle medium (DMEM) supplemented with 10% heat inactivated fetal bovine serum (FBS), 1% penicillin-streptomycin (P/S) and 2mM L-Glutamine in humidified atmosphere (37°, 5% CO_2 incubator). When they reached 90% confluence, they were rinsed with 1X Phosphate-buffered saline (PBS) and detached by using trypsin-EDTA. After trypsinization, detached cells were collected with 5 ml of complete DMEM and centrifuged at 300xg for 5 minutes at room temperature. The supernatant was then discarded, the pellets were suspended in complete DMEM and split 1:4. For cell culture experiments, cells were counted using trypan blue.

Senescent cells were generated by allowing cell cultures to reach the point of replicative exhaustion, which typically occurred after approximately 50-52 passages. The progress of cell division was monitored daily using microscopy. Once cell replication ceased, the cultures were incubated for an additional period of 6-8 weeks before the cells were harvested.

2.1.1. Cryopreservation of stock cells

To create a chronological cell stock collection, at least 1 plate of cell pellets from each passage were frozen. Firstly, cells were washed 1X PBS, detached with trypsin-EDTA and recovered by 5 mL of complete DMEM after trypsin treatment. They were the centrifuged at 300xg for 5 minutes and the pellet was resuspended in 1 mL of freezing medium containing complete DMEM and 10% DMSO. Each cell suspension was transferred to freezing vials. Cells were left at -80° C in isopropanol box overnight and then transferred to -80° C fridge. For long term storage, cells were transferred to nitrogen tank.

2.1.2. Thawing of frozen cells

One vial of the cells was placed into water bath at 37° C until the ice became a cell suspension. Then, the fibroblast cells were gently resuspended and transferred to a 15 mL falcon tube with 10 mL of DMEM. Cells were then centrifuged at 300xg for 5 minutes to completely remove DMSO. The supernatant was removed, and the pellet

was then resuspended in complete culture medium. Cells were seeded into cell-culture dishes and incubated for 24 hours at 37°, 5% CO_2 incubator. Next day, the culture medium was refreshed.

2.2. BrdU Staining Flow Cytometry

The nucleotide analog BrdU incorporation and staining is a method frequently used in cell aging and proliferation studies (Itahana, Campisi and Dimri, 2007; Schorl and Sedivy, 2007; De Cecco et al., 2019). Anti-BrdU (FITC) antibody staining was performed following BrdU incorporation to show the proliferation rate of fibroblast cells and thus to distinguish early senescence and late senescence stage cells. The protocol was prepared based on the manufacturer's guidelines (eBioscience™ BrdU Staining Kit for Flow Cytometry FITC- Catalog Number: 8811-6600). Any deviations from the guideline have been given with corresponding literature (Dolbeare et al., 1983). For this protocol, cells were seeded at 30% confluency in 10-cm cell culture dishes and allowed to attach for 24 hours. Next day, 10 uμ BrdU was added to each dish to label dividing cells and cells were incubated for 48 hours at 37 ℃, 5% CO_2 (Hewitt, von Zglinicki and Passos, 2013). After the incubation, cells were harvested with trypsin-EDTA and centrifuged for 5 minutes at 300xg. Supernatant was removed, and cells were washed with 2 mL of staining buffer (1X PBS with 5% FBS) then centrifuged at 400xg for 5 minutes. Following centrifugation, cells were resuspended in 300 µl PBS and 100 µl of each cell suspension was aliquoted to eppendorf tubes. After gently vortexing the cell suspensions, 1ml of 1X BrdU Staining Buffer working solution which includes 250 µl of Buffer Concentrate + 750 µl of Fixation/Permeabilization Diluent was added. This mixture was incubated for 20 minutes at room temperature in the dark. Cells were then washed twice with 500 µl of staining buffer at 5000xg for 3 min. Later, the supernatant was discarded and 100 µL of the DNase I working solution (700 µL of 1X PBS with 5% FBS) was added to each pellet. Samples were incubated for 1 hour at 37°C in the dark. Following the incubation, cells were washed twice with staining buffer at 5000xg for 3 min. For each cell, 75 µl of staining buffer containing 5 µl of Anti-BrdU fluorochrome-conjugated antibody was added to the cell pellets and incubated for 30 minutes at room temperature in the dark. Afterward, cells were washed twice with staining buffer at 5000xg for 3 min and resuspended in 500 µl staining buffer. Finally, data were collected and analyzed with 488 nm excitation. The cell population was determined in the forward and sideways scatter dot plot, and dead cells were excluded from the

analysis. Events were depicted in a green fluorescence histogram compared to the unstained control, where the y-axis indicates cell number, and the x-axis indicates BrdU fluorescence intensity on a log scale.

2.3. Immuno-FISH

γ-H2AX immunofluorescence staining was performed to show telomere shortening and DNA damage in the young, early senescent, and late senescent fibroblasts, and telomeres were also marked by fluorescent in situ hybridization (FISH) (Marchesini et al., 2016). Here, a specially developed DNA-FISH protocol was performed simultaneously with immunofluorescent staining (Chaumeil, Micsinai and Skok, 2013). First, 12 mm glass coverslips were sterilized on day 1 and inserted in 12-well plates. Fibroblast cells were seeded in the 12 well-plates with coverslips at a density of $4x10^4$ cells per well and incubated for 48 hours. On day 3, the medium was aspirated, and the cells were washed twice with 500 µl of PBS for 2 minutes each. Cells were then fixed with 500 µl of freshly made 4% (v/v) formaldehyde in 1X PBS. After 10 minutes of incubation at room temperature, formaldehyde was removed, and cells were washed three times for 5 minutes at room temperature with 500 µl of PBS. The fixed cells were then permeabilized with 500 µl of 0.5% (v/v) Triton-X + 0.5% (w/v) Saponin in PBS solution and incubated for 30 minutes at room temperature. Cells were then washed with 500 µl PBS three times and blocking was performed by treating them with 200 µl 1x PBG (2% (v/v) fish gelatin + 5% (w/v) BSA in PBS) containing 100 µg/ml RNAseA solution (Thermo Fisher Scientific, EN0531) for 1 hour at room temperature. Again, cells were washed three times with 500 µl of PBS. After blocking, the coverslips were transferred to a humidity chamber (150 mm petri dish with moist blotting paper + parafilm sheet) placed on parafilm cell side up and incubated with 150 µl of γ-H2AX primary antibody (Abcam, ab81299, 1:250) diluted in 1x PBG overnight at 4°C. On day 4, the primary antibody solution was removed, and the cells were washed 5 times with 100 µl of PBST (PBS + 0.1% (v/v) Tween-20) at room temperature and each wash was performed for 5 minutes. 150 µl of 0.3 µg/µl secondary antibody (Abcam, ab150080) diluted in 1x PBG were added and incubated for 30 minutes at room temperature in the dark. The cells were then washed 5 times with 100 µl of PBST at room temperature and each wash was performed for 5 minutes. For refixation of cells, 150 µl of freshly made 4% (v/v) formaldehyde in 1X PBS was added at room temperature and incubated for 10 minutes. Cells were also re-permeabilized with 0.2% (v/v) Triton + 0.2% (w/v) Saponin in 1X PBS for 10 minutes

at room temperature. Following the addition 10 mM glycine in deionized water, the cells were incubated for 30 minutes at room temperature and washed 3 times (5 minutes each) with 100 µl of 1x PBS. The coverslips were dehydrated for 5 minutes with 100 µl of 70%, 85%, and 100% cold ethanol, respectively, and then air-dried. For each slide, 200 nM PNA probe (PNA Bio,) was prepared in 20 µl of hybridization buffer (1M Tris-HCl + 60% (v/v)) Formamide (BioBasic, FB0211) + 0.5% Blocking reagent (Roche, 11096176001)) and heated at 85°C for 5 minutes. Next, the hybridization buffer was placed on pre-warmed slides and covered with a coverslip containing cells (cell side down). The slides with coverslips were sealed with a heat resistant liquid rubber and they were heated at 85°C for 10 minutes. The slides were then placed in the humidity chamber for 2 hours at room temperature in the dark. Following the hybridization step, coverslips were removed from the slides cell side up and placed on parafilm to perform washing. Cells were washed twice (15 min each) with wash solution I (10% BSA (v/v) + 1M Tris-HCl + 70% (v/v) Formamide) and then 3 times (5 min each) with wash solution II (1M Tris-HCl + 5M NaCl + 1% (v/v) Tween-20). Mounting media with DAPI (Abcam, ab104139) was added to the slides and the coverslip with the cells was placed inside these slides. The coverslips on the slides were sealed with nail polish and allowed to dry in the dark for approximately 30 minutes. The slides were stored at 4°C until the next day. On day 5, cells were visualized with a confocal microscope (Zeiss LSM880, Jena Germany).

2.4. Real Time- Quantitative PCR (RT-qPCR)

For qPCR analysis, 70% confluent fibroblast cells were rinsed with PBS, detached by using trypsin-EDTA and centrifuged for 5 minutes at 300xg. Then, total RNAs of the cells were extracted using Macherey-Nagel™ NucleoSpin™ RNA Mini Kit (Macherey-Nagel, 740955.50) according to manufacturer's instructions.

For cDNA synthesis, 1 µg of isolated total RNA was reverse transcribed using OneScript® Plus cDNA Synthesis Kit (Abm, G236) with oligo dTs and the qPCR reaction was performed in 96-well plates using BlasTaq™ 2X qPCR Master Mix (Abm, G891). Relative expression levels of p53, p16, p21, IL6, MMP1 and MMP3 genes were analyzed by using CFX Connect Real-Time PCR Detection System (Bio-Rad Laboratories), normalized to β-Actin, and calculated by Livak method (Livak and Schmittgen, 2001). Each experiment was performed in biological and technical triplicates. Data was expressed as mean ± standard error and analysis of significance

was performed with student's t-test using the GraphPad Prism 8.0 software for Windows (GraphPad Software, La Jolla California USA, www.graphpad.com).

Table 1. RT-qPCR protocol.

Stages	Temperature (°C)	Time (second)	Number of Cycles
Enzyme Activation	**95**	**300**	**1**
Denaturation	**95**	**30**	**40**
Annealing	**58**	**30**	
	72	**30**	
Melt Curve	**65 to 95**	**5**	**1**

Table 2. Primer Sequences

IL6	*TTCGGTCCAGTTGCCTTCTC*	*TGTTTTCTGCCAGTGCCTCT*
IL8	*GTTTTTGAAGAGGGCTGAGAATTC*	*CCCTACAACAGACCCACACAATAC*
MMP1	*AGTGGCCCAGTGGTTGAAAA*	*GCATGGTCCACATCTGCTCT*
MMP3	*GGCAAGACAGCAAGGCATAG*	*CCCGTCACCTCCAATCCAAG*
p21	*AGTCAGTTCCTTGTGGAGCC*	*CATTAGCGCATCACAGTCGC*
p53	*TGAAGCTCCCAGAATGCCAG*	*ACATCTTGTTGAGGGCAGGG*
p16	*CGGAAGGTCCCTCAGACATC*	*CCCTGTAGGACCTTCGGTGA*
ACTB	*AAGGATTCCTATGTGGGCGAC*	*CGTACAGGGATAGCACAGCC*

2.5. Western Blotting

When cells were reached 70% confluency, they were washed twice with PBS and collected with trypsin. Then they were lysed with lysis buffer including phosphatase and protease inhibitors. Then, they were sonicated by using Q125 Sonicator (Q Sonica, Q125-110, U.S.A.) with 50% amplitude for 25 seconds for three times. The samples were incubated for 30 seconds on ice between pulses. The lysates were clarified by centrifugation at 16.000xg for 15 min at 4°C, and the supernatant was transferred to a new tube. Concentrations of protein lysates were measured by using Bio Rad DC protein assay kit (Bio-Rad Laboratories, 5000111) utilizing spectrophotometer at 750 nm. Sample protein concentrations were normalized in accordance with bovine serum albumin (BSA) protein of a known concentration. Then,

4X Laemli buffer (Bio-Rad Laboratories, 161-0747) was added to the proteins and they were heated at 100°C for 5 min. Then, 50 µg of samples were loaded onto 5-8% polyacrylamide gel and run at 100 Volt for 90 min. Then, proteins were wet-transferred onto PVDF membranes and the membranes were blocked for 1 hour at room temperature with 5% nonfat dry milk in TBST. Membranes were incubated with the Beta-actin (Cell Signaling Technology, 4970S, 1:5000), p21 (Cell Signaling Technology, 2947S, 1:1000) and γ-H2AX (Abcam, ab81299, 1:5000) primary antibodies overnight at +4ºC. Following primary antibody incubations and extensive washing with TBST, secondary antibodies conjugated with horse-radish peroxidase (HRP) (Cell Signaling Technology, 7074S, 1:5000) were incubated 2 hours at room temperature. After washing the membrane with TBST for three times, chemiluminescent reaction was detected using ECL+ western blot detection kit (ABclonal, RM02867) according to the manufacturer's protocols. The emitted chemiluminescence, duration depends on the specific antibody. Images were acquired with the Vilber Fusion Solo S optical system (Vilber Lourmat, France).

2.6. DNA isolation

DNA of fibroblast cells, previously characterized as young, early senescent, and late senescent, was isolated to perform next generation whole genome sequencing. Fibroblast cells were seeded at a density of $3x10^6$ cells per dish and rinsed with PBS, detached by using trypsin-EDTA. Cells were centrifuged at 300xg for 5 minutes before the isolation. Isolation was performed using the Invitrogen™ PureLink™ Genomic DNA Mini Kit (Thermo Fisher Scientific, K182001) according to the manufacturer's instructions. The concentrations of isolated DNAs were measured with the Maestro Nano spectrophotometer (MaestroGen, MN-917, Thaiwan) and qualities were checked with agarose gel electrophoresis.

2.7. Library Preparation

In this study, the PCR-free Library (Treangen and Salzberg, 2011) approach was used instead of the polymerase chain reaction (PCR)-based sequence library since, the PCR-free Library method is more suitable for analyzing repetitive DNA sequences. For library preparation, the Illumina Truseq PCR-free Library Preparation Kit was utilized, which requires 1-2 µg of genomic DNA sample.

2.8. The chromatin immunoprecipitation (ChIP) sample preparation

The chromatin immunoprecipitation (ChIP) method was applied with γ-H2AX antibody, a double-stranded DNA damage marker, to map endogenous DNA damage occurring in young, early senescence, and late senescence stages in HDF cells. ChIP assay was performed using SimpleChIP® Plus Enzymatic Chromatin IP Kit with Magnetic Beads (Cell Signaling Technology, 9005) according to the manufacturer's protocol and any deviations from the guideline have been given. Firstly, cells were seeded at a density of $2x10^6$ cells per dish and for each analysis $8x10^6$ cells were used. For fixation and crosslinking, 270µl of 37% formaldehyde was added to the cell culture dishes containing complete DMEM. Then, 2 ml of 10X glycine was added to the dishes and swirled to mix, incubated for 5 minutes. The media with formaldehyde and glycine was removed and cells were washed twice with 10 ml of ice cold 1X PBS. After the addition of 1 ml ice cold PBS containing 5µl of 200X Protease Inhibitor Cocktail (PIC) to the dishes, the cells were scraped and all the dishes from the same sample were combined into a 15 ml conical tube. They were then centrifuged at 2,000xg for 5 minutes at 4°C and the supernatant was removed. Cells were resuspended in 1 ml ice-cold 1X Buffer A which supplied with the kit, containing + 0.5µl 1M DTT + 5 µl 200X PIC per IP prep and incubated on ice for 10 minutes by inverting the tube in every 2 minutes. The samples were centrifuged at 2,000xg for 5 min at 4°C. After centrifugation, the supernatant was removed, and the pellet was resuspended in 1 ml of ice-cold 1X Buffer B + 0.55 µl 1M DTT. The centrifugation process was repeated, and the pellet was resuspended in 100 µl 1X Buffer B + DTT. The sample was then transferred to an Eppendorf tube. 0,5 µl of Micrococcal Nuclease (Cell Signaling Technology, 10011) was added to the IP prep, mixed by inverting the tube, and incubated for 20 minutes at 37°C with frequent mixing in the thermo-shaker (Thermo-Shaker, MS100). The digestion process was stopped by adding 10 µl of 0.5M EDTA (Cell Signaling Technology, 7011) and the tube was incubated on ice for 2 minutes. The nuclei were then pelleted by centrifugation at 16,000xg for 1 min at 4°C, and the supernatant was removed. The nuclear pellet was resuspended in 100µl of 1X ChIP Buffer + 0.5 µl 200X PIC and incubated on ice for 10 min. Afterward, 500µl of lysate was sonicated three times to break the nuclear membrane by using Q125 Sonicator (Q Sonica, Q125-110, U.S.A.) with 30% amplitude for 25 seconds. The samples were incubated for 30 seconds on ice between pulses. The lysates were clarified by centrifugation at 9,500xg for 10 min at 4°C, and the supernatant was transferred to a

new tube. This cross-linked chromatin preparation was checked by loading on a hematocytometer, visualized with a microscope, and stored at -80°C until further use. To check the chromatin digestion and concentration, 100µl of nuclease free water, 6 µl 5 M NaCl (Cell Signaling Technology, 7010), and 2µl RNase A (Cell Signaling Technology, 7013) were added to the 50µl of chromatin sample. After incubation at 37°C for 30 minutes, 2 µl Proteinase K (Cell Signaling Technology, 10012) was added to the solution and incubated at 65°C for 4 hours. 10µl of sample was run on a 1% agarose gel. Also, the concentrations of the samples were quantified with the Maestro Nano spectrophotometer (MaestroGen, MN-917, Thaiwan). For chromatin immunoprecipitation, 400 µl of 1X ChIP Buffer + 2µl 200X PIC was prepared and 5µg of chromatin was added to the solution. Then, 10µl of this mixture was transferred to the Eppendorf tube as 2% input and stored at -20°C until further use. Following, γ-H2AX antibody (Abcam, ab81299, 1:250) was added to the remaining precipitate and the samples were incubated overnight at 4°C with rotation. Next day, 30 µl of Protein G Magnetic Beads was added to each sample and, they were incubated for 2 hours at 4°C with rotation. By using a magnetic separation rack (Cell Signaling Technology, 7017), each sample with protein G magnetic beads was pelleted and supernatants were removed. The samples were washed three times with 1 ml of low salt solution for 5 minutes at 4°C with rotation. Then, 1 ml of high salt solution was added to the beads and incubated at 4°C for 5 minutes with rotation. Each sample with protein G magnetic beads was pelleted with the magnetic separation rack, and supernatants were removed. Pellets were resuspended with 150 µl 1X ChIP Elution Buffer and for the chromatin elution, incubated for 30 minutes at 65°C in a thermo shaker at 1,200 rpm. Protein G magnetic beads was pelleted by placing the tubes in the magnetic separation rack. The supernatants were then transferred to new tubes. 150 µl 1X ChIP Elution Buffer was also added to the 2% input samples. 6 µl 5M NaCl and 2 µl Proteinase K (Cell Signaling Technology, 10012) was added to all samples and incubated for 4 hours at 65°C. Then DNAs were purified. For the purification, firstly, 5 volumes of DNA Binding Buffer (Cell Signaling Technology, 10007) were added for every 1 volume of DNA sample. The samples were transferred to a DNA spin column in collection tube and centrifuged at 16,000 x g for 30 seconds. After centrifugation, the liquid in the collection tube was discarded and 750 µl of DNA Wash Buffer (Cell Signaling Technology, 10008) was added to the spin column and centrifuged at 16,000 x g for 30 seconds. The liquid in the collection tube was discarded and 50 µl of DNA Elution

Buffer (Cell Signaling Technology, 10009) was added to each spin column placed into the clean Eppendorf tube. Lastly, the samples were centrifuged at 16,000 x g for 30 seconds to elute DNA and spin column was discarded. The eluate, purified and immunoprecipitated DNA, was stored at -20°C until CHIP-sequencing.

2.9. Agarose Gel Electrophoresis

DNA fragments were separated using agarose gel electrophoresis with standard buffers and loading solutions. Agarose gels with 1% concentration were used for this study. 1 gram of agarose (Sigma, A9539) was dissolved in 100 ml of 1X TAE buffer (BioShop, TAE222.1) and ethidium bromide (Bio Basic, D00197) was added for visualization of the gel. DNA samples were mixed with Loading dye (Ampliqon, A608104) and loaded onto the gel. The 1 kb ladder (Abm, G106) was used to approximate the size and amount of DNA on the gels. The gel was run at 100 Volts for 30-45 minutes using the Owl EasyCast Mini Gel Electrophoresis System (Thermo Scientific, B1A) and images were acquired with the Vilber Fusion Solo S optical system (Vilber Lourmat, France).

2.10. Bioinformatics analysis of ChIP-Sequencing

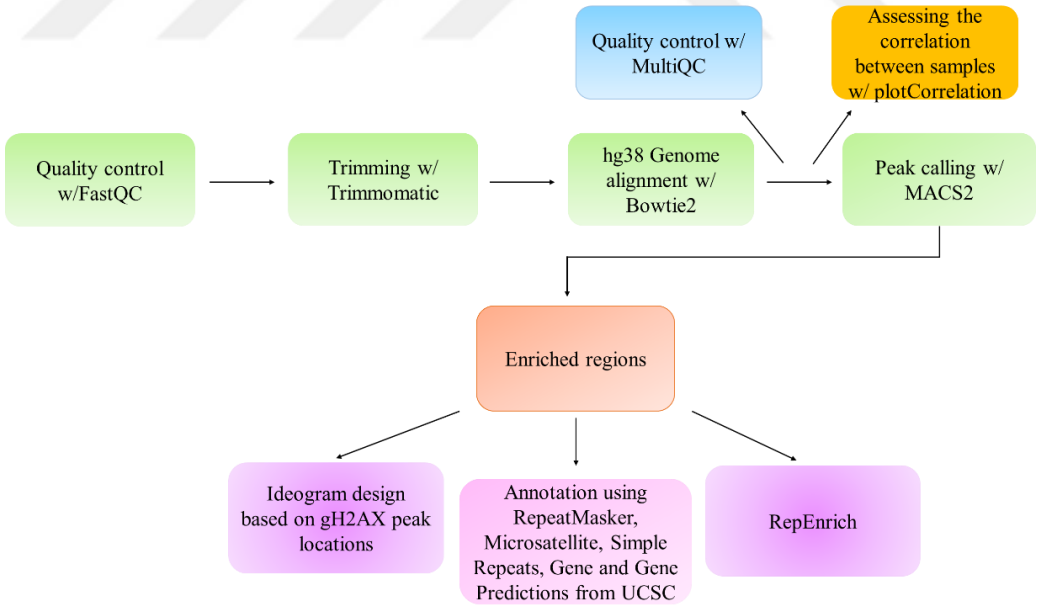

Figure 19. Schematic representation of the methods used for ChIP-seq analysis in this thesis.

The first step involved assessing the quality of the raw sequence reads, which were in fastq.gz format, using Fastq Quality Check (FastQC) (Babraham Bioinformatics, 2023). FastQC is a tool utilized to evaluate the quality of sequence

reads generated by NGS platforms. The quality control procedures conducted in this study involved various checks, such as examining sequence quality scores, detecting overrepresented sequences or adapters, assessing duplication levels, and analyzing sequence length distributions and per-base sequence content.

Next, low-quality reads were removed to eliminate misleading data. Trimmomatic (Bolger, Lohse and Usadel, 2014), a tool designed for Illumina NGS data, was used to remove adapter and illumina-specific sequences in which were in fastq.gz format. Also, the read was scanned with a 4-base wide sliding window, cutting when the average quality per base drops below 20.

The trimmed reads were aligned to the human reference genome GRCh38 (hg38) using Bowtie2 (Langmead and Salzberg, 2012), a widely used short read aligner in NGS analysis. To ensure accurate quality control, MultiQC (Ewels et al., 2016) was applied to the outputs of FastQC, Trimmomatic, and Bowtie2 to provide a comprehensive summary of quality control metrics across all samples and datasets. It provides valuable information on several quality checks, including sequence counts, sequence quality histograms, per-sequence quality scores, per-base sequence content, per-sequence GC content, adapter content, and identification of overrepresented sequences.

Following, to assess the correlation between samples, the QC modules of deepTools (Ramírez et al., 2016), a software program for NGS data analysis, were utilized. The read coverage over multiple genomic regions from each input BAM file obtained after alignment was calculated using the multiBamSummary tool. Pearson correlation between the samples is then computed and visualized using the plotCorrelation tool (Ramírez et al., 2016).

Next, MACS2 (Model-based Analysis of ChIP-seq), a peak caller (Feng et al., 2012), was employed to identify enriched regions (peaks) of γ-H2AX in the data. To perform peak calling, MACS2 first estimates the background signal by using control samples (input). It then scans the ChIP-seq dataset to identify regions where the number of sequencing reads is significantly higher than the estimated background. These regions represent potential binding sites of the γ-H2AX protein. Then, MACS2 models paired peaks, and aligns them based on the midpoint between their centers. In this analysis, a minimum false discovery rate (FDR) cutoff of 0.05 was determined to identify significant regions. Following, histograms were created using ggplot2 (Wickham, 2009) based on these peaks, to compare γ-H2AX peak count and intensity.

Additionally, from the peak calling results, chromosomal ideograms were generated using the NCBI genome decoration page (NCBI, 2017), to visualize the genomic regions enriched with γ-H2AX based on ChIP-seq data.

Furthermore, annotation was performed to provide additional context and information about the identified peaks. To annotate the peaks, firstly the data format was changed to GTF file by using Homer tool (Heinz et al., 2010). Then, by using the "AnnotatePeaks" tool (Heinz et al., 2010), and RepeatMasker (Smit, AFA, Hubley, R & Green, 2015) or GENCODE - Release 43 (GRCh38.p13) (Frankish et al., 2021), γ-H2AX peak scores and locations were identified for different classes of repeats including simple repeats, microsatellites, and centromeric repeats as well as for genes in the GENCODE project. Histograms were created using ggplot2 based on these annotations to compare the peaks from three groups (young, early senescence and late senescence). Peak scores from each group were used to estimate the number of peaks falling into different intensity ranges.

RepEnrich (Criscione et al., 2014) was employed to elucidate the role of repetitive elements in genetic regulation, particularly in the context of their interaction with γ-H2AX and their distribution across the genome. RepEnrich facilitates this analysis by utilizing the Bowtie1 aligner to map sequence reads to the genome for both trimmed ChIP and input samples. It distinguishes reads that exhibit unique genomic mappings, classifying them into various subfamilies of repetitive elements based on their overlap with genomic instances annotated by RepeatMasker (Smit, AFA, Hubley, R & Green, 2015). In cases where reads map to multiple locations, RepEnrich conducts separate mappings to repetitive element assemblies, which are constructed from genomic instances annotated by RepeatMasker for distinct repetitive element subfamilies.

Lastly, to explore the relationships and interactions among genes that have γ-H2AX enrichment, ShinyGO v.0.76.3 was employed. ShinyGO (Ge, Jung and Yao, 2020), a powerful analytical tool for gene-ontology analysis. For the analysis, a minimal size of genes annotated by Ontology term for testing of 10, a maximal size of genes annotated for testing of 2000 with the FDR cutoff as 0.05. Since there were fewer than 5 genes found in each gene group for young cells, the young cells did not pass the filter and their results were not included.

CHAPTER 3: RESULTS

3.1. Replicative Lifespan and Senescence Characteristics of Fibroblast Cell Strains

The replicative behavior of fibroblast cells was monitored during passaging into senescence. Senescent cells were generated by allowing cell cultures to reach where they stop dividing. In analysis, cell strains from a single vial were used and they maintained in culture as at least triplicates from the beginning until they reach senescence. The population doubling (PD) graphs were prepared according to the PD they arrive the laboratory. For IMR-90 fibroblasts, the start PD was 27 for fresh vials ordered from ATCC. For WI-38, the start PD was 32 ordered from ATCC. For HDF fibroblasts, the start PD was 18 for fresh vials. The cell strain specific transition into senescence of each of the fibroblast cell strains was detected by using immuno-FISH staining, BrdU labeling and observation under microscopy.

The starting of senescence was earliest in IMR-90 strains during their span in culture compared to the other fibroblast cell strains. Indeed, HDF fibroblasts showed the most extended replicative lifespan.

Three specific time points were determined for each cell line on the population doubling graphs (Figure 21). These time points include young cells (early PD) at the initial stage of linear PD growth, early senescent cells (middle to late PD) during the start of senescence, late senescent cells (late PD) at the advanced stage of senescence with limited growth. Since the growth rate of each strain differs, the PD values that they are considered as young, pre-senescent, early senescent and late senescent also differ. In the experiments, cells at the young, early senescent, and late senescent stages were utilized.

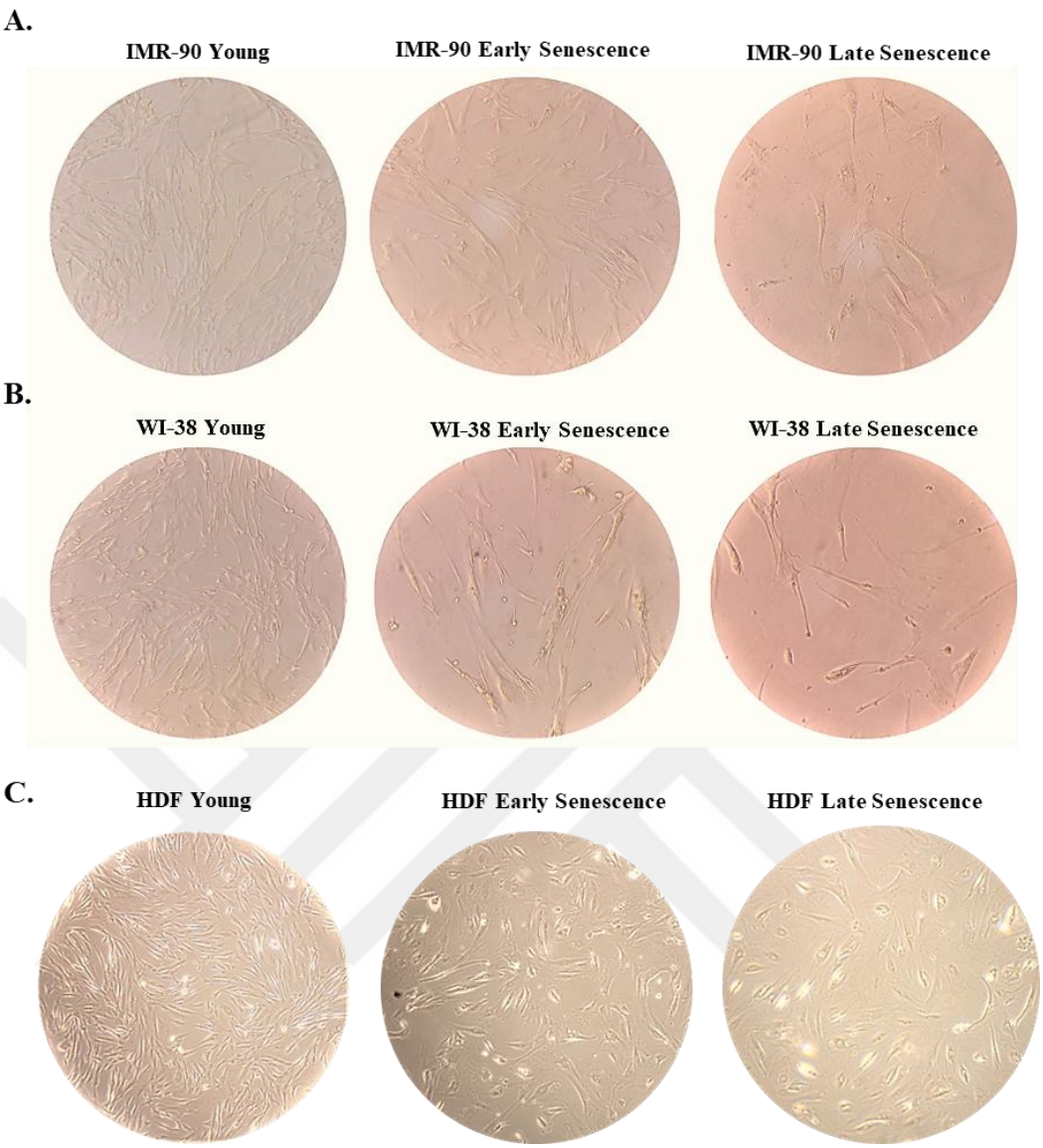

Figure 20. Bright field microscopy images depicting the stages of replicative senescence in (A) IMR90, (B) WI38, and (C) HDF fibroblast cells.

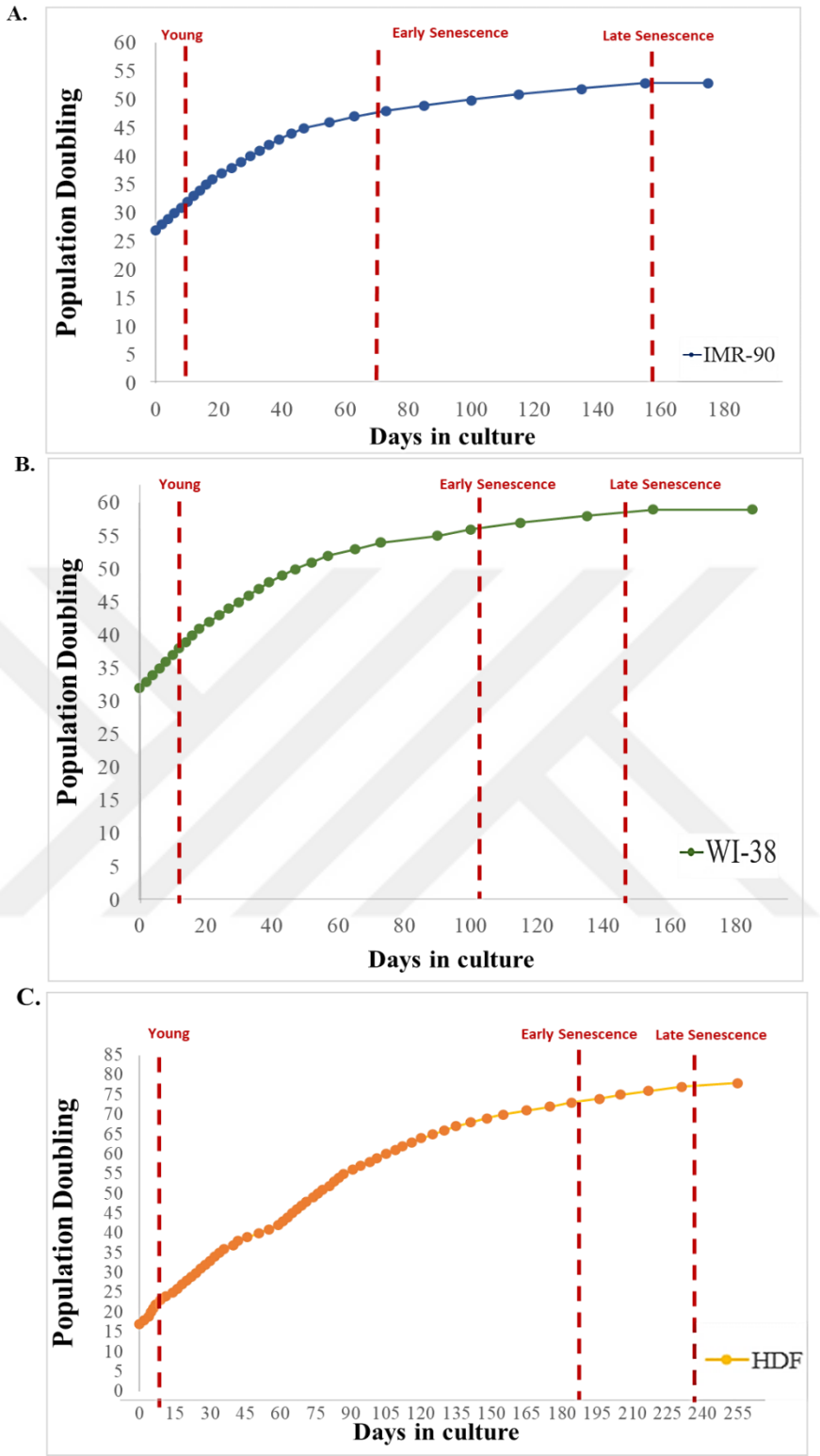

Figure 21. Population doubling graphs of (A) IMR90, (B) WI38, and (C) HDF fibroblast cells. Time points when young, pre-senescent, early senescent, and late senescent cells used in other work packages are indicated by dashed red lines.

For the experiments, the population doubling (PD) was taken as 32 for young cells, while for early senescent cells PD was 49 and for late senescent cells it was 53

for IMR-90 young cells. Similarly, for WI-38 fibroblasts, the PD was 40 for young cells, 55 for early senescent cells and 58 for senescent cells. For HDF fibroblasts, the PD was 36 for young cells, 74 for early senescent cells and 78 for senescent cells.

3.2. BrdU Incorporation Analysis Reveals Differential Proliferation Rates in Fibroblast Cell Senescence

Nucleotide analog BrdU incorporation and staining is a frequently used method in cell senescence and proliferation studies (Itahana et al., 2007; Schorl and Sedivy, 2007; De Cecco et al., 2019). In this study, anti-BrdU (FITC) antibody staining was utilized after BrdU incorporation to assess the proliferation rate of fibroblast cells. This method allowed for the differentiation between young, early senescent, and late senescent cells. The percentage of BrdU positive cells corresponds to the early population doubling stage of the cell. Following 72 hours of BrdU incorporation, 85-95% of young cells, 5-10% of early senescent cells and 0% of senescent cells exhibited BrdU signal in accordance with the literature. These findings align with the measurements of cell proliferation obtained from the population doubling graphs taken at the specified time intervals.

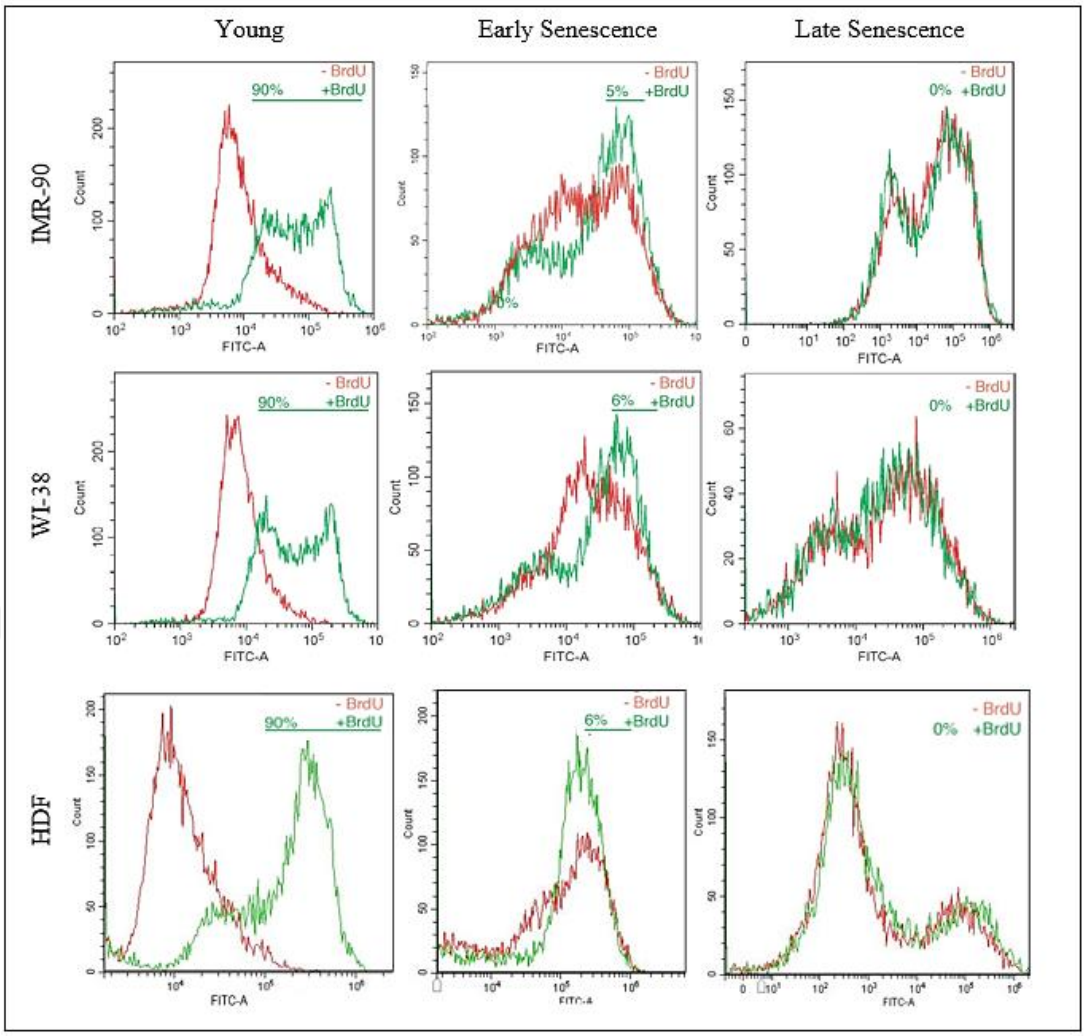

Figure 22. Analysis of fibroblast proliferation rate using BrdU incorporation staining by flow cytometry.

3.3. Immunofluorescence and Fluorescence in Situ Hybridization (immuno-FISH) Analysis Reveals Dynamic Telomere Loss and DNA Damage Patterns in Fibroblast Cell Senescence

A specialized technique called immuno-FISH was performed to investigate potential non-telomeric regions that activate the DNA damage response (DDR) and subsequently induce senescence. This technique combines immunofluorescent staining of γ-H2AX, a marker of DNA damage, with telomere labeling using fluorescence in situ hybridization (FISH), allowing to demonstrate telomere loss and DNA damage concurrently in young, early senescent, and late senescent fibroblasts (Fumagalli et al., 2012; Marchesini et al., 2016). Confocal microscopy images confirmed the colocalization of these signals. In young cells, it is observed that there are numerous and bright telomere signals (green). Telomere signals decreased in both

number and intensity in early senescent cells and were barely detectable in late senescent cells, which aligns with findings from previous studies. γ-H2AX (red) was rarely observed in young cells and appeared with lower intensity at different locations in early senescent cells. Some of these damaged areas were near telomeres, while others were distant from telomeres. These findings support the hypothesis that endogenous DNA damage occurring during replicative aging is not exclusively confined to telomeres. Interestingly no DNA damage markers were detected in deep senescent cells. Upon reviewing the literature, it was observed that similar immuno-FISH assays were conducted only in early senescent cells (Jiang and Pugh, 2009).

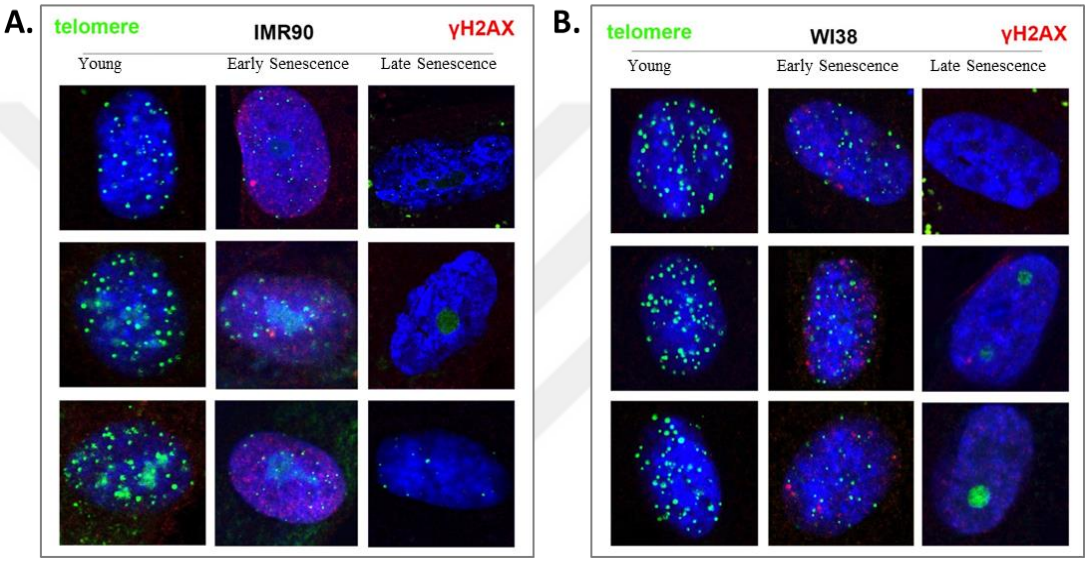

Figure 23. ImmunoFISH staining for telomeres and γ-H2AX in fibroblasts (A) IMR-90 cells, (B) WI-38 cells. The nucleus is stained with DAPI DNA dye (blue), while telomeres are green and γ-H2AX is red.

3.4. Differential Expression of Cell Cycle and SASP Factors in Young, Early Senescent, and Late Senescent Fibroblast Cells Revealed by RT-qPCR Analysis

Following the isolation of RNA from young, early senescent, and late senescent cells quantitative real-time PCR (RT-qPCR) was performed to assess the expression levels of cell cycle and SASP factors that were explained in the *Section 1.7.1.9* at the mRNA level, as shown in Figure 24. According to the results of the experiment, early senescent and senescent cells express genes such as p53, p16, and p21, which are the cell cycle regulators, as well as SASP genes like IL6, IL8, and MMP3 significantly higher than the young proliferating cells. In contrast, young cells show much lower expression of these genes. These results are consistent with the literature (De Cecco et al., 2019).

Interestingly, the expression levels in senescent cells were lower than those in early senescent samples, which is consistent with the findings related to the DNA damage marker γ-H2AX.

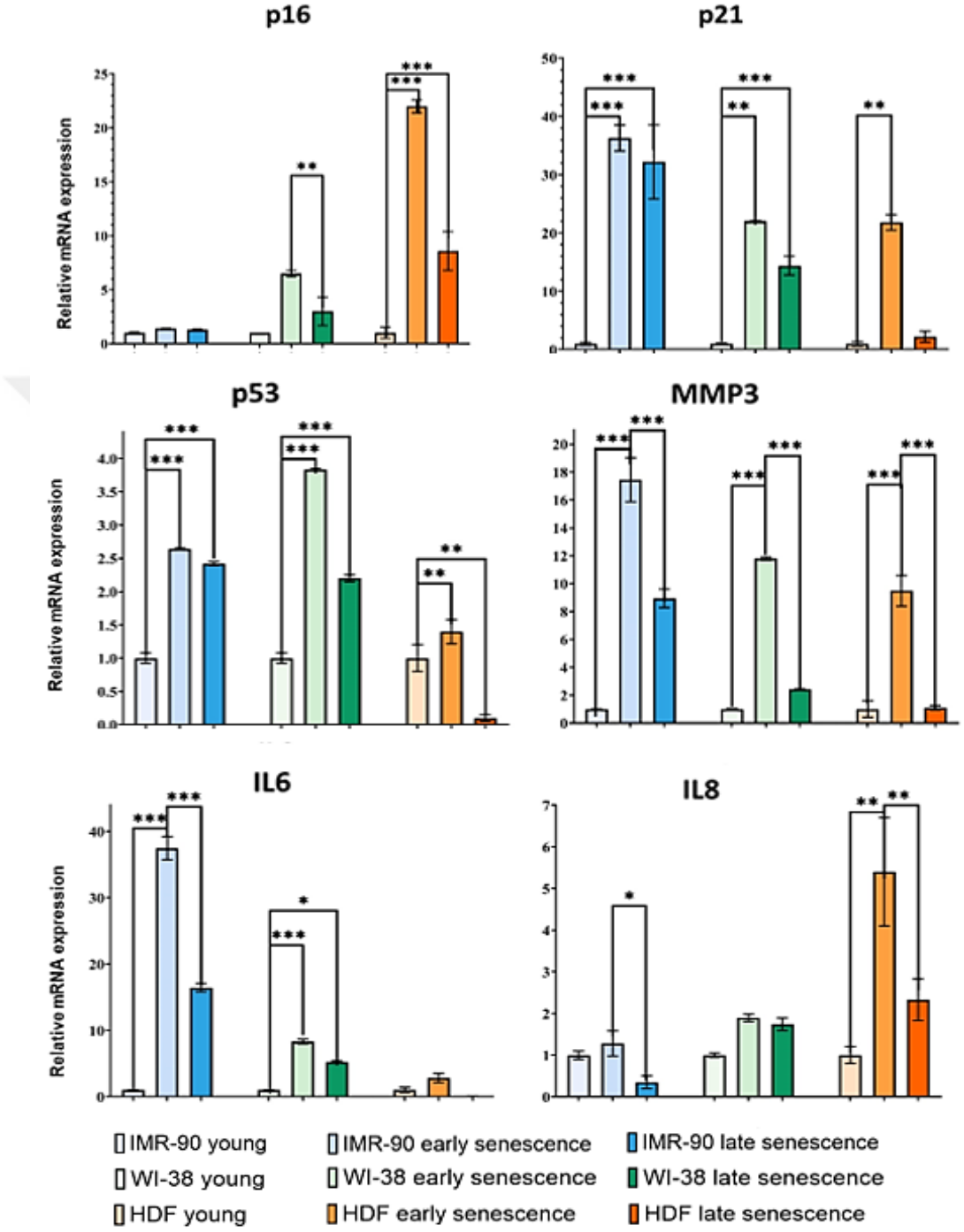

Figure 24. Analysis of the expression of genes that are cell cycle inhibitors and SASP gene expressions in young, early senescent, and late senescent fibroblasts using quantitative real-time PCR (RT-qPCR).

3.5. Dynamic Protein Expression Changes in p21 and γ-H2AX During Cellular Senescence

According to the Western blot results, the protein expression of the cell cycle regulator p21 in IMR-90 and WI-38 cells exhibited a similar pattern to the qPCR results, showing an increase in early senescent samples compared to late senescent and young ones. This congruence between gene expression and protein abundance implies a robust regulatory role for p21 in influencing cell cycle dynamics during the course of cellular senescence response (Figure 25).

Furthermore, a similar pattern emerged concerning γ-H2AX levels within the same cell lines. In early senescent cells, it was observed that substantial elevation in γ-H2AX, which is indicative of heightened DNA damage response activation. However, in late senescent cells, a noteworthy decrease in γ-H2AX levels was observed. These results suggest dynamic changes in the DNA damage response as cells transition from early to late senescence.

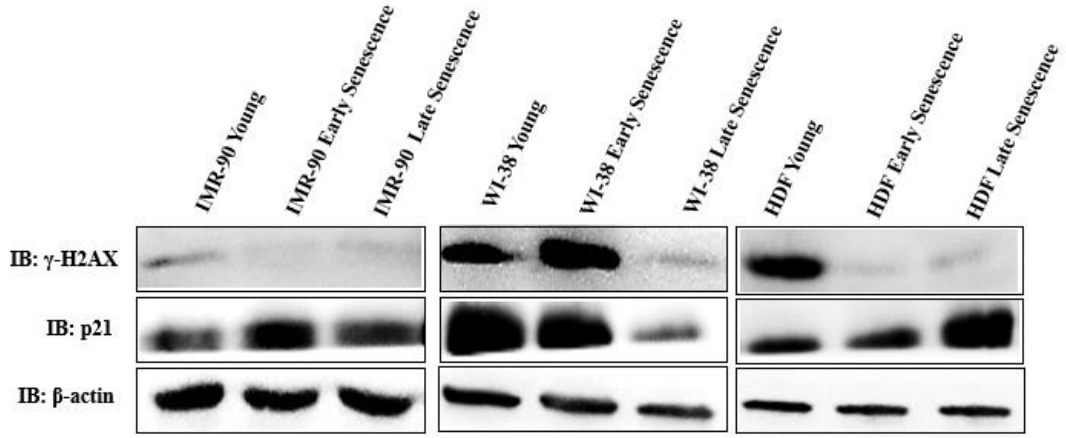

Figure 25. Western blot image of total protein lysates obtained from young, early senescent, and late senescent fibroblasts. Immuno-blotted proteins were indicated on the left panel of the image.

3.6. Quality Control Results of Fibroblast DNAs for Whole-Genome Next-Generation Sequencing

The DNA samples obtained from three different stages (young, early senescent, late senescent) of three characterized fibroblast lines (IMR-90, WI-38, and HDF cells) were utilized for the whole genome sequencing (WGS) process. The quality and quantity of the DNA samples were assessed using Nanodrop and Qubit measurements, and agarose gel electrophoresis was performed as an additional quality check. The obtained results, (Table 3) indicated that the DNA samples met the

necessary criteria in terms of purity and concentration for the subsequent WGS analysis.

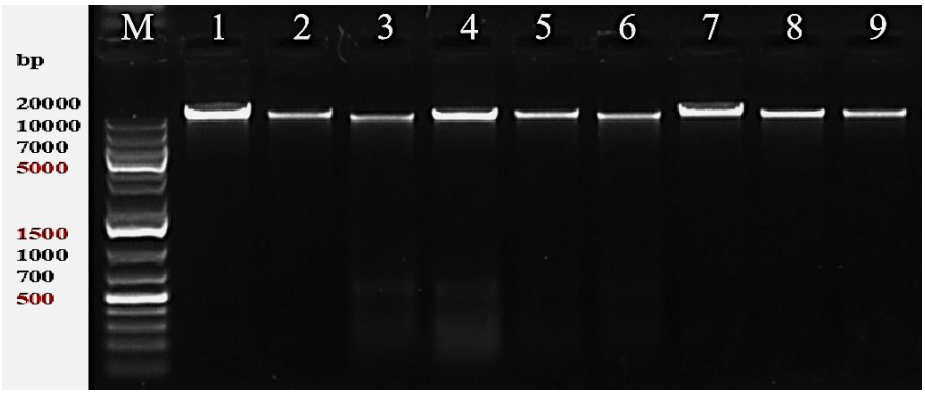

Figure 26. Agarose gel electrophoresis images of young, early senescent and late senescent fibroblast DNAs sent to next generation whole genome sequencing. M: DNA ladder. The sample numbers are as shown in Table 3.

Table 3. Quality control results of young, early senescent, and late senescent fibroblast DNAs for whole-genome next-generation sequencing. The quality of the samples was measured using Nanodrop micro spectrophotometer and Qubit fluorometer devices.

		Nanodrop Results			Qubit Results
	Sample Name	**Concentration (ng/µl)**	**A260/280**	**A260/230**	**Concentration (ng/µl)**
1	WI-38-young	63.6	1.8	2.07	70
2	WI-38-early senescence	23.4	1.73	1.99	22.4
3	WI-38-late senescence	25.7	1.88	2.03	7.38
4	IMR-90-young	131.6	1.97	2.06	63.2
5	IMR-90-early senescence	45.3	1.85	1.92	27.6
6	IMR-90-late senescence	19.1	1.71	1.77	8.1
7	HDF-young	99.3	1.84	1.93	94.6
8	HDF-early senescence	44.7	1.77	1.5	34.8
9	HDF late senescence	33.5	1.78	1.81	23.6

3.7. Quality Control Results of Fibroblast Data for ChIP-sequencing

The quality control results of the WGS and ChIP-seq sequencing data of young, early senescent, and late senescent fibroblast cells, are given in Table 4. In the table, the column "Raw reads" in the quality control results represents the total amount of raw data reads, while the "Raw data" column indicates the value in gigabytes (G) obtained by multiplying the raw reads with the sequence length. Accordingly, each sample, has a raw data output exceeding 90 G, with a total raw data amount of 864.0 G. Additionally, the "Effective" percentage in the table represents the ratio of clean reads to raw reads. Clean reads are obtained by filtering out low-quality regions,

adapter sequences, and reads that fail to meet minimum quality criteria. In this regard, all of the samples have an "effective" percentage exceeding 93%. Furthermore, the "Error" column indicates the percentage of possible errors during the sequencing process. This rate is calculated as 0.03% for all samples, indicating a very low error rate in our next-generation sequencing. The Q20 value in the table represents a 1% error rate (i.e., every 100 bp sequencing read may contain one error), corresponding to a call accuracy of 99%. The Q30 quality score represents a 0.1% error rate (i.e., every 1000 bp sequencing read may contain one error). When sequencing quality reaches Q30, nearly all reads will be perfect without any errors or ambiguities. Therefore, Q30 is considered a criterion for quality in NGS. Finally, the GC percentage in the table indicates the ratio of the number of G and C bases to the total number of bases. This ratio is used to assess the distribution of GC content and determine the separation between AT and GC. According to the complementary base pairing rule, the content of AT and GC should be similar in each sequencing cycle. In this regard, the GC percentage is suitable for all samples.

Table 4. The quality control results of the WGS and ChIP-seq data of young, early senescent, and late senescent fibroblast cells.

	Sample	Raw reads	Raw data	Effective(%)	Error(%)	Q20(%)	Q30(%)	GC(%)
ChIP Samples	HDF-young	29157188	4.4	83.66	0.03	97.27	92.72	48.18
	HDF-young (10% input)	24280802	3.6	60.09	0.03	97.43	93.28	51.03
	HDF-early senescence	38592268	5.8	66.55	0.03	97.68	93.68	48.86
	HDF-early senescence (10% input)	30793250	4.6	60.19	0.03	97.47	93.24	49.61
	HDF-late senescence	41992184	6.3	72.69	0.03	97.31	92.98	51.08
	HDF-late senescence (10% input)	13849734	2.1	43.61	0.03	97.56	93.61	52.38
WGS Samples	WI-38-young	721818900	108.3	94.43	0.03	95.29	89.24	41.1
	WI-38-early senescence	869262194	130.4	96.6	0.03	95.97	90.24	40.99
	IMR-90-young	757136498	113.6	93.46	0.03	95.37	89.25	41.11
	HDF-young	623731138	93.6	93.99	0.03	95.83	90.16	41.12
	HDF-early senescence	756303656	113.4	97.07	0.03	96.17	90.57	40.98
	HDF-late senescence	719152454	107.9	96.74	0.03	96	90.28	40.96
	IMR-90-early senescence	530331524	94.6	98.16	0.03	94.95	88.12	40.96
	IMR-90-early senescence	100295852		97.88	0.03	95.44	89.17	40.98
	IMR-90-late senescence	456484070	102.3	98.12	0.03	95.43	89.11	41.02
	IMR-90-late senescence	225779812		98.16	0.03	96.69	91.73	41.07

3.8. Quality Control Results of γ-H2AX ChIP-seq HDF fibroblasts

To investigate the endogenous DNA damage occurring at different stages (young, early senescent, and late senescent) in HDF cells, the chromatin immunoprecipitation (ChIP) method with the γ-H2AX antibody was performed. The immunoprecipitated DNA was then subjected to ChIP-seq analysis. Optimization of the ChIP procedure involved treating the cells with varying amounts of MNase (5, 7.5,

10 µl) as depicted in Figure 27.A.

The quality control results of the samples prepared for ChIP-seq analysis, including input samples representing young, early senescent, and late senescent HDF cells, are presented in Table 5. The input samples underwent all steps except for the treatment with the H2AX antibody and serve as positive controls for chromatin immunoprecipitation. Additionally, the samples were subjected to Nanodrop and qubit quality measurements, as well as agarose gel electrophoresis, with the gel images shown in Figure 27.B. The samples were found to be appropriate for ChIP-seq analysis.

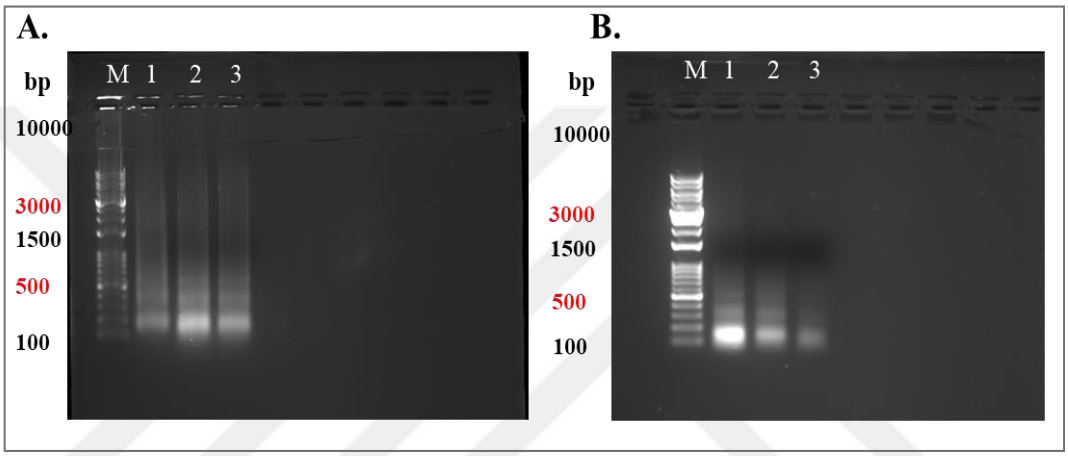

Figure 27. Agarose gel electrophoresis image showing MNase enzyme concentration optimization for chromatin immunoprecipitation process. (A) Image of 3 different amounts of MNase (5, 7.5, 10 µl) tested in HDF fibroblasts. B. Chromatin immunoprecipitation was performed with optimum MNase concentration to young, early senescent and late senescent HDF cells.

Table 5. Nanodrop micro spectrophotometer and Qubit fluorometer quality control results of young, early senescent, and late senescent HDF fibroblast DNAs and input samples.

Sample Name	Nanodrop Results			Qubit Results
	Concentration (ng/µl)	A260/280	A260/230	Concentration (ng/µl)
HDF-young	7.8	1.43	1.11	2.16
HDF-young (10% input)	3.2	1.33	0.59	0.23
HDF-early senescence	11.8	1.73	1.42	4.68
(10% input)	3	1.26	0.76	0.01
HDF-late senescence	7.5	1.58	1.12	0.67
HDF-late senescence (10% input)	2.5	1.15	0.57	0.01

3.9. γ-H2AX ChIP-seq Results of HDF Fibroblasts

3.9.1. FastQC Quality Control Results

The FASTQC GC content results of γ-H2AX ChIP-seq for HDF fibroblasts are presented in Figure 28. The sequence lengths of all samples are 150 bp. For HDF young sample, GC% content is 48% and the total sequence number is 19800806. For HDF young input, GC% content is 50% and the total sequence number is 22203647. For HDF early senescent samples, GC% content is 50% and the total sequence number is 22203647. For HDF early senescent inputs, GC% content is 49% and the total sequence number is 23825769. For HDF late senescent samples, GC% content is 50% and the total sequence number is 20996092. For HDF late senescent inputs, GC% content is 51% and the total number is 59223634.

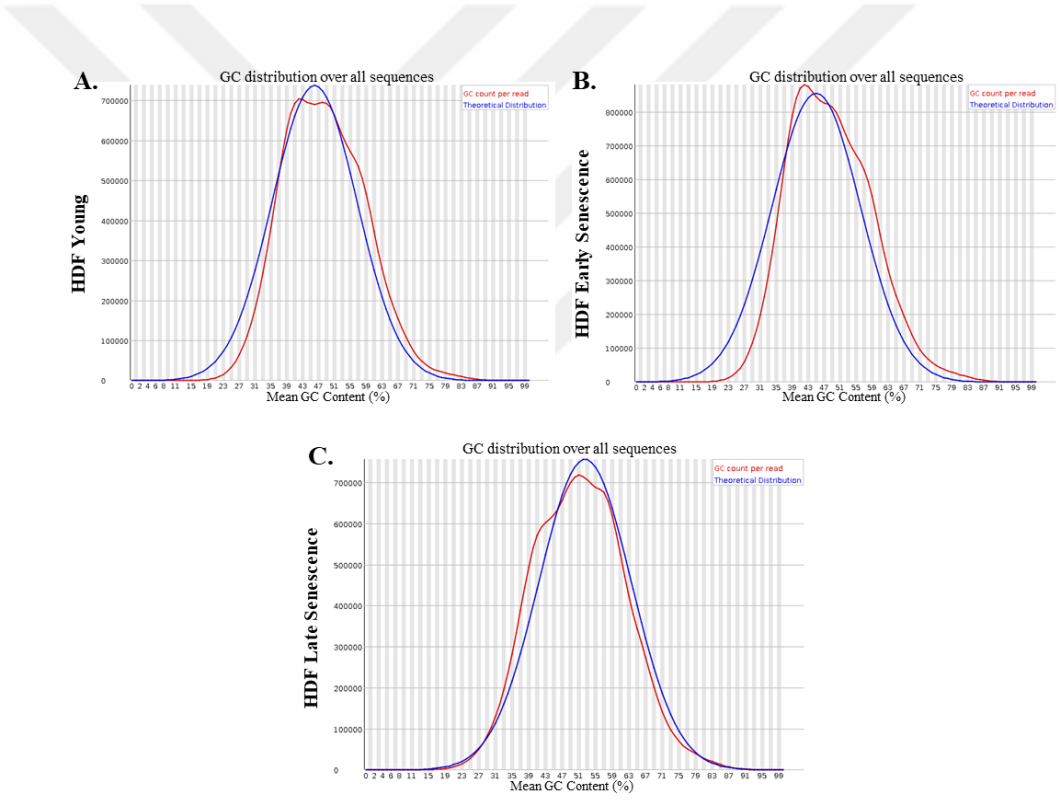

Figure 28. The representative FASTQC- GC content results of γ-H2AX ChIP-seq HDF (A) Young, (B) Early senescent (C) Late senescent fibroblasts.

The per sequence and per base quality scores in FASTQC data is an initial indicator of the sequencing data quality. These scores are represented on the graph, with the quality scores displayed on the y-axis. A higher quality score signifies better base call accuracy. The graph includes visual indicators as the yellow box representing the 25th and 75th percentiles, a red line indicating the median, and whiskers indicating the 10th and 90th percentiles. The average quality score for the nucleotide is

represented by a blue line.

The graph's background color distinguishes different quality levels: green for very good quality calls, orange for calls of reasonable quality, and red for calls of bad quality. Typically, as the sequencing run progresses, the quality of base calls tends to deteriorate, leading to an increased occurrence of calls falling into the orange region towards the end of a read. Analyzing these metrics reveals that the base quality scores for the first nucleotide are high, with a majority of reads having scores above 28 (Figure 29).

Per sequence quality scores in FASTQC data provide an overall assessment of read quality, enabling the identification of regions with low-quality or problematic sequences. These scores are represented using the Phred scale. The graph plots the average quality score on the x-axis and the number of sequences with that average on the y-axis. As shown in Figure 30, most of the readings have a high average quality score without any bumps in low quality values.

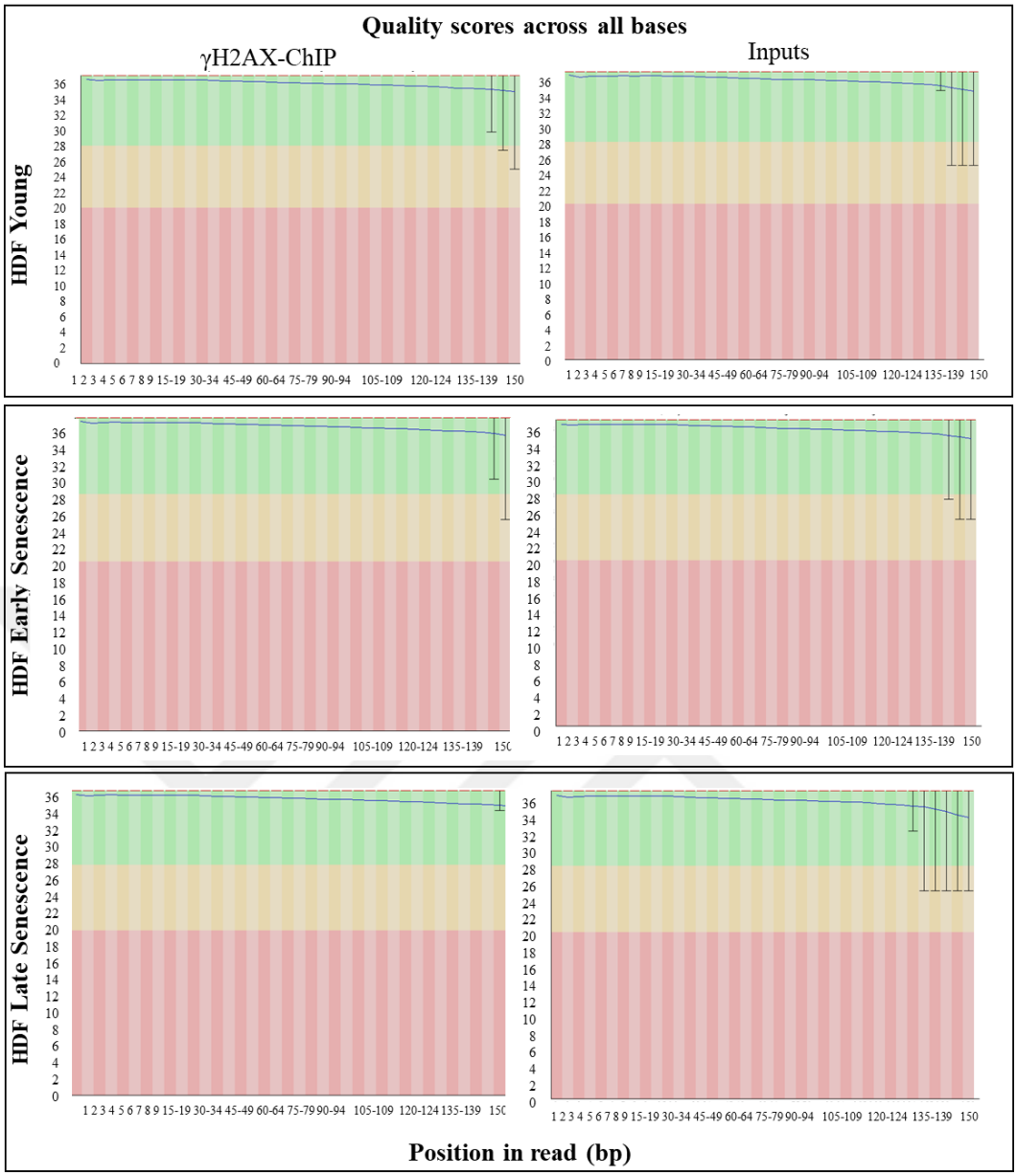

Figure 29. γ-H2AX ChIP-seq per base quality score results of HDF young, early senescent, late senescent fibroblasts and their input controls.

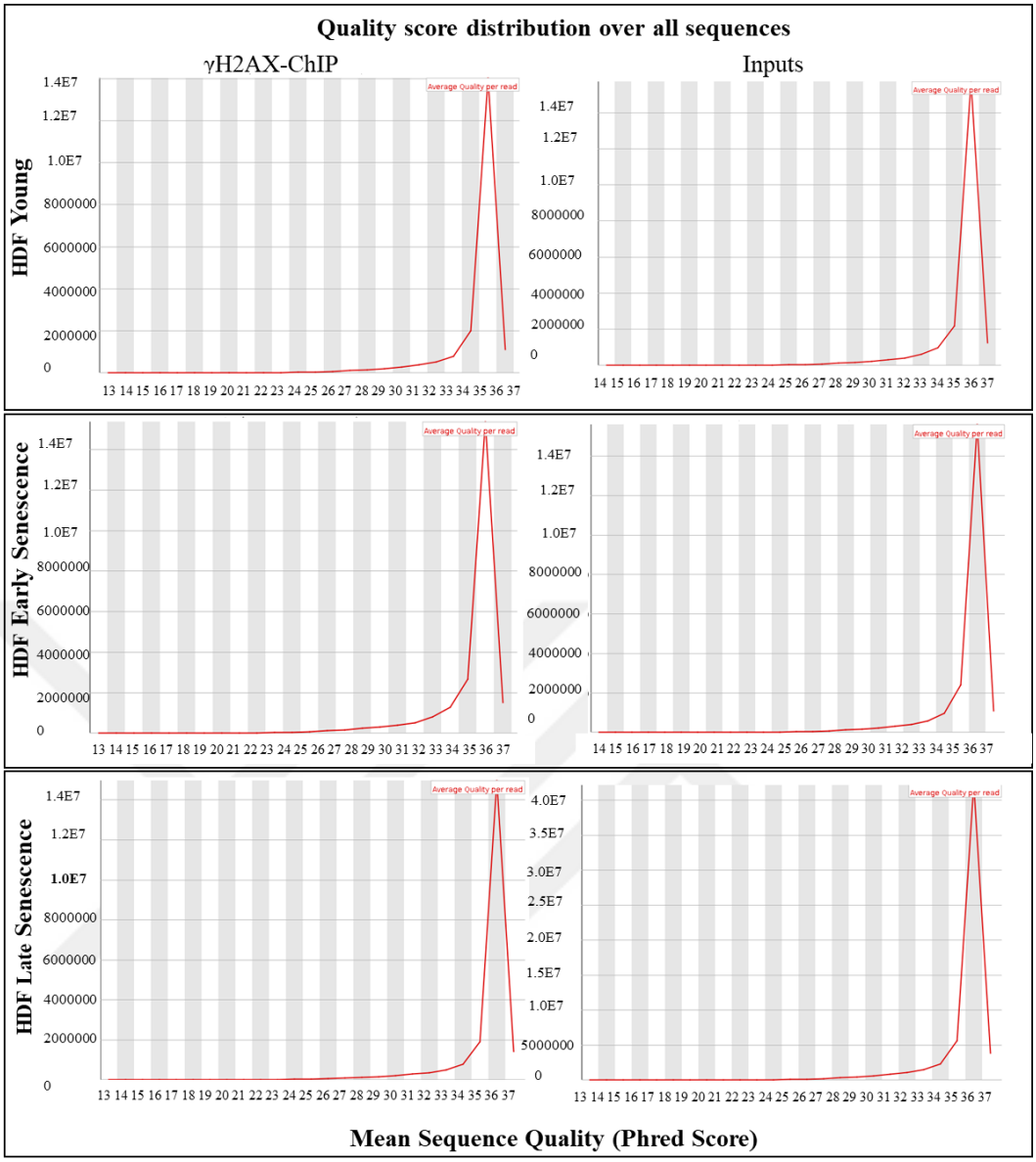

Figure 30. γ-H2AX ChIP-seq per sequence quality scores of HDF young, early senescent, late senescent fibroblasts and their input controls.

3.9.2. Quality Control and Correlation Analysis of Trimmed and Aligned γ-H2AX ChIP-seq Samples

After removing low-quality reads and aligning the data to the hg38 reference genome, quality checks were performed using MultiQC to ensure accurate data quality. The trimmed and aligned samples were represented as green lines in the graph, with the y-axis representing the quality scores. Higher scores indicate better base calls. The results indicated that the mean quality value across each base position in the reads was very good, as depicted in Figure 31. Additionally, the per sequence quality score report demonstrated that a subset of our data after trimming exhibited consistently high-quality values.

Figure 31. The overall quality control of output files from FastQC, Trimmomatic and Bowtie2 analysis. Green lines represent (A) Mean quality scores and (B) per sequence quality scores of all HDF samples, including inputs.

Moreover, the correlation plot (Figure 32) illustrates the relationship between read counts across different samples used in the analysis, as measured by the Pearson correlation coefficient. It provides insights into the interconnections among various variables. The main diagonal line, marked as 1.00, indicates perfect correlation of each variable with itself. The color transition from blue to red signifies a decrease from the maximum correlation value of 1.00.

Based on the Pearson correlation coefficient values, which exceed 0.5 for all aligned samples, it can be concluded that there is a strong positive correlation between the read coverages of the samples.

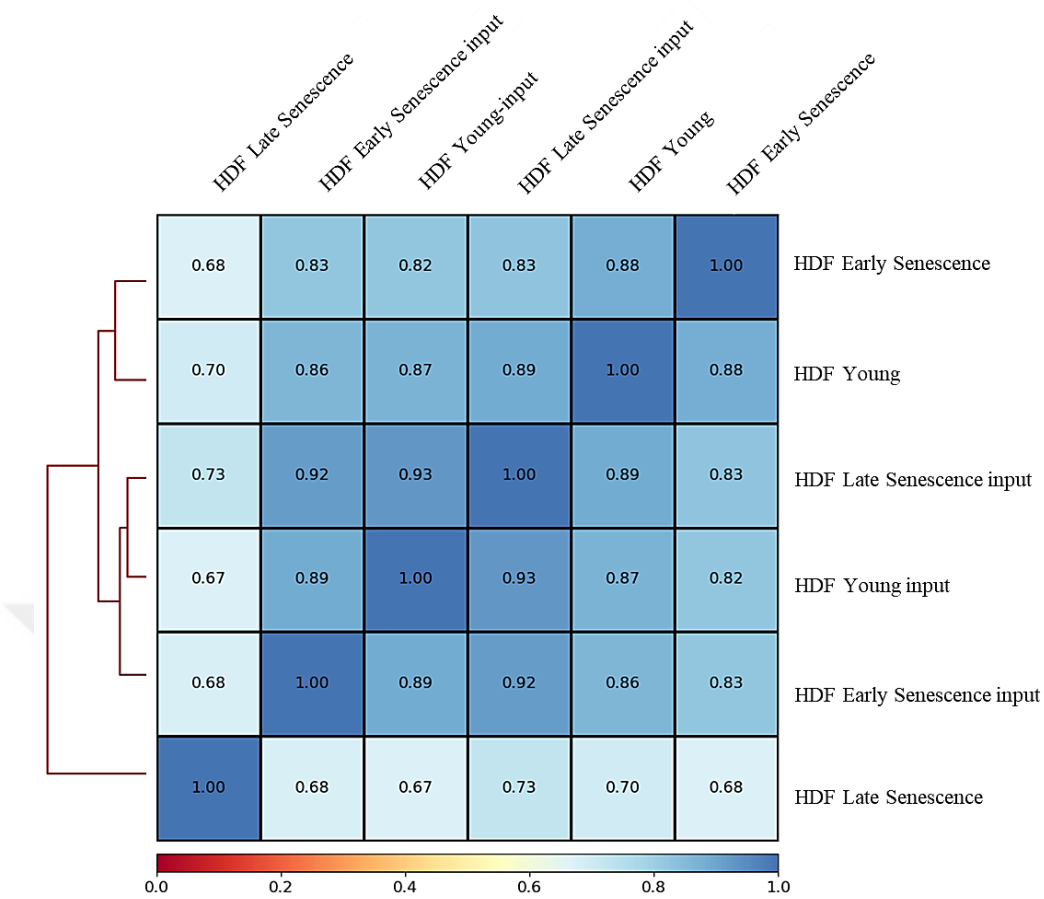

Figure 32. The correlation plot illustrating the relationship between read counts of different samples used in the analysis, measured by the Pearson correlation coefficient.

3.9.3. Analysis of γ-H2AX Peaks and Peak Scores in Young, Early Senescent, and Late Senescent Samples

Peak calling is a critical step in the analysis of ChIP-seq data, specifically for identification of the summit, which is the highest point within each peak, providing the precise location of the γ-H2AX-DNA interaction. Additionally, MACS2 assigns a score to each peak, reflecting the strength of the signal. The significance of the peaks is estimated by comparing them to the background signal while controlling for false discovery rate (FDR). The significant peaks were plotted based on their peak scores on histogram. According to the histogram results, the count and the intensity of γ-H2AX peaks that are significant compared to inputs, increased in early senescence compared to late senescence and were the lowest in the young samples. As shown in Figure 33, the young samples showed minimal peak scores, while the summits in early and late senescent samples were notably higher than the young sample.

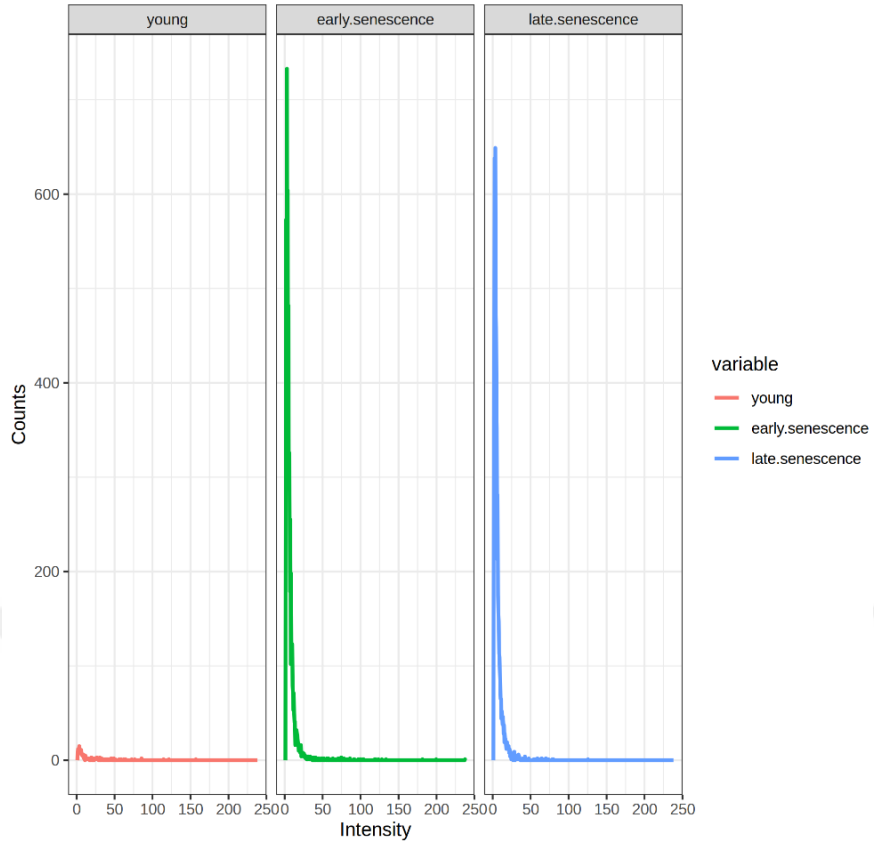

Figure 33. The demonstration of γ-H2AX in HDF young, early senescent and late senescent samples. Histogram estimates the number peaks falling into each intensity range.

Then, by mapping the peaks onto the chromosomal ideogram, a visual representation of the genome-wide distribution of γ-H2AX peaks across the genome was visualized. As depicted in Figure 34, the intensity of γ-H2AX was lower in HDF young samples compared to the early and late senescence ones. Additionally, it has been observed that the chromosomal distribution of γ-H2AX increases in telomeric regions in aging cells, as proposed, but it is also significantly elevated in non-telomeric regions.

A.

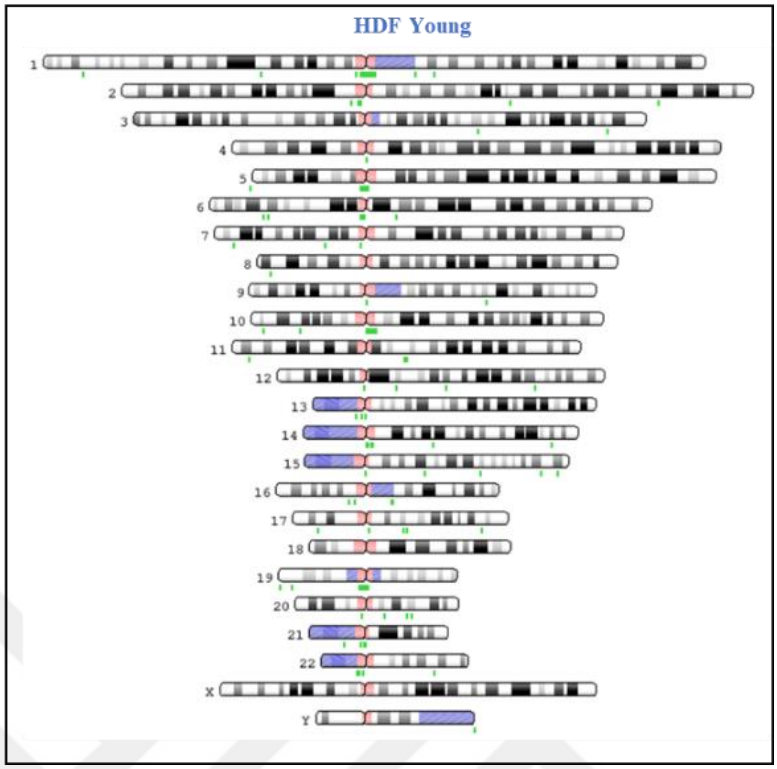
HDF Young
1
2
3
4
5
6
7
8
9
10
11
12
13
14
15
16
17
18
19
20
21
22
X
Y

B.

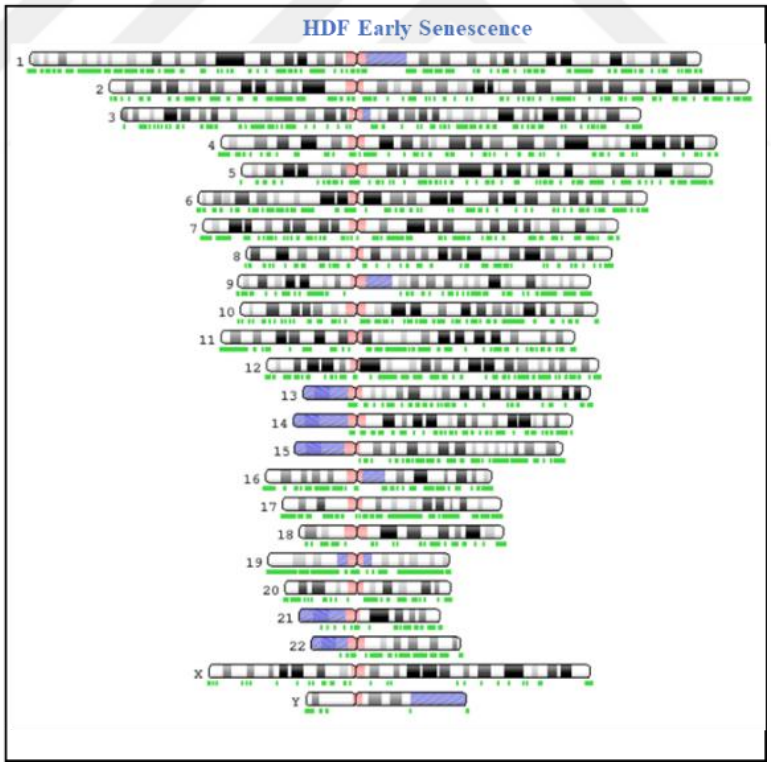
HDF Early Senescence
1
2
3
4
5
6
7
8
9
10
11
12
13
14
15
16
17
18
19
20
21
22
X
Y

C.

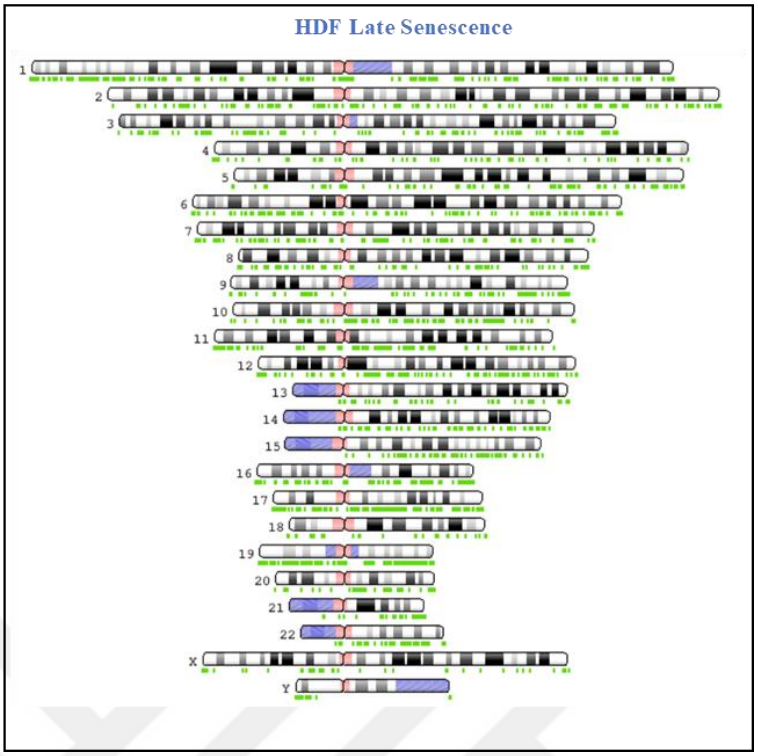

Figure 34. γ-H2AX chromosomal ideogram that gives the distribution along the human chromosomes in HDF young, early, and late senescent samples.

3.9.4. RepeatMasker Annotation and Analysis of γ-H2AX Peaks in Repetitive Elements

To identify repetitive elements exhibiting the DNA damage marker γ-H2AX, repeat masker annotations were applied to the peak calling outputs. Initially, a plot was generated to visualize the distribution of repeats identified by the RepeatMasker annotation. The analysis revealed the peaks of γ-H2AX in repetitive elements during early senescence. Furthermore, late senescent samples exhibited a pronounced peak, indicating a high accumulation of γ-H2AX in repetitive elements.

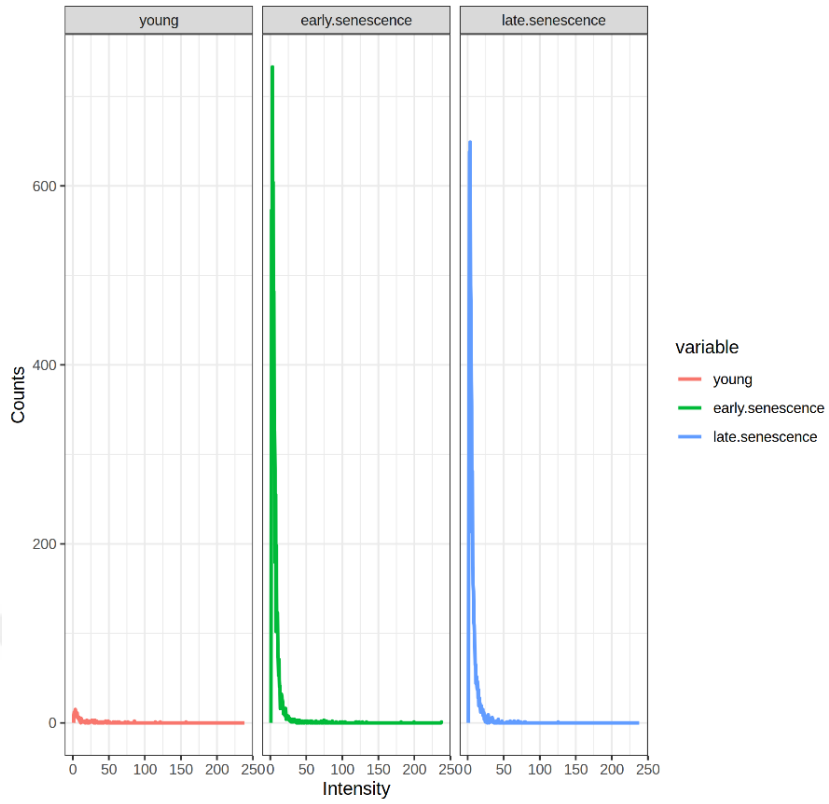

Figure 35. The γ-H2AX peaks on repetitive elements.

Subsequently, separate histograms were plotted for the repeats that were suggested to be associated with senescence in the previous studies (De Cecco et al., 2013; Booth and Brunet, 2016; Nakao, Tanaka and Koga, 2020; Soto-Palma et al., 2022). The results revealed that γ-H2AX accumulation in the L1 repeat was nearly absent in young cells but increased in early and late senescent cells. A similar pattern was noticed for the ALR/alpha satellite and Alu repeats. In comparison to the young sample, the L1, ALR/alpha, and Alu repeats demonstrated higher peaks in γ-H2AX binding sites of senescent cells. This observation implies that as cells undergo aging and accumulate DNA damage, repetitive elements within the γ-H2AX binding regions tend to exhibit heightened peak scores. In contrast to the aforementioned repeats, the subtelomeric TAR repeat displayed a distinct pattern. In young cells, no significant peak scores of the sub-telomeric repeat was observed in γ-H2AX binding sites. In addition, the peak scores of early and late senescent cells were tested statistically with the Mann Whitney U test, but no significant difference was observed ($p > 0.05$).

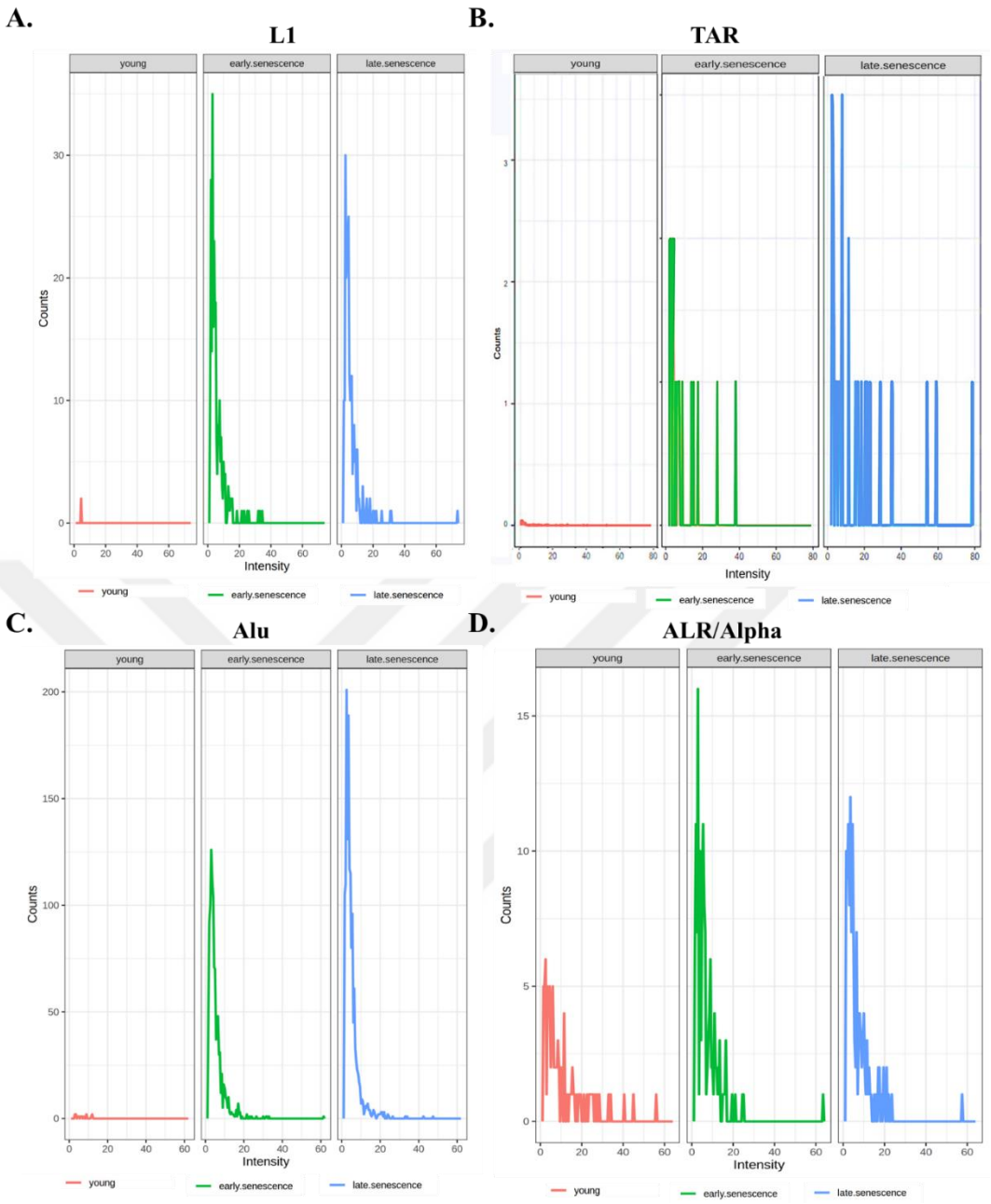

Figure 36. The depiction of γ-H2AX on (A) L1 repeat (B) TAR repeat (C) Alu repeat and (D) Alr/alpha repeat.

3.9.5. γ-H2AX ChIP Enrichment in Repetitive Elements Using RepEnrich

In the analysis, RepEnrich was employed to investigate ChIP γ-H2AX enrichment within repetitive elements in young, early and late senescent HDF cells, focusing on the subtelomeric repeats. Surprisingly, the results revealed a consistent increase in the levels of these three telomeric repeats in both early and late senescent cells compared to young cells. Notably, in early senescent cells γ-H2AX enrichment within the repeat elements exceeded those observed in late senescent cells (Figure 37). These findings were consistent across most of the repetitive element classes, including simple repeats, satellite repeats, and other repetitive elements (Table 6).

These intriguing results suggest that subtelomeric repeats, specifically Rep522, LSAU, and TAR, exhibit elevated γ-H2AX enrichment in late senescent cells displaying the most significant changes. This phenomenon could signify a unique regulatory mechanism in senescent cells, shedding light on the role of γ-H2AX in the maintenance of genomic stability during cellular aging.

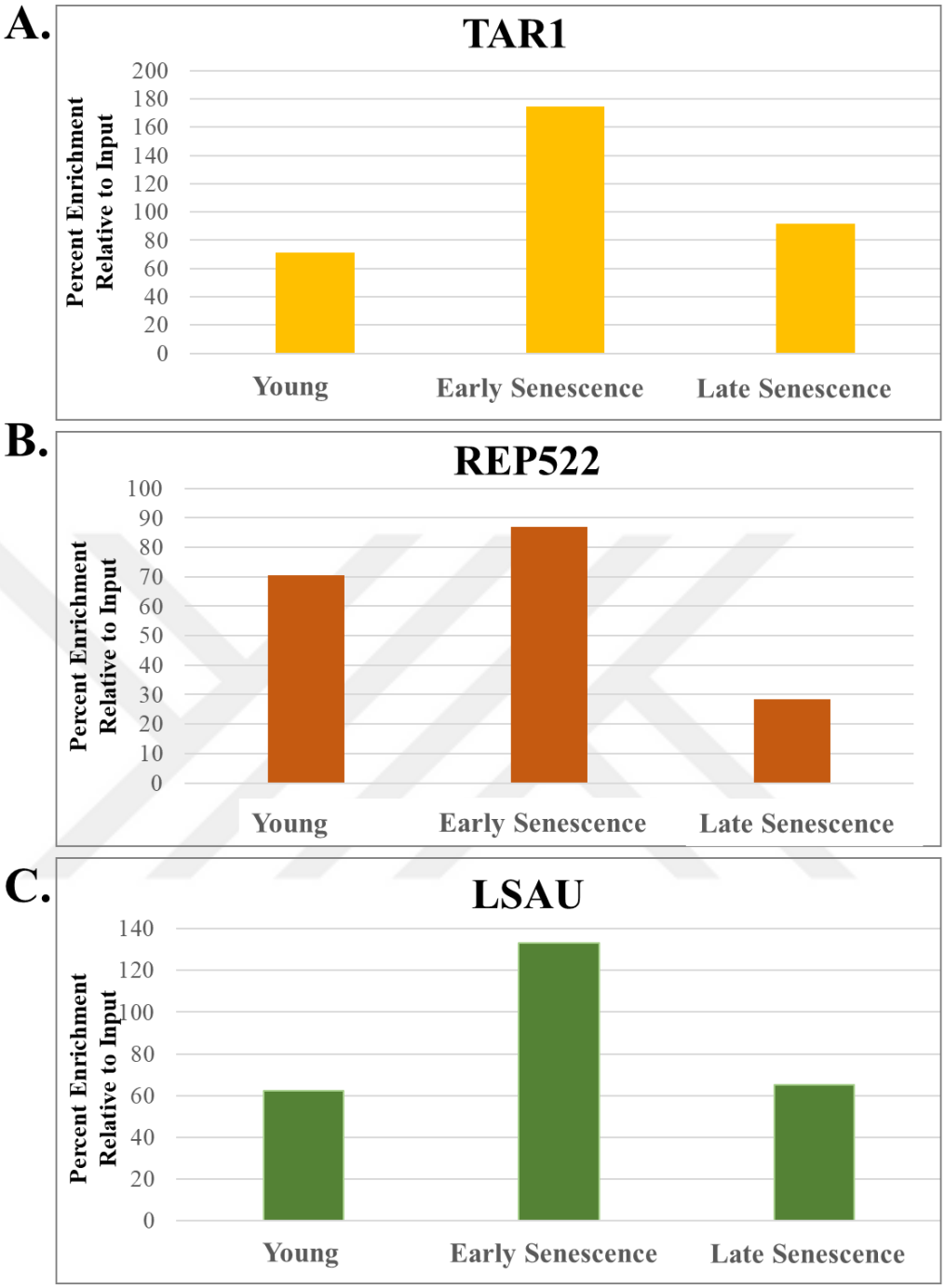

Figure 37. γ-H2AX ChIP Enrichment in Telomeric Repeats. (A) TAR1 repeat (B) REP522 repeat (C) LSAU repeat.

Table 6. γ-H2AX ChIP Enrichment in Various Repetitive Elements. *Samples with fold change values greater than 2 were considered significant for the named repeats, while those with values exceeding 10 were deemed significant for simple repeats. Young: Young HDF cells, Early Sen: Early Senescent HDF cells, Late Sen: Late Senescent HDF cells.*

	Percent Enrichment Relative to Input			**(Fold Change)**		
Repeat	**Young**	**Early Sen**	**Late Sen**	**Early Sen vs Young**	**Late Sen vs Young**	**Late Sen vs Early Sen**
TELOMERIC REPEATS						
_CCCTAA_n	124.29	164.44	69.85	1.32	0.56	0.42
_TTAGGG_n	119.05	125.64	65.79	1.06	0.55	0.52
SIMPLE REPEATS						
_CATGGA_n	11.76	125.00	33.33	10.63	2.83	0.27
_CCCTTCG_n	6.25	159.09	43.18	25.45	6.91	0.27
_CCTGCGC_n	4.88	143.33	60.24	29.38	12.35	0.42
_CGCGGCT_n	10.71	345.45	139.13	32.24	12.99	0.40
_CGGC_n	27.08	297.14	77.42	10.97	2.86	0.26
_CTCACCT_n	7.41	190.91	42.55	25.77	5.74	0.22
_GAGGCTGG_n	7.69	83.33	23.81	10.83	3.10	0.29
_GCCCTGC_n	3.03	156.25	40.30	51.56	13.30	0.26
_GCCGCCA_n	27.59	292.86	49.02	10.62	1.78	0.17
NAMED REPEATS						
Eulor4	84.85	213.64	63.64	2.52	0.75	0.30
LSAU	62.30	133.19	65.35	2.14	1.05	0.49
MARE10	157.50	343.33	111.24	2.18	0.71	0.32
MER75A	82.19	200.00	56.67	2.43	0.69	0.28
TAR1	71.54	174.37	91.93	2.44	1.29	0.53
UCON57	150.00	323.08	77.78	2.15	0.52	0.24
UCON60	137.93	333.33	92.86	2.42	0.67	0.28
UCON69	81.82	203.45	60.00	2.49	0.73	0.29
tRNA-Tyr-TAC	109.09	225.00	35.96	2.06	0.33	0.16
tRNA-Val-GTY	60.00	169.57	117.39	2.83	1.96	0.69

Table 6 (continued). Table 6. γ-H2AX ChIP Enrichment in Various Repetitive Elements. Samples with fold change values greater than 2 were considered significant for the named repeats, while those with values exceeding 10 were deemed significant for simple repeats. *Young: Young HDF cells, Early Sen: Early Senescent HDF cells, Late Sen: Late Senescent HDF cells.*

	Percent Enrichment Relative to Input			**(Fold Change)**		
Repeat	**Young**	**Early Sen**	**Late Sen**	**Early Sen vs Young**	**Late Sen vs Young**	**Late Sen vs Early Sen**
ALL SATELLITES						
ACRO1	98.37	126.78	51.59	1.29	0.52	0.41
ALR_Alpha	180.46	152.11	70.01	0.84	0.39	0.46
BSR_Beta	144.44	130.24	46.02	0.90	0.32	0.35
CER	150.67	149.23	51.40	0.99	0.34	0.34
D20S16	90.61	109.65	40.64	1.21	0.45	0.37
GSAT	96.36	104.02	30.21	1.08	0.31	0.29
GSATII	78.47	95.98	33.20	1.22	0.42	0.35
GSATX	90.18	93.74	30.55	1.04	0.34	0.33
HSAT4	147.10	126.26	40.19	0.86	0.27	0.32
HSAT5	79.24	97.16	29.44	1.23	0.37	0.30
HSATI	114.69	101.41	43.89	0.88	0.38	0.43
LSAU	62.30	133.19	65.35	2.14	1.05	0.49
MSR1	79.84	109.27	43.18	1.37	0.54	0.40
REP522	70.43	87.02	28.47	1.24	0.40	0.33
SATR1	141.28	122.20	43.86	0.86	0.31	0.36
SATR2	149.45	126.46	46.27	0.85	0.31	0.37
SST1	74.34	102.47	31.70	1.38	0.43	0.31
TAR1	71.54	174.37	91.93	2.44	1.29	0.53
GAATG_n	163.90	185.86	53.28	1.13	0.33	0.29

3.9.6. Gene Ontology (GO) Analysis Reveals Functional Significance of γ-H2AX Binding Sites During Senescence

In this study, it was investigated that the presence of γ-H2AX peaks in genes associated with various KEGG pathways and biological processes in early senescent and late senescent cells. The aim of this analysis is to assess whether DNA damage tended to clustered within gene rich regions and explore its possible connection with age-related characteristics

Findings revealed that there may be an association of γ-H2AX peaks and the genes related to bacterial invasion of epithelial cells, ribosome function, focal adhesion, ECM-receptor interaction, actin cytoskeleton organization, PI3K-Akt pathway, some infectious diseases, cardiomyopathy, microRNAs and proteoglycans in cancer (Figure 38A). These findings suggest the involvement of DNA damage response in various biological processes, including immune response, increased susceptibility to bacterial infections, cellular signaling, protein synthesis, cellular adhesion, vascular processes, ECM dynamics, DNA damage response mechanisms and age-related diseases, overall cellular homeostasis during early senescence. These results highlight the broad impact of DNA damage on various cellular processes and their potential implications in age related phenotypes and diseases (Figure 38A).

Also, for the late senescent cells, analysis of gene ontology terms related to the KEGG was performed. Notably, genes involved in the p53 signaling pathway, which is the master cell cycle regulator, found to be potentially related with DNA damage response. Furthermore, various types of cancer, pathways related to cellular processes such as Focal Adhesion, Apoptosis, Regulation of Actin Cytoskeleton, and Tight Junctions exhibited γ-H2AX peaks in late senescent cells. These pathways are essential for maintaining in cell structure, adhesion, intercellular communication, DNA damage response and cell cycle control. The presence of DNA damage in their associated genes suggests potential disruptions in these processes can induce SASP formation during late senescence. Additionally, the AGE-RAGE signaling pathway in Diabetic Complications and the PI3K-Akt signaling pathway, both implicated in age-related diseases and cellular signaling, showed γ-H2AX peaks, further highlighting the involvement of DNA damage in late senescence-associated pathologies (Figure 38B).

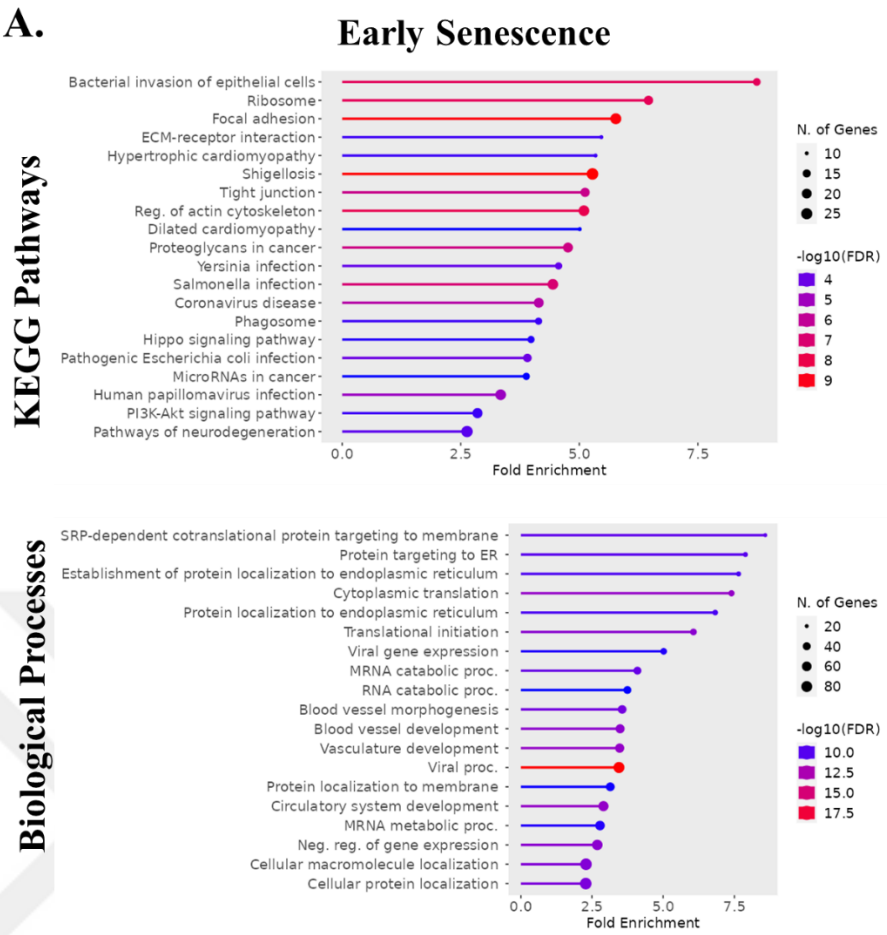

Figure 38. Gene Ontology (GO) term analysis of γ-H2AX peaks in (A) Early Senescent cells and (B) Late Senescent cells. The figure depicts the specific KEGG pathways and biological processes associated with DNA damage and cellular senescence.

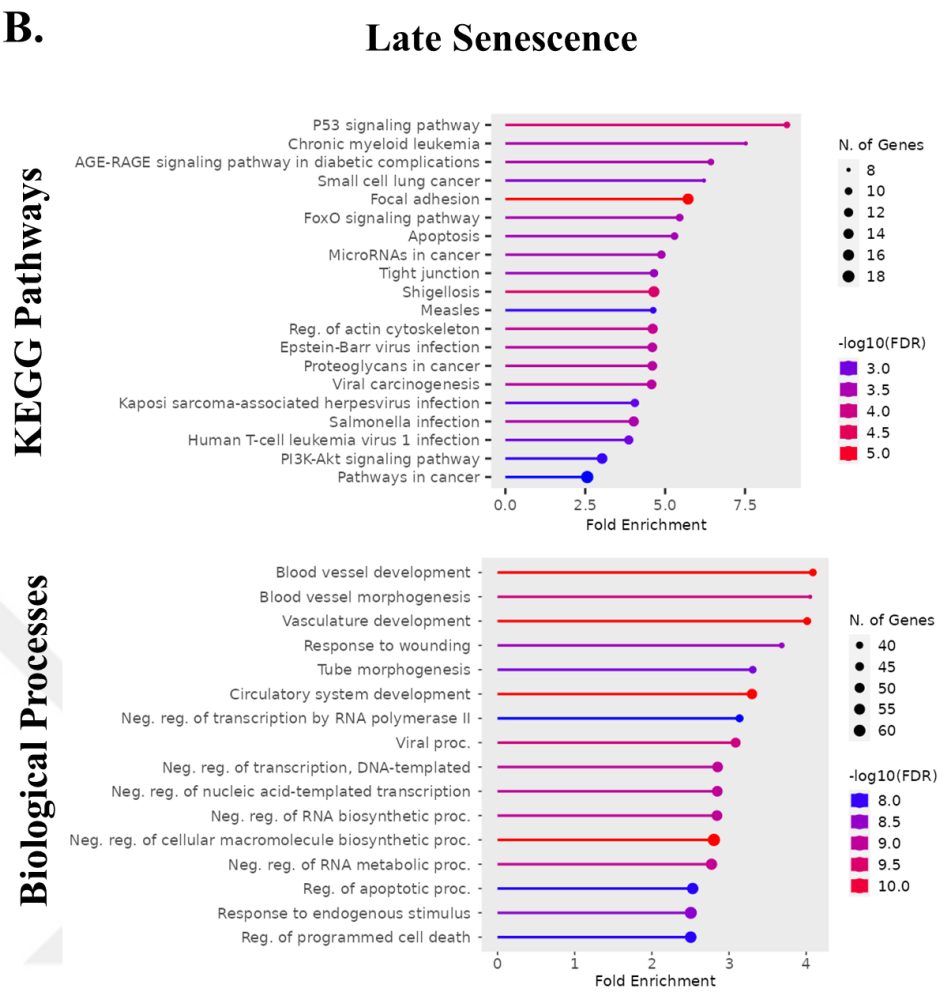

Figure 38 (continued). Gene Ontology (GO) term analysis of γ-H2AX peaks in (A) Early Senescent cells and (B) Late Senescent cells. The figure depicts the specific KEGG pathways and biological processes associated with DNA damage and cellular senescence.

Regarding biological processes, γ-H2AX peaks were found be related with blood vessel morphogenesis, blood vessel development, and vasculature development suggests a potential link between DNA damage and altered vascular processes during late senescence. Processes related to cell migration, tube morphogenesis, and locomotion also exhibit γ-H2AX peaks, indicating the impact of DNA damage on cellular mobility and tissue remodeling (Figure 38B).

CHAPTER 4: DISCUSSION

One prominent alteration involves the gradual shortening of telomeres, which are repetitive DNA sequences located at the ends of chromosomes. This progressive telomere shortening triggers DNA damage response mechanisms, particularly those involved in repairing double-strand DNA breaks. Previous research studies (Nakamura et al., 2008; Jullien et al., 2013; Marchesini et al., 2016) have indicated that DNA damage is not limited to telomeric regions but can occur in other genomic regions as well. However, the specific affected regions and the spontaneous occurrence of such damage have not been thoroughly investigated. Building upon these existing findings, the primary objective of this study is to identify the regions that undergo DNA damage during replicative senescence and these regions can include gene rich regions, and regulatory elements outside of telomeres. Additionally, considering the inherent instability and susceptibility to replication errors of repetitive DNA structures, this study aims to determine repetitive motifs that contribute to the overall DNA damage observed in replicative senescence.

The results obtained from wet lab experiments and ChIP-seq analysis revealed an increment trend of γ-H2AX peaks in both early and late senescent cells compared to young cells. These findings are consistent with the previous research indicating the accumulation of DNA damage markers in aging cells (Nakamura et al., 2008; Jullien et al., 2013). Utilizing the immunoFISH technique, it was observed that young cells exhibit minimal presence of the DNA damage marker γ-H2AX, while early senescent cells show its presence at various locations. Notably, it has been shown that some of these damaged regions are located close to telomeres, while others are located distant. Furthermore, these results are supported when the γ-H2AX accumulated regions were mapped onto the chromosomal ideogram. When examining the ideogram, it is observed that DNA damage is not only localized in telomeric regions, but also spreads throughout the chromosome. These findings support the hypothesis of this study, suggesting that endogenous DNA damage occurring during replicative aging is not confined solely to telomeres.

Interestingly, in ImmunoFISH experiments, it was observed that late senescent cells did not exhibit any detectable presence of the DNA damage marker. Moreover, the ChIP-seq analysis also revealed distinct characteristics of γ-H2AX peaks between early and late senescent cells. In both cell populations, a higher number of γ-H2AX

peaks were observed compared to young cells. Consistent with the data obtained from wet-lab experiments, it was particularly notable that early senescent cells exhibited a more pronounced increase in DNA damage response marker, γ-H2AX. Reviewing the existing literature, it is noteworthy that similar immunoFISH applications have primarily focused on pre-senescent cells (mid-point between young and the senescent cells) (Nakamura et al., 2008; Jullien et al., 2013; Marchesini et al., 2016). Currently, there is a lack of literature regarding the investigation of the DNA damage marker across different stages of senescence. Furthermore, qPCR results indicated that in early senescent cells, the expression levels of cell cycle regulators and SASP genes, which are also associated with the DNA damage response (DDR), were found to be higher in comparison to late senescent cells.

It is known that the DNA damage repair response operates differently in senescent cells (da Silva and Schumacher, 2019), which may explain the decrease in DNA damage marker accumulation during late senescence. Normally, when cells experienced extensive DNA damage, the activation of a complex signaling network known as the DDR is triggered. DDR senses DNA damage and initiates a cascade of events to repair the damage and halt cell cycle progression (Jackson and Bartek, 2009). However, cells that have transitioned into a state of complete senescence might progressively deactivate their DNA repair mechanisms as they approach the final stages of their lifecycle. This decline in γ-H2AX may signify a transition in the cellular response to DNA damage. In earlier stages of senescence or when cells are actively repairing DSBs, higher levels of γ-H2AX is observed, possibly indicating ongoing repair efforts. However, when the cell reaches the end of senescence, it may shut down the DDR mechanism. This phenomenon finds support in a study that observed a noteworthy suppression of the expression of genes responsible for orchestrating the DNA damage response in cells that had fully undergone the aging process (Collin et al., 2018). This alteration in DNA repair processes in senescent cells could have profound implications for genome stability and the overall cellular health in aging organisms.

Moreover, the correlation between reduced γ-H2AX signals and decreased expression of SASP genes potentially suggests a coordinated response. It is possible that deeply senescent cells, experiencing a reduced DNA damage response and repair activity, may strategically reduce SASP as part of a controlled mechanism to modulate

senescence-associated processes. This intriguing association calls for further investigation to uncover the precise molecular mechanisms at play.

Furthermore, this observation could be attributed to a mechanism similar to that seen in embryogenesis. It is well-established that embryonic senescence can be induced by various factors, including DNA damage. During embryogenesis, cells undergo rapid proliferation and differentiation, exposing them to a multitude of stresses and signals that can activate the senescence program. These developmental processes may involve tight regulation of DNA damage response mechanisms, resulting in effective repair and clearance of DNA lesions (Muñoz-Espín et al., 2013; Sacco, Belloni and Latella, 2021). As a consequence, late senescent cells may exhibit a lower burden of DNA damage and a decrease in the expression of senescence-associated genes. This suggests that the molecular mechanisms underlying embryogenesis and late senescence may share common regulatory pathways that influence DNA damage response and senescence-associated gene expression.

In our study, as IMR-90 and HDF cells progressed into deep senescence, we observed a decrease in the protein expression of γ-H2AX. The different outcomes between protein expression analysis and protein-DNA interaction analysis (ChIP-sequencing), may be attributed to several factors. Firstly, γ-H2AX expression and its DNA binding activity are subject to distinct regulatory mechanisms. While protein expression may increase in response to various cellular signals, the immediate effect on protein-DNA interactions may not always align. This is particularly relevant in aging or DNA damage scenarios where elevated γ-H2AX expression may not instantaneously reflect increased DNA binding. Secondly, the presence and identity of interaction partners can greatly influence the binding capability of γ-H2AX to DNA. Changes in these partners under different conditions can modulate the protein's DNA interaction profile. Additionally, epigenetic alterations on DNA may affect γ-H2AX's binding properties. DNA damage or epigenetic modifications can lead to a shift in the regions where γ-H2AX prefers to bind. Lastly, γ-H2AX's dynamic nature as part of the DNA damage response can impact its binding kinetics, contributing to differences in observed DNA interactions.

In this study, it was also aimed to identify specific DNA motifs that are vulnerable to DNA damage. During cellular senescence, it has been observed that the expression of repetitive DNA elements such as LINEs and SINEs undergoes changes (De Cecco et al., 2013; Booth and Brunet, 2016; Nakao, Tanaka and Koga, 2020; Soto-

Palma et al., 2022). Since they have the ability to move and insert themselves in different locations within the genome, this mobility can lead to genomic rearrangements, insertional mutagenesis, and alterations in gene expression patterns, all of which can disrupt normal cellular functions and contribute to genomic instability. For instance, L1 retrotransposons were upregulated in senescent cells and the activation of L1 elements has been implicated in genomic instability and the pro-inflammatory state associated with senescence (De Cecco et al., 2013). Also, Alr/alpha satellite was found to be upregulated in late senescence (Karakülah and Yandim, 2020). Similarly, Alu elements, a type of SINE repeats, show dysregulated expression in senescent cells. The altered expression of Alu elements in senescence may contribute to DNA damage response and senescence-associated phenotypes (Simon et al., 2019). Specifically, it is known that alpha satellites are predominantly found in these regions and copy number alterations in these satellite arrays may cause accumulation of DNA damage. Possibly by inducing genomic instability due to stalled replication forks caused by unresolved secondary structures, and re-replication of highly repetitive DNAs.

Consistent with the previous literature, an enrichment trend was observed for the telomeric repeats, some of the simple repeats and satellites, according to RepEnrich analysis results. Indeed, repetitive regions can be more susceptible to DNA damage since errors can occur more frequently in these regions during DNA replication and repair processes. Additionally, repetitive elements can be hotspots for genetic recombination and rearrangements, which can lead to DNA damage.

GO term analysis was performed to determine whether DNA damage clustered in gene-rich regions and to investigate whether there was a potential association with age-related phenotypes. It turns out that genes associated with the bacterial invasion of epithelial cells may have a potential relevance. It was previously shown that the presence of DNA damage promote the secretion of essential SASP components and can disrupt the normal functioning of immune cells, subsequently, impairing their ability to mount an effective defense against bacterial pathogens in senescence (Prattichizzo et al., 2018; Bana and Cabreiro, 2019). This highlights the importance of maintaining genomic integrity for efficient immune function.

The p53 signaling pathway plays a critical role in coordinating cellular responses to DNA damage and cellular stress. Activation of p53 serves as a protective mechanism to halt cell cycle progression and initiate DNA repair processes, allowing

cells to respond appropriately to DNA damage and maintain genomic integrity (Williams and Schumacher, 2016). In our study, we observed the presence of γ-H2AX peaks in genes associated with the p53 signaling pathway in late senescent cells, potentially indicating the activation of repair pathways in response to DNA damage, in line with the previous results.

In the study, it was observed a relation between DNA damage and the ribosomal pathways in early senescent cells. Ribosomes play a crucial role in protein synthesis, and impaired ribosome biogenesis can result in structural alterations of the nucleolus (Turi et al., 2019). These alterations observed in various age-related diseases, including cardiovascular diseases, neurodegenerative diseases, and cancer (Hetman and Pietrzak, 2012; Hariharan and Sussman, 2014; Turi et al., 2019). Furthermore, our analysis revealed a correlation between genes associated with these age-related diseases and DNA damage in senescent cells. This finding suggests that the dysregulation of ribosomal pathways and the accumulation of DNA damage are interconnected processes during cellular senescence and can be initiative for age-related diseases.

Interestingly, GO term analysis revealed the AGE-RAGE signaling pathway in Diabetic Complications and the PI3K-Akt signaling pathway, both implicated in age-related diseases and cellular signaling, showed γ-H2AX peaks in late senescent cells. The binding of advanced glycation end products (AGEs) to their receptor RAGE triggers downstream signaling events, including the activation of the PI3K/Akt pathway which is responsible for regulating critical cellular processes such as cell growth, survival, and metabolism (Abdelmageed et al., 2019). This activation in turn, lead to increased oxidative stress, impaired mitochondrial function, and altered protein homeostasis, which are characteristic features of both senescence and the age-related diseases. In line with the our GO-term analysis, previous research highlighting the role of the AGE-RAGE pathway in the development and progression of diabetic complications, neurodegeneration, and cardiovascular diseases (Senatus and Schmidt, 2017; Kong et al., 2020; Snelson, Lucut and Coughlan, 2022). Also, these findings align with our WGS analysis (data not shown). These observations suggest that these signaling pathways may exacerbate DNA damage, leading to cellular dysfunction and the manifestation of senescence.

Despite the valuable insights gained from this study, there are certain limitations that should be acknowledged. First, the molecular characterization of the

cells was incomplete. While various techniques were employed to investigate different aspects of cellular senescence, additional molecular analyses could have provided a more comprehensive understanding of the underlying mechanisms. Second, the ChIP-seq data used in the analysis was obtained from a single cell line. The use of multiple cell lines would have strengthened the findings and allowed for a better generalization of the results. Third, the replicas of the experiments used in the ChIP-seq were limited. Future studies should aim to include larger sample sizes and rigorous replication to ensure robustness. Addressing these limitations in future studies would contribute to a more comprehensive understanding of the molecular mechanisms underlying cellular senescence and DNA damage, further strengthening the conclusions drawn from this research.

CHAPTER 5: CONCLUSION

In conclusion, in this thesis, it was aimed to unravel the occurrence and distribution of endogenous DNA damage outside of telomeres during the process of replicative senescence. By employing advanced techniques such as immuno-FISH and γ-H2AX detection, it was discovered that DNA damage is not confined solely to telomeric regions but manifests throughout the genome during senescence.

Another key focus of this study was to investigate the regions that are vulnerable to DNA damage. Through the utilization of γ-H2AX ChIP-seq analysis, we unraveled some of repetitive elements, including LINEs, SINEs, and Alr/alpha repeats, within regions exhibiting DNA damage during senescence. These findings strongly suggest the involvement of repetitive DNA elements in the DNA damage response.

Additionally, our research has been extended to identify whether DNA damage exhibits clustering patterns in gene-rich regions and explore its potential association with age-related phenotypes in both early and late senescent cells using GO term analysis. Intriguingly, immune system pathways, cell death mechanisms, neurodegeneration, vascularization processes, type II diabetes-related pathways, and cancer-related pathways emerged as intricately linked to DNA damage during senescence.

Moreover, we observed a notable disparity in DNA damage and SASP gene expression between early and late senescence. The higher levels of DNA damage signals, the expression of SASP and cell cycle regulator genes in early senescence, as compared to the late stage, may be attributed to the switching off the DNA damage response mechanism during late senescence. Indeed, existing literature has highlighted the pivotal roles played by DNA damage response (DDR) and DNA repair pathways in the context of senescent cells.

To summarize, our research offers valuable insights into the occurrence and distribution of endogenous DNA damage beyond telomeres during replicative senescence. The identification of specific repetitive DNA motifs contributing to DNA damage adds a layer of complexity to our understanding. Additionally, the elucidation of key pathways and biological processes associated with DNA damage during senescence enhances our comprehension of the underlying mechanisms driving age-related diseases. Although previously unexplored, our results suggest that DNA alterations may have the potential to trigger age-related diseases.

Looking ahead, validation in wet lab experiments is necessary to confirm the findings and provide further evidence for the role and the molecular mechanisms of DNA damage response in senescence. Future studies should delve deeper into the precise mechanisms of DNA repair, the impact of repetitive DNA elements on genomic instability, and the development of therapeutic interventions aimed at mitigating DNA damage during senescence. By pursuing these avenues of research and conducting experimental validation, we can advance our knowledge of senescence biology and pave the way for innovative strategies to address age-related health challenges.

REFERENCES

Abdelmageed, M. E. (2019) '*Cinnamaldehyde ameliorates STZ-induced rat diabetes through modulation of IRS1/PI3K/AKT2 pathway and AGEs/RAGE interaction.*', Naunyn-Schmiedeberg's archives of pharmacology, Vol. 392(2), pp. 243–258.

Al Aboud, N. M., Tupper, C. and Jialal, I. (2023) '*Genetics, Epigenetic Mechanism.*', in. Treasure Island (FL).

Acosta, J. C. (2013) '*A complex secretory program orchestrated by the inflammasome controls paracrine senescence*', Nature Cell Biology, Vol. 15(8), pp. 978–990.

Aird, K. M. and Zhang, R. (2013) '*Detection of senescence-associated heterochromatin foci (SAHF).*', Methods in molecular biology (Clifton, N.J.), Vol. 965, pp. 185–196.

Alberts B, Johnson A, Lewis J, Raff M, Roberts K, W. P. (2002) Molecular biology of the cell. 4th ed. New York: Garland Science/Taylor & Francis LLC.

Alessio, N.. (2023) 'P*rogression of irradiated mesenchymal stromal cells from early to late senescence: Changes in SASP composition and anti-tumour properties',* Cell Proliferation, Vol. n/a(n/a), p. e13401.

Almatarneh, M. H. (2022) 'C*omputational Insights in DNA Methylation: Catalytic and Mechanistic Elucidations for Forming 3-Methyl Cytosine*', Journal of Chemistry. Edited by J. Corchado, 2022, p. 2673396.

Ambros, V. (2004) '*The functions of animal microRNAs*', Nature, Vol. 431(7006), pp. 350–355.

Amtmann, A., Ma, H. and Wagner, D. (2015) *'Chromatin and Epigenetics*.', Plant physiology. United States, pp. 1185–1188.

Anwar, S. L., Wulaningsih, W. and Lehmann, U. (2017) *'Transposable Elements in Human Cancer: Causes and Consequences of Deregulation.*', International journal of molecular sciences, 18(5).

Argueso, J. L. (2008) '*Double-strand breaks associated with repetitive DNA can reshape the genome*', Proceedings of the National Academy of Sciences, Vol. 105(33), pp. 11845–11850.

Armanios, M. (2009) '*Short telomeres are sufficient to cause the degenerative defects associated with aging.*', American journal of human genetics, Vol. 85(6), pp. 823–832.

De Azambuja, K. (2014) *'Validation of an HPV16-mediated carcinogenesis mouse*

model', In vivo (Athens, Greece), Vol. 28(5), pp. 761–767. Available at: https://pubmed.ncbi.nlm.nih.gov/25189887.

Babraham Bioinformatics (2023) FastQC. Available at: https://www.bioinformatics.babraham.ac.uk/projects/fastqc/.

Bana, B. and Cabreiro, F. (2019) '*The Microbiome and Aging.*', Annual review of genetics, 53, pp. 239–261.

Barski, A. (2007) '*High-resolution profiling of histone methylations in the human genome.*', Cell, 129(4), pp. 823–837.

Beck, C. R. (2011) '*LINE-1 elements in structural variation and disease.*', Annual review of genomics and human genetics, 12, pp. 187–215.

Bernstein, C. (2013) *'DNA Damage, DNA Repair and Cancer*', in Chen, C. (ed.). Rijeka: IntechOpen, p. Ch. 16.

Bodnar, A. G.. (1998) '*Extension of life-span by introduction of telomerase into normal human cells.'* Science (New York, N.Y.), Vol. 279(5349), pp. 349–352.

Bolger, A. M., Lohse, M. and Usadel, B. (2014) *'Trimmomatic: a flexible trimmer for Illumina sequence data',* Bioinformatics, 30(15), pp. 2114–2120.

Bonneville, R. (2017) '*Landscape of Microsatellite Instability Across 39 Cancer Types'*, JCO Precision Oncology, Vol. (1), pp. 1–15.

Booth, L. N. and Brunet, A. (2016) '*The Aging Epigenome.*', Molecular cell, Vol. 62(5), pp. 728–744. d

Borodkina, A.. (2014) '*Interaction between ROS dependent DNA damage, mitochondria and p38 MAPK underlies senescence of human adult stem cells.'*, Aging, Vol. 6(6), pp. 481–495.

Bourré (2020) DNA Damage Response (DDR), Crown Bioscience. Available at: https://blog.crownbio.com/dna-damage-responseitle.

Branzei, D. and Foiani, M. (2008) '*Regulation of DNA repair throughout the cell cycle.'*, Nature reviews. Molecular cell biology, Vol. 9(4), pp. 297–308.

Brown, T. (2002) 'Genomes.', in. Oxford: Wiley-Liss. Available at: https://www.ncbi.nlm.nih.gov/books/NBK21134/.

Bulbiankova, D. (2023) '*Hallmarks and Biomarkers of Skin Senescence: An Updated Review of Skin Senotherapeutics.',* Antioxidants (Basel, Switzerland), 12(2).

Burma, S. (2001) '*ATM phosphorylates histone H2AX in response to DNA double-strand breaks*.', The Journal of biological chemistry, Vol. 276(45), pp. 42462–42467.

Campisi, J., Dimri, G., and Hara, E. (1996) In Handbook of the Biology of Aging.

Fourth Edi. Edited by E. S. and J. Rowe. New York: Academic Press.

Campisi, J. (1996) '*Replicative Senescence: An Old Lives' Tale?*', Cell, Vol. 84(4), pp. 497–500.

Campisi, J. (2013) '*Aging, cellular senescence, and cancer.*', Annual review of physiology, 75, pp. 685–705.

Capparelli, C. (2012) '*CDK inhibitors (p16/p19/p21) induce senescence and autophagy in cancer-associated fibroblasts, "fueling" tumor growth via paracrine interactions, without an increase in neo-angiogenesis'*, Cell Cycle, Vol. 11(19), pp. 3599–3610.

De Cecco, M. (2013) '*Genomes of replicatively senescent cells undergo global epigenetic changes leading to gene silencing and activation of transposable elements*', Aging Cell, Vol. 12(2), pp. 247–256.

De Cecco, M. et al. (2019) '*L1 drives IFN in senescent cells and promotes age-associated inflammation'*, Nature, Vol. 566(7742), pp. 73–78.

Chaffey, N. (2003) 'Alberts, B., Johnson, A., Lewis, J., Raff, M., Roberts, K. and Walter, P. Molecular biology of the cell. 4th edn.', Annals of Botany, Vol. 91(3), p. 401.

Chang, H. H. Y. (2017) *'Non-homologous DNA end joining and alternative pathways to double-strand break repair',* Nature Reviews Molecular Cell Biology, Vol. 18(8), pp. 495–506.

Chatterjee, N. and Walker, G. C. (2017) '*Mechanisms of DNA damage, repair, and mutagenesis',* Environmental and Molecular Mutagenesis, Vol. 58(5), pp. 235–263.

Chauhan, T. (2021) What is Heterochromatin?- Constitutive and Facultative Heterochromatin Explained. Available at: https://geneticeducation.co.in/what-is-heterochromatin-constitutive-and-facultative-heterochromatin-explained/.

Chaumeil, J., Micsinai, M. and Skok, J. A. (2013) '*Combined immunofluorescence and DNA FISH on 3D-preserved interphase nuclei to study changes in 3D nuclear organization.*', Journal of visualized experiments : JoVE, Vol. (72), p. e50087.

Chen, H. et al. (2015) *'MacroH2A1 and ATM Play Opposing Roles in Paracrine Senescence and the Senescence-Associated Secretory Phenotype'*, Molecular Cell, Vol. 59(5), pp. 719–731.

Chen, J.-H., Hales, C. N. and Ozanne, S. E. (2007) '*DNA damage, cellular senescence and organismal ageing: causal or correlative?'*, Nucleic Acids Research, Vol. 35(22), pp. 7417–7428.

Chen, T. (2022) '*DNA damage response inhibition-based combination therapies in cancer treatment: Recent advances and future directions*', Aging and Cancer, Vol. 3(1), pp. 44–67.

Childs, B. G. (2015) '*Cellular senescence in aging and age-related disease: from mechanisms to therapy.'*, Nature medicine, Vol. 21(12), pp. 1424–1435.

Chowdhury, D. (2005) '*gamma-H2AX dephosphorylation by protein phosphatase 2A facilitates DNA double-strand break repair.*', Molecular cell, Vol. 20(5), pp. 801–809.

Collado, M. and Serrano, M. (2010) '*Senescence in tumours: evidence from mice and humans*', Nature Reviews Cancer, Vol. 10(1), pp. 51–57.

Coppé, J.-P.. (2008) '*Senescence-associated secretory phenotypes reveal cell-nonautonomous functions of oncogenic RAS and the p53 tumor suppressor.*', PLoS biology, Vol. 6(12), pp. 2853–2868.

Coppé, J.-P. (2010) '*The senescence-associated secretory phenotype: the dark side of tumor suppression.*', Annual review of pathology, Vol. 5, pp. 99–118.

Criscione, S. W. (2014) '*Transcriptional landscape of repetitive elements in normal and cancer human cells*', BMC Genomics, Vol. 15(1), p. 583.

Criscione, S. W., Teo, Y. V. and Neretti, N. (2016) '*The Chromatin Landscape of Cellular Senescence.*', Trends in genetics : TIG, Vol. 32(11), pp. 751–761.

d'Adda di Fagagna, F. (2003) '*A DNA damage checkpoint response in telomere-initiated senescence*.', Nature, Vol. 426(6963), pp. 194–198.

d'Adda di Fagagna, F. (2008) '*Living on a break: cellular senescence as a DNA-damage response'*, Nature Reviews Cancer, Vol. 8(7), pp. 512–522.

Dai, L. (2014) '*Expression and detection of LINE-1 ORF-encoded proteins', Mobile Genetic Elements*, Vol. 4(3), p. e29319.

Davalos, A. R. (2010) '*Senescent cells as a source of inflammatory factors for tumor progression.'*, Cancer metastasis reviews, Vol. 29(2), pp. 273–283.

Deininger, P. (2011) '*Alu elements: know the SINEs*', Genome Biology, Vol. 12(12), p. 236.

Densham, R. M. and Morris, J. R. (2017) '*The BRCA1 Ubiquitin ligase function sets a new trend for remodelling in DNA repair.*', Nucleus (Austin, Tex.), Vol. 8(2), pp. 116–125.

Dimri, G. P. (1995) *'A biomarker that identifies senescent human cells in culture and in aging skin in vivo.*', Proceedings of the National Academy of Sciences, Vol. 92(20),

pp. 9363–9367.

Dolbeare, F. (1983) '*Flow cytometric measurement of total DNA content and incorporated bromodeoxyuridine*.', Proceedings of the National Academy of Sciences of the United States of America, Vol. 80(18), pp. 5573–5577.

Dumétier, B. (2022) '*Repeat Element Activation-Driven Inflammation: Role of NFκB and Implications in Normal Development and Cancer?*', Biomedicines, Vol. 10, p. 3101.

Efeyan, A. and Serrano, M. (2007) 'p*53: Guardian of the Genome and Policeman of the Oncogenes'*, Cell Cycle, Vol. 6(9), pp. 1006–1010.

Elbakry, A. and Löbrich, M. (2021) 'H*omologous Recombination Subpathways: A Tangle to Resolve*.', Frontiers in genetics, Vol. 12, p. 723847.

Ellegren, H. (2004) '*Microsatellites: simple sequences with complex evolution'*, Nature Reviews Genetics, Vol. 5(6), pp. 435–445.

Ershova, E. S. (2019) '*Copy Number Variation of Human Satellite III (1q12) With Aging*', Frontiers in Genetics, Vol. 10.

Evans, D., Graumann, K. and Bryant, J. (2013) Annual Plant Reviews: Plant Nuclear Structure, Genome Architecture and Gene Regulation.

Ewels, P. (2016) '*MultiQC: summarize analysis results for multiple tools and samples in a single report*', Bioinformatics, Vol. 32(19), pp. 3047–3048.

Fagagna, F. d'Adda di (2003) *'A DNA damage checkpoint response in telomere-initiated senescence',* Nature, Vol. 426(6963), pp. 194–198.

Fan, Y. (2020) *'Senescent Cell Depletion Through Targeting BCL-Family Proteins and Mitochondria*', Frontiers in Physiology, 11.

Feng, J. (2012) '*Identifying ChIP-seq enrichment using MACS*', Nature Protocols, Vol. 7(9), pp. 1728–1740.

Feschotte, C. and Pritham, E. J. (2007) '*DNA transposons and the evolution of eukaryotic genomes*.', Annual review of genetics, Vol. 41, pp. 331–368.

Frankish, A. (2021) '*GENCODE 2021*.', Nucleic acids research, Vol. 49(D1), pp. D916–D923.

Fumagalli, M. (2012) '*Telomeric DNA damage is irreparable and causes persistent DNA-damage-response activation.*', Nature cell biology, Vol. 14(4), pp. 355–365.

Gadgil, R. (2017) '*Replication stalling and DNA microsatellite instability.*', Biophysical chemistry, Vol. 225, pp. 38–48.

Ge, S. X., Jung, D. and Yao, R. (2020) *'ShinyGO: a graphical gene-set enrichment*

tool for animals and plants.', Bioinformatics (Oxford, England), Vol. 36(8), pp. 2628–2629.

Gee, M. (2018) *'DNA damage repair in ovarian cancer: Unlocking the heterogeneity'*, Journal of Ovarian Research, Vol. 11.

Gilbert (2000) 'Developmental Biology.', in. Sunderland (MA): Sinauer Associates. Available at: https://www.ncbi.nlm.nih.gov/books/NBK10041/.

Goodwin, S., McPherson, J. D. and McCombie, W. R. (2016) 'C*oming of age: ten years of next-generation sequencing technologies*', Nature Reviews Genetics, 17(6), pp. 333–351.

Gorgoulis, V. G. and Halazonetis, T. D. (2010) *'Oncogene-induced senescence: the bright and dark side of the response.'*, Current opinion in cell biology, Vol. 22(6), pp. 816–827.

Gregory, T. R. (2005) '*Synergy between sequence and size in Large-scale genomics',* Nature Reviews Genetics, Vol. 6(9), pp. 699–708.

Guo, J. (2022) '*Aging and aging-related diseases: from molecular mechanisms to interventions and treatments'*, Signal Transduction and Targeted Therapy, Vol. 7(1), p. 391.

Haberle, V. and Stark, A. (2018) *'Eukaryotic core promoters and the functional basis of transcription initiation'*, Nature Reviews Molecular Cell Biology, Vol. 19(10), pp. 621–637.

Hachmo, Y. (2020) '*Hyperbaric oxygen therapy increases telomere length and decreases immunosenescence in isolated blood cells: a prospective trial.'*, Aging, Vol. 12(22), pp. 22445–22456.

Hadjiargyrou, M. and Delihas, N. (2013) '*The Intertwining of Transposable Elements and Non-Coding RNAs'*, International Journal of Molecular Sciences, pp. 13307–13328.

Halazonetis, T. D., Gorgoulis, V. G. and Bartek, J. (2008) '*An Oncogene-Induced DNA Damage Model for Cancer Development'*, Science, Vol. 319(5868), pp. 1352–1355.

Hamsanathan, S. and Gurkar, A. U. (2022) *'Lipids as Regulators of Cellular Senescence'*, Frontiers in Physiology, Vol. 13.

Hariharan, N. and Sussman, M. A. (2014) *'Stressing on the nucleolus in cardiovascular disease.'*, Biochimica et biophysica acta, Vol. 1842(6), pp. 798–801.

Hayflick, L. and Moorhead, P. S. (1961) *'The serial cultivation of human diploid cell strains*', Experimental Cell Research, Vol. 25(3), pp. 585–621.

Heinz, S. (2010) '*Simple combinations of lineage-determining transcription factors prime cis-regulatory elements required for macrophage and B cell identities.',* Molecular cell, Vol. 38(4), pp. 576–589.

Helman, E. (2014) '*Somatic retrotransposition in human cancer revealed by whole-genome and exome sequencing.',* Genome research, Vol. 24(7), pp. 1053–1063.

Henikoff, S. (2008) *'Nucleosome destabilization in the epigenetic regulation of gene expression',* Nature Reviews Genetics, Vol. 9(1), pp. 15–26.

Herbig, U. (2006) *'Cellular Senescence in Aging Primates*', Science, Vol. 311(5765), p. 1257.

Hernandez-Segura, A., Nehme, J. and Demaria, M. (2018) '*Hallmarks of Cellular Senescence',* Trends in Cell Biology, Vol. 28(6), pp. 436–453.

Hetman, M. and Pietrzak, M. (2012) '*Emerging roles of the neuronal nucleolus.*', Trends in neurosciences, Vol. 35(5), pp. 305–314.

Hewitt, G. (2012) '*Telomeres are favoured targets of a persistent DNA damage response in ageing and stress-induced senescence*', Nature Communications, Vol. 3(1), p. 708.

Hewitt, G., von Zglinicki, T. and Passos, J. F. (2013) '*Cell sorting of young and senescent cells.*', Methods in molecular biology (Clifton, N.J.), Vol. 1048, pp. 31–47.

Hinz, J. M. (2005) '*Influence of double-strand-break repair pathways on radiosensitivity throughout the cell cycle in CHO cells*', DNA Repair, Vol. 4(7), pp. 782–792.

Hu, L. (2022) *'Why Senescent Cells Are Resistant to Apoptosis: An Insight for Senolytic Development*', Frontiers in Cell and Developmental Biology, Vol. 10.

Issa, J.-P. (2003) '*Age-related epigenetic changes and the immune system',* Clinical Immunology, Vol. 109(1), pp. 103–108.

Itahana, K., Campisi, J. and Dimri, G. P. (2007) '*Methods to detect biomarkers of cellular senescence: the senescence-associated beta-galactosidase assay.',* Methods in molecular biology (Clifton, N.J.), Vol. 371, pp. 21–31.

Iyer, R. R. (2015) *'DNA Triplet Repeat Expansion and Mismatch Repair'*, Annual Review of Biochemistry, Vol. 84(1), pp. 199–226.

Jackson, S. P. and Bartek, J. (2009) *'The DNA-damage response in human biology and disease',* Nature, Vol. 461(7267), pp. 1071–1078.

Jiang, C. and Pugh, B. F. (2009) '*Nucleosome positioning and gene regulation: advances through genomics'*, Nature Reviews Genetics, Vol. 10(3), pp. 161–172.

Jin, B., Li, Y. and Robertson, K. D. (2011) '*DNA Methylation: Superior or Subordinate in the Epigenetic Hierarchy?'*, Genes & Cancer, Vol. 2(6), pp. 607–617.

Jullien, L. (2013) '*Eroded human telomeres are more prone to remain uncapped and to trigger a G2 checkpoint response'*, Nucleic Acids Research, Vol. 41(2), pp. 900–911.

Kadonaga, J. T. (2012) *'Perspectives on the RNA polymerase II core promoter'*, WIREs Developmental Biology, Vol. 1(1), pp. 40–51.

Kanaki, T., Makrantonaki, E. and Zouboulis, C. C. (2016) '*Biomarkers of skin aging.*', Reviews in endocrine & metabolic disorders, Vol. 17(3), pp. 433–442.

Karakülah, G. and Yandim, C. (2020) 'S*ignature changes in the expressions of protein-coding genes, lncRNAs, and repeat elements in early and late cellular senescence.'*, Turkish journal of biology = Turk biyoloji dergisi, Vol. 44(6), pp. 356–370.

Karakülah, G. and Yandim, C. (2021) 'I*dentification of differentially expressed genomic repeats in primary hepatocellular carcinoma and their potential links to biological processes and survival*.', Turkish journal of biology = Turk biyoloji dergisi, Vol. 45(5), pp. 599–612.

Kastenhuber, E. R. and Lowe, S. W. (2017) *'Putting p53 in Context.*', Cell, Vol. 170(6), pp. 1062–1078.

Kazazian, H. H. J. (2004) 'M*obile elements: drivers of genome evolution*.', Science (New York, N.Y.), Vol. 303(5664), pp. 1626–1632.

Kim, J.-I. (2009) '*A highly annotated whole-genome sequence of a Korean individual'*, Nature, Vol. 460(7258), pp. 1011–1015.

Kishikawa, T. (2016) '*Satellite RNAs promote pancreatic oncogenic processes via the dysfunction of YBX1*.', Nature communications, Vol. 7, p. 13006.

Kong, Y. (2020) '*Pathological Mechanisms Linking Diabetes Mellitus and Alzheimer's Disease: the Receptor for Advanced Glycation End Products (RAGE).',* Frontiers in aging neuroscience, Vol. 12, p. 217.

Koso, H. (2012) '*Transposon mutagenesis identifies genes that transform neural stem cells into glioma-initiating cells*', Proceedings of the National Academy of Sciences, Vol. 109(44), pp. E2998–E3007.

Kumari, R. and Jat, P. (2021) *'Mechanisms of Cellular Senescence: Cell Cycle Arrest and Senescence Associated Secretory Phenotype*', Frontiers in Cell and Developmental Biology, Vol. 9.

Kuo, L. J. and Yang, L.-X. (2008) 'G*amma-H2AX - a novel biomarker for DNA double-strand breaks*.', In vivo (Athens, Greece), Vol. 22(3), pp. 305–309.

Lamm, E., Harman, O. and Veigl, S. J. (2020) '*Before Watson and Crick in 1953 Came Friedrich Miescher in 1869.*', Genetics, Vol. 215(2), pp. 291–296.

Lander, E. S. (2001) 'I*nitial sequencing and analysis of the human genome.'*, Nature, Vol. 409(6822), pp. 860–921.

Langmead, B. and Salzberg, S. L. (2012) '*Fast gapped-read alignment with Bowtie 2'*, Nature Methods, Vol. 9(4), pp. 357–359.

Le, N. Q. K. (2019) 'C*lassifying Promoters by Interpreting the Hidden Information of DNA Sequences via Deep Learning and Combination of Continuous FastText N-Grams '*, Frontiers in Bioengineering and Biotechnology . Available at: https://www.frontiersin.org/articles/10.3389/fbioe.2019.00305.

Lee, E. et al. (2012) '*Landscape of somatic retrotransposition in human cancers.'*, Science (New York, N.Y.), Vol. 337(6097), pp. 967–971.

Lettieri-Barbato, D. et al. (2022) '*MicroRNAs, Long Non-Coding RNAs, and Circular RNAs in the Redox Control of Cell Senescenc*e.', Antioxidants (Basel, Switzerland), Vol. 11(3).

Li, G.-M. (2008) '*Mechanisms and functions of DNA mismatch repair*', Cell Research, Vol. 18(1), pp. 85–98.

Liao, Z. (2021) '*Cellular Senescence: Mechanisms and Therapeutic Potential.',* Biomedicines, Vol. 9(12).

Limas, J. C. and Cook, J. G. (2019) 'P*reparation for DNA replication: the key to a successful S phase*.', FEBS letters, Vol. 593(20), pp. 2853–2867.

Livak, K. J. and Schmittgen, T. D. (2001) 'A*nalysis of relative gene expression data using real-time quantitative PCR and the 2(-Delta Delta C(T)) Method.*', Methods (San Diego, Calif.), Vol. 25(4), pp. 402–408.

Lopes-Paciencia, S. (2019) '*The senescence-associated secretory phenotype and its regulation'*, Cytokine, Vol. 117, pp. 15–22.

López-Otín, C. (2013) '*The hallmarks of aging.*', Cell, Vol. 153(6), pp. 1194–1217.

Loscalzo, J. and Handy, D. E. (2014) '*Epigenetic modifications: basic mechanisms and role in cardiovascular disease* (2013 Grover Conference series).', Pulmonary circulation, Vol. 4(2), pp. 169–174.

Lowndes, N. F. and Toh, G. W.-L. (2005) 'DN*A Repair: The Importance of Phosphorylating Histone H2AX'*, Current Biology, Vol. 15(3), pp. R99–R102.

de Magalhães, J. P. (2013) '*How ageing processes influence cancer.*', Nature reviews. Cancer. England, pp. 357–365.

Mah, L.-J., El-Osta, A. and Karagiannis, T. C. (2010) '*γH2AX as a molecular marker of aging and disease'*, Epigenetics, Vol. 5(2), pp. 129–136.

Marchesini, M. (2016) '*PML is required for telomere stability in non-neoplastic human cells*', Oncogene, Vol. 35(14), pp. 1811–1821.

Mardis, E. R. (2008) *'Next-Generation DNA Sequencing Methods*', Annual Review of Genomics and Human Genetics, Vol. 9(1), pp. 387–402.

Marthandan, S. (2015) '*Similarities in Gene Expression Profiles during In Vitro Aging of Primary Human Embryonic Lung and Foreskin Fibroblasts*.', BioMed research international, 2015, p. 731938.

Marthandan, S. (2016) '*Conserved Senescence Associated Genes and Pathways in Primary Human Fibroblasts Detected by RNA-Seq.*', PloS one, Vol. 11(5), p. e0154531.

Martins, S. G. (2021) 'L*inking Oxidative Stress and DNA Damage to Changes in the Expression of Extracellular Matrix Components.*', Frontiers in genetics, Vol. 12, p. 673002.

Massey, T. H. and Jones, L. (2018) 'T*he central role of DNA damage and repair in CAG repeat diseases.*', Disease models & mechanisms, Vol. 11(1).

Matsuno, Y. (2019) *'Replication stress triggers microsatellite destabilization and hypermutation leading to clonal expansion in vitro*', Nature Communications, Vol. 10(1), p. 3925.

Mattick, J. S. and Makunin, I. V (2006) '*Non-coding RNA.*', Human molecular genetics, Vol. 15 Spec No, pp. R17-29.

Merck (no date) DNA Damage and Repair. Available at: https://www.sigmaaldrich.com/TR/en/technical-documents/technical-article/research-and-disease-areas/cancer-research/dna-damage-and-repair.

Metzker, M. L. (2010) '*Sequencing technologies — the next generation'*, Nature Reviews Genetics, Vol. 11(1), pp. 31–46.

Di Micco, R. (2006) '*Oncogene-induced senescence is a DNA damage response triggered by DNA hyper-replication.*', Nature, Vol. 444(7119), pp. 638–642.

Di Micco, R. (2021) '*Cellular senescence in ageing: from mechanisms to therapeutic opportunities'*, Nature Reviews Molecular Cell Biology, Vol. 22(2), pp. 75–95.

Mijit, M. (2020) '*Role of p53 in the Regulation of Cellular Senescence.*',

Biomolecules, Vol. 10(3).

Mirkin, S. M. (2007) '*Expandable DNA repeats and human disease.*', Nature, Vol. 447(7147), pp. 932–940.

Mitra, M. (2019) '*DNA Repairing and its Mechanism in the Cell*', 3, pp. 116–119.

Molinaro, C., Martoriati, A. and Cailliau, K. (2021) '*Proteins from the DNA Damage Response: Regulation, Dysfunction, and Anticancer Strategies.*', Cancers, 13(15).

Molnár, F. (2016) Mechanisms of Gene Regulation, Mechanisms of Gene Regulation, Second Edition.

Moore, L. D., Le, T. and Fan, G. (2013) *'DNA Methylation and Its Basic Function*', Neuropsychopharmacology, Vol. 38(1), pp. 23–38..

Morozova, O., Hirst, M. and Marra, M. A. (2009) '*Applications of New Sequencing Technologies for Transcriptome Analysis*', Annual Review of Genomics and Human Genetics, Vol. 10(1), pp. 135–151.

Morris, S. A. (2023) Microsatellite. Available at: https://www.genome.gov/genetics-glossary/Microsatellite (Accessed: 6 October 2023).

Muñoz-Espín, D. (2013) '*Programmed Cell Senescence during Mammalian Embryonic Development*', Cell, Vol. 155(5), pp. 1104–1118.

Muñoz-Espín, D. and Serrano, M. (2014) '*Cellular senescence: from physiology to pathology*', Nature Reviews Molecular Cell Biology, Vol. 15(7), pp. 482–496.

Muñoz-López, M. and García-Pérez, J. L. (2010) '*DNA transposons: nature and applications in genomics.*', Current genomics, Vol. 11(2), pp. 115–128.

Murakami, Y. (2013) '*Heterochromatin and Euchromatin BT - Encyclopedia of Systems Biology*', in Dubitzky, W. (eds). New York, NY: Springer New York, pp. 881–884.

Mylonas, A. and O'Loghlen, A. (2022) '*Cellular Senescence and Ageing: Mechanisms and Interventions*', Frontiers in Aging, Vol. 3.

Nacarelli, T. and Sell, C. (2017) 'T*argeting metabolism in cellular senescence, a role for intervention*', Molecular and Cellular Endocrinology, Vol. 455, pp. 83–92.

Nakamura, A. J. (2008) *'Both telomeric and non-telomeric DNA damage are determinants of mammalian cellular senescence*', Epigenetics & Chromatin, Vol. 1(1), p. 6.

Nakamura, A. J. (2009) 'Telomere-dependent and telomere-independent origins of endogenous DNA damage in tumor cells.', Aging, Vol. 1(2), pp. 212–218..

Nakao, M., Tanaka, H. and Koga, T. (2020) '*Cellular Senescence Variation by*

Metabolic and Epigenomic Remodeling', Trends in Cell Biology, Vol. 30(12), pp. 919–922.

Nakato, R. and Sakata, T. (2021) '*Methods for ChIP-seq analysis: A practical workflow and advanced applications*', Methods, Vol. 187, pp. 44–53.

Narita, Masashi (2003) '*Rb-Mediated Heterochromatin Formation and Silencing of E2F Target Genes during Cellular Senescence*', Cell, Vol. 113(6), pp. 703–716.

National Insitute on Aging (NIA), H. (2023) Understanding the Dynamics of the Aging Process. Available at: https://www.nia.nih.gov/about/aging-strategic-directions-research/understanding-dynamics-aging (Accessed: 6 October 2023).

NCBI (2017) Genome Decoration Page. Available at: https://www.ncbi.nlm.nih.gov/genome/tools/gdp.

Neurohr, G. E. (2019) '*Excessive Cell Growth Causes Cytoplasm Dilution And Contributes to Senescence.*', Cell, Vol. 176(5), pp. 1083-1097.e18.

Nojadeh, J. N., Behrouz Sharif, S. and Sakhinia, E. (2018) '*Microsatellite instability in colorectal cancer.*', EXCLI journal, Vol. 17, pp. 159–168.

Novak, K. (2005) *'In vivo veritas*', Nature Reviews Cancer, Vol. 5(9), p. 668.

Okada, N. (1991) *'SINEs: Short interspersed repeated elements of the eukaryotic genome.*', Trends in ecology & evolution, Vol. 6(11), pp. 358–361.

Pace, J. K. 2nd and Feschotte, C. (2007) '*The evolutionary history of human DNA transposons: evidence for intense activity in the primate lineage.*', Genome research, Vol. 17(4), pp. 422–432.

Pagni, S. (2022) '*Non-coding regulatory elements: Potential roles in disease and the case of epilepsy*', Neuropathology and Applied Neurobiology, Vol. 48(3), p. e12775.

Paramos-de-Carvalho, D., Jacinto, A. and Saúde, L. (2021) *'The right time for senescence'*, eLife. Edited by M. E. Bronner, Vol. 10, p. e72449.

Park, P. J. (2009) '*ChIP–seq: advantages and challenges of a maturing technology'*, Nature Reviews Genetics, Vol. 10(10), pp. 669–680.

Pavlicek, A., Kapitonov, V. V and Jurka, J. (2006) '*Human Repetitive DNA BT - Encyclopedic Reference of Genomics and Proteomics in Molecular Medicine'*, in. Berlin, Heidelberg: Springer Berlin Heidelberg, pp. 822–831.

Pérez, R. F. (2018) '*Distinct chromatin signatures of DNA hypomethylation in aging and cancer.'*, Aging cell, Vol. 17(3), p. e12744.

Pilié, P. G. (2019) '*State-of-the-art strategies for targeting the DNA damage response in cancer*', Nature Reviews Clinical Oncology, Vol. 16(2), pp. 81–104.

Plohl, M., Meštrović, N. and Mravinac, B. (2014) '*Centromere identity from the DNA point of view*', Chromosoma, Vol. 123(4), pp. 313–325.

Porokhovnik, L. N. (2021) '*The Role of Human Satellite III (1q12) Copy Number Variation in the Adaptive Response during Aging, Stress, and Pathology: A Pendulum Model*', Genes.

Prattichizzo, F. (2018) '*Short-term sustained hyperglycaemia fosters an archetypal senescence-associated secretory phenotype in endothelial cells and macrophages.*', Redox biology, Vol. 15, pp. 170–181.

Rabinovitch, R. C. (2017) *'AMPK Maintains Cellular Metabolic Homeostasis through Regulation of Mitochondrial Reactive Oxygen Species*.', Cell reports, Vol. 21(1), pp. 1–9.

Rahimian, E. (2020) '*DNA repair pathways as guardians of the genome: Therapeutic potential and possible prognostic role in hematologic neoplasms*', DNA Repair, Vol. 96, p. 102951.

Ramel, C. (1997) '*Mini- and microsatellites.'*, Environmental health perspectives, Vol. 105 Suppl(Suppl 4), pp. 781–789.

Ramírez, F. (2016) *'deepTools2: a next generation web server for deep-sequencing data analysis'*, Nucleic Acids Research, Vol. 44(W1), pp. W160–W165.

Rayess, H., Wang, M. B. and Srivatsan, E. S. (2012) '*Cellular senescence and tumor suppressor gene p16'*, International Journal of Cancer, Vol. 130(8), pp. 1715–1725.

Reddy, J. P. and Li, Y. (2011) '*Oncogene-Induced Senescence and its Role in Tumor Suppression*', Journal of Mammary Gland Biology and Neoplasia, Vol. 16(3), pp. 247–256.

Rogakou, E. P. (1998) '*DNA double-stranded breaks induce histone H2AX phosphorylation on serine 139*.', The Journal of biological chemistry, Vol. 273(10), pp. 5858–5868.

Rudolph, K. L. (1999) 'L*ongevity, Stress Response, and Cancer in Aging Telomerase-Deficient Mice'*, Cell, Vol. 96(5), pp. 701–712.

Rutgers Medical School (2023) *Causes of Telomere Shortening and Dysfunction*. Available at: https://njms.rutgers.edu/departments/molecular_genetics/faculty/herbig/TDIS.php.

Sacco, A., Belloni, L. and Latella, L. (2021) 'F*rom Development to Aging: The Path to Cellular Senescence*.', Antioxidants & redox signaling, Vol. 34(4), pp. 294–307.

Saksouk, N., Simboeck, E. and Déjardin, J. (2015) 'Constitutive heterochromatin

formation and transcription in mammals', Epigenetics & Chromatin, 8(1), p. 3.
Sanidas, I. (2019) '*A Code of Mono-phosphorylation Modulates the Function of RB.*', Molecular cell, Vol. 73(5), pp. 985-1000.e6.
Schorl, C. and Sedivy, J. M. (2007) '*Analysis of cell cycle phases and progression in cultured mammalian cells.',* Methods (San Diego, Calif.), Vol. 41(2), pp. 143–150.
Senatus, L. M. and Schmidt, A. M. (2017) '*The AGE-RAGE Axis: Implications for Age-Associated Arterial Diseases.*', Frontiers in genetics, Vol. 8, p. 187.
Serrano, M. (1997) '*Oncogenic ras provokes premature cell senescence associated with accumulation of p53 and p16INK4a.*', Cell, Vol. 88(5), pp. 593–602.
Shammas, M. A. (2011) '*Repetitive sequences, genomic instability, and Barrett's esophageal adenocarcinoma*', Mobile Genetic Elements, Vol. 1(3), pp. 208–212.
Shastri, N. (2018) '*Genome-wide Identification of Structure-Forming Repeats as Principal Sites of Fork Collapse upon ATR Inhibition.*', Molecular cell, Vol. 72(2), pp. 222-238.e11.
Shen, Y. (2012) '*A Steroid Receptor–MicroRNA Switch Regulates Life Span in Response to Signals from the Gonad*', Science, Vol. 338(6113), pp. 1472–1476.
Siddiqi, S., Mills, J. and Matushansky, I. (2010) '*Epigenetic remodeling of chromatin architecture: exploring tumor differentiation therapies in mesenchymal stem cells and sarcomas.',* Current stem cell research & therapy, Vol. 5(1), pp. 63–73.
da Silva, P. F. L. and Schumacher, B. (2019) *'DNA damage responses in ageing.',* Open biology, Vol. 9(11), p. 190168.
Simna, S. P. and Han, Z. (2022) *'Prospects of Non-Coding Elements in Genomic DNA Based Gene Therapy.',* Current gene therapy, Vol. 22(2), pp. 89–103.
Simon, M. (2019) '*LINE1 Derepression in Aged Wild-Type and SIRT6-Deficient Mice Drives Inflammation.',* Cell metabolism, Vol. 29(4), pp. 871-885.e5.
Smit, AFA, Hubley, R & Green, P. (2015) RepeatMasker Open-4.0.
Smith, U. (2021) '*Cellular senescence and its role in white adipose tissue',* International Journal of Obesity, Vol. 45(5), pp. 934–943.
Snelson, M., Lucut, E. and Coughlan, M. T. (2022) '*The Role of AGE-RAGE Signalling as a Modulator of Gut Permeability in Diabetes.',* International journal of molecular sciences, Vol. 23(3).
Soto-Palma, C. (2022) *'Epigenetics, DNA damage, and aging.',* The Journal of clinical investigation, Vol. 132(16).
Storer, M. (2013) '*Senescence is a developmental mechanism that contributes to*

embryonic growth and patterning.', Cell, Vol. 155(5), pp. 1119–1130.

Sun, L. (2021) *'Chromatin and Epigenetic Rearrangements in Embryonic Stem Cell Fate Transitions*', Frontiers in Cell and Developmental Biology, Vol. 9.

Sun, L., Yu, R. and Dang, W. (2018) *'Chromatin Architectural Changes during Cellular Senescence and Aging.'*, Genes, Vol. 9(4).

Sun, P. (2007) '*PRAK is essential for ras-induced senescence and tumor suppression.',* Cell, Vol. 128(2), pp. 295–308.

Sundararajan, R. and Freudenreich, C. H. (2011) '*Expanded CAG/CTG repeat DNA induces a checkpoint response that impacts cell proliferation in Saccharomyces cerevisiae.'*, PLoS genetics, Vol. 7(3), p. e1001339.

Tiedje, C. (2012) '*The p38/MK2-driven exchange between tristetraprolin and HuR regulates AU-rich element-dependent translation.'*, PLoS genetics, 8(9), p. e1002977.

Ting, D. T. (2011) *'Aberrant overexpression of satellite repeats in pancreatic and other epithelial cancers.'*, Science (New York, N.Y.), Vol. 331(6017), pp. 593–596.

Tomasova, K. (2020) *'DNA Repair and Ovarian Carcinogenesis: Impact on Risk, Prognosis and Therapy Outcome'*, Cancers, Vol. 12, p. 1713.

Treangen, T. J. and Salzberg, S. L. (2011) '*Repetitive DNA and next-generation sequencing: computational challenges and solutions.',* Nature reviews. Genetics, Vol. 13(1), pp. 36–46.

Turi, Z. (2019) *'Impaired ribosome biogenesis: mechanisms and relevance to cancer and aging.'*, Aging, Vol. 11(8), pp. 2512–2540.

Ugalde, A. P., Español, Y. and López-Otín, C. (2011) *'Micromanaging aging with miRNAs: new messages from the nuclear envelope.'*, Nucleus (Austin, Tex.), Vol. 2(6), pp. 549–555.

Ulitsky, I. (2011) '*Conserved function of lincRNAs in vertebrate embryonic development despite rapid sequence evolution.',* Cell, Vol. 147(7), pp. 1537–1550.

Victorelli, S. and Passos, J. F. (2017) 'Telomeres and Cell Senescence - Size Matters Not', eBioMedicine, 21, pp. 14–20.

Vos, L. J., Famulski, J. K. and Chan, G. K. T. (2006) '*How to build a centromere: from centromeric and pericentromeric chromatin to kinetochore assembly.*', Biochemistry and cell biology = Biochimie et biologie cellulaire, Vol. 84(4), pp. 619–639.

Wahls, W. P., Wallace, L. J. and Moore, P. D. (1990) '*Hypervariable minisatellite DNA is a hotspot for homologous recombination in human cells'*, Cell, 60(1), pp. 95–

103.

Wei, X. (2021) '*Heterochromatin-dependent transcription of satellite DNAs in the Drosophila melanogaster female germline'*, eLife. Edited by D. Weigel, Vol. 10, p. e62375.

Weinberg, M. S. and Wood, M. J. A. (2009) *'Short non-coding RNA biology and neurodegenerative disorders: novel disease targets and therapeutics.'*, Human molecular genetics, Vol. 18(R1), pp. R27-39.

Western Oregon University (no date) Ch450 and Ch451: Biochemistry - Defining Life at The Molecular Level. Available at: https://wou.edu/chemistry/courses/online-chemistry-textbooks/ch450-and-ch451-biochemistry-defining-life-at-the-molecular-level/chapter-12-dna-damage-repair-and-mutations/ (Accessed: 6 December 2023).

Wickham, H. (2009) ggplot2: Elegant Graphics for Data Analysis, Springer-Verlag New York. Available at: https://ggplot2.tidyverse.org/.

Williams, A. B. and Schumacher, B. (2016) *'p53 in the DNA-Damage-Repair Process.',* Cold Spring Harbor perspectives in medicine, Vol. 6(5).

Yandım, C. (2012) Heterochromatin Effects In Friedreich's Ataxia And Sexual Dimorphism.

Yandım, C. and Karakülah, G. (2019a) *'Dysregulated expression of repetitive DNA in ER+/HER2- breast cancer'*, Cancer Genetics, Vol. 239, pp. 36–45.

Yandım, C. and Karakülah, G. (2019b) '*Expression dynamics of repetitive DNA in early human embryonic development.',* BMC genomics, Vol. 20(1), p. 439.

Yandım, C. and Karakülah, G. (2022) *'Repeat expression is linked to patient survival and exhibits single nucleotide variation in pancreatic cancer revealing LTR70:r.879A>G'*, Gene, Vol. 822, p. 146344.

von Zglinicki, T. (2002) '*Oxidative stress shortens telomeres', Trends in Biochemical Sciences*, Vol. 27(7), pp. 339–344.

Zhang, L. (2014) *'The structure and retrotransposition mechanism of LTR-retrotransposons in the asexual yeast Candida albicans',* Virulence, Vol. 5(6), pp. 655–664.

Zhang, W. (2008) *'Comparison of global DNA methylation profiles in replicative versus premature senescence'*, Life Sciences, Vol. 83(13), pp. 475–480.

Zhu, Q. (2011) *'BRCA1 tumour suppression occurs via heterochromatin-mediated silencing.',* Nature, Vol. 477(7363), pp. 179–184.